



GLOBAL MARITIME

MARINE, OFFSHORE AND ENGINEERING CONSULTANTS

11767 Katy Freeway, Suite 660, Houston, Texas 77079

Telephone: (281) 558 3690 Facsimile: (281) 558 0541

Email: agm@globalmaritimeus.com Website: www.globalmaritime.com

MINERALS MANAGEMENT SERVICE

ASSESSMENT OF PERFORMANCE OF
DEEPWATER FLOATING PRODUCTION FACILITIES
DURING HURRICANE LILI

FINAL REPORT

Report No: GMH-3704-1377 Rev 1

DOCUMENT DETAILS AND ISSUE RECORD

AUTHOR: Alberto Morandi

| Revision | Date | Details | Author | Checked | Approved |
|----------|----------|------------------------|--------|----------|----------|
| 0 | 04.08.04 | For Submittal to MMS | ACM | DM / JAM | ACM |
| 1 | 06.30.04 | Incorporating Comments | ACM | DM | ACM |
| | | | | | |

C:\ Public\Project Files\Job No. 1377 MMS\Report\GMH_3704_1377_Rv1.doc

EXECUTIVE SUMMARY

Several deep water floating production facilities are currently in operation in the Gulf of Mexico, with many more planned for the future. Hurricane Lili provided an opportunity to verify the performance of such units in the field during a major environmental event. The present study collected and assessed information on the performance of deepwater production facilities that were impacted by Lili, aiming to provide further insight into critical design issues and develop recommendations for improvement in design and operation practices for deep water floating production installations. The principal conclusions and recommendations are summarized below.

1st Objective: Identify the units that were closest to Lili's track and most likely to be impacted by it.

The units that were closest to Lili were: ChevronTexaco's Genesis Spar and Typhoon Mono-Column Tension Leg Platform (TLP), ENI's Morpeth and Allegheny Mono-Column TLPs, Conoco's Jolliet TLP, Shell's Brutus TLP and El Paso's Prince TLP. Typhoon was the unit located closest to Lili's track and subjected to the most severe environmental conditions.

2nd Objective: Collect information on any observed damage to such units and assess its significance. If significant structural damage was observed, identify potential abnormal loading (such as loss of air gap or collision) and failure mechanisms.

In general, no damage to structural members was observed. Inspection data indicated damage to secondary structures located in the air gap such as ladders and boat landings (up to 55ft above sea level) but no evidence of air gap loss was found. In general, the units were subject to motions that led to damage of some topsides equipment.

3rd Objective: Assess the environmental conditions during Lili and if these were of a sufficiently large magnitude to test the design of the units affected. Identify and collect any measured data that would assist in assessing the performance of the units. Verify if the performance of the units during Lili stayed within their design limits.

The hindcast study and the measurements obtained of wind (for Brutus) and of current (for Genesis) suggest that the environmental conditions during Hurricane Lili were sufficient to test the response of Typhoon, Brutus and Genesis relative to their design events.

Motion and tendon tension measurements were obtained for Brutus and verified to be within design limits. Tendon tension measurements were obtained for Typhoon and were also within design limits. Tendon tensions were calculated for Allegheny and found to be within the design limits.

| It is noted that no monitoring data was available for Allegheny, Jolliet, Prince and Genesis as their monitoring systems were not operational during Lili. Valuable monitoring data was not recorded precisely when such platforms were subject to a major environmental event. A contributing factor for this occurrence was that the units were evacuated during Hurricane Isidore and powering of the monitoring system had not been restored (or failed) during Lili. It is understood that some units are currently upgrading the batteries that power their monitoring systems.

4th Objective: Verify the data collected against current knowledge from the point of view of design environmental conditions and assess any safe / unsafe bias.

High quality buoy data provided the best indication of winds and waves during Lili and Oceanweather's hindcast model provided an accurate representation of the data measured at the buoys. The measurements obtained from the production units concerning environmental conditions were disappointing and no wave measurements at all were available from any of the units considered here. Wind measurements were obtained for Brutus but the buoy data was considered more applicable as it was measured nearer to the standard 10m height above sea level and without potential interference from nearby structures.

Some relevant current data was measured for Genesis but the data for the 29m column of water near the surface was discarded due to interference of the side lobes of the Acoustic Doppler Current Profiler (ADCP) unit. Given the complexity of modeling hurricane currents, the design current profiles examined achieved a reasonable level of competence in terms of capturing the global current loading. Relative to the measurements, the hindcast model under-predicted the surface currents and over-predicted deep currents.

Overall the analysis of Hurricane Lili data suggested that the design and hindcast models were reasonably competent in predicting key hurricane environmental data.

5th Objective: Verify the data collected against current knowledge from the point of view of design response / performance models and assess any safe / unsafe bias.

Detailed analyses of the monitoring data suggested an overall safe side bias in the design models for Brutus with room for future investigation. Minimum tendon tension was an important criterion for the design of Brutus in its intact condition and it was noted that the minimum tendon tensions during Lili did not at all approach a critical condition of zero tension.

Detailed analysis of the monitoring data indicated that, given the uncertainties involved in determining the environmental conditions during Lili, the design models for Typhoon predicted tendon tensions that were reasonably close to the measurements. The results however suggest that there is little room for reducing conservatism in such design models for some critical headings.

6th Objective: Review past operational experience and briefly document key issues of concern to the industry. These are understood to be prediction of meteorological data, its translation into design bases, and the impact of vortex shedding effects on the behavior of risers and TLP tendons as well as on the motions and therefore global performance of deepwater floating production installations. Assess if the data collected during Lili sheds new light into these issues.

High frequency tendon tension response components during Lili were apparent at 0.5 Hz or higher for both Brutus and Typhoon indicating potential vortex shedding effects on the tendons. However, the magnitude of such effects was small and did not significantly contribute to the total tendon tension. No significant riser Vortex Induced Vibration (VIV) was reported. Such behavior was in contrast to that observed, for example, for Allegheny during the Millennium Eddy where VIV on the tendons and risers was enough to excite modes of vibration of the TLP structure.

Vortex Induced Motions (VIM) was not identified for the TLPs as the vortex shedding frequency may be close to the surge and sway resonant periods. The overall tendon tensions as well as the comparisons of specific components of the design recipe did not suggest any unforeseen tension components. The observations suggest that, for Brutus and Typhoon, VIM was not of concern.

Recommendations.

Damage was observed to deck equipment in some units due to the motions during Lili. A review of the procedures for securing critical equipment during major environmental events is recommended. Damage was also observed to equipment located in the air gap of some of the units. Such damage appears to be consistent with design predictions for wave crest, wave run-up and green water loading but a more detailed assessment should be carried out in the future.

Several units were subject to severe environmental loading not only during Lili, but also during previous major environmental events. The impact of all such events on the integrity of structural components, tendons, moorings, anchors and risers should be carefully investigated.

The data measured during Lili provided evidence of vortex shedding effects on TLP tendons but the magnitude of such effects did not increase the overall tension values beyond design predictions. On a more general note, vortex shedding may affect risers and tendons but also the global motions of spars. Such motions may have a knock-on effect on other areas such as the integrity of structural components, moorings and risers. This study provided evidence of the competence of the tools and procedures available to the industry (both in terms of analysis and measurement) when modeling an event such as Lili. The industry should work diligently in applying such tools and expertise to achieve similar competence in modeling VIV and VIM to reduce undue operational costs. This study provided evidence that some operators and designers are indeed working diligently to address the complex issues related to metocean data and its translation into design bases as well as those issues related to VIV and VIM in deepwater structures. An industry wide effort into reviewing and documenting existing prediction methods and best design practices on such issues would be beneficial for the future operation of deep water production units in the Gulf of Mexico.

The offshore industry has previously conducted useful studies where computer programs for advanced analysis (such as pushover analysis of platforms) were benchmarked. Computer programs presently used for the prediction of motions, tendon / mooring loads and riser response should be subject to similar benchmarking. The outcome of such study would provide an insight into specific areas where future research would be most beneficial.

There is a clear economical benefit in designing operations to be maintained during high currents.

Extensive literature is available related to reliability-based methods for TLP design. A co-ordinated effort to collate such information and develop a risk-based approach to the design and integrity management of TLPs worldwide could be beneficial to the industry. A similar approach to the design of risers could be also beneficial.

KEYWORDS

| | | | |
|------|-------------|------|-----|
| MMS | Hurricane | Lili | TLP |
| Spar | Performance | | |

TABLE OF CONTENTS

| SECTION | PAGE |
|---|-----------|
| 1. INTRODUCTION..... | 8 |
| 1.1 INSTRUCTIONS | 8 |
| 1.2 AIMS AND OBJECTIVES OF THE PROJECT | 8 |
| 1.3 SCOPE OF WORK | 9 |
| 1.4 OUTLINE OF THE REPORT | 10 |
| 2. BACKGROUND | 11 |
| 2.1 HISTORICAL PERSPECTIVE..... | 11 |
| 2.2 PERFORMANCE AND RELIABILITY OF FLOATING PRODUCTION FACILITIES | 13 |
| 2.3 METEOROLOGICAL DATA..... | 13 |
| 2.4 IMPACT OF HIGH CURRENTS ON DEEP WATER OPERATIONS | 16 |
| 2.5 VORTEX SHEDDING EFFECTS AND VORTEX INDUCED VIBRATION (VIV)..... | 17 |
| 2.6 'TRADITIONAL' GLOBAL PERFORMANCE ANALYSIS OF FLOATING SYSTEMS..... | 19 |
| 3. ENVIRONMENTAL CONDITIONS DURING HURRICANE LILI..... | 20 |
| 3.1 HURRICANE LILI'S TRACK AND INTENSITY | 20 |
| 3.2 HINDCAST STUDY BY OCEANWEATHER INC..... | 24 |
| 3.3 MAXIMUM WINDS AND SEASTATES | 26 |
| 3.4 DIRECTIONALITY OF WINDS AND SEASTATES | 31 |
| 3.5 CURRENT..... | 33 |
| 4. INSPECTION RESULTS FOR INSTALLATIONS AFFECTED BY LILI | 38 |
| 4.1 ALLEGHENY AND TYPHOON - SEASTAR® MONO-COLUMN TLP DESIGNS | 38 |
| 4.2 PRINCE - MODEC TLP DESIGN | 45 |
| 4.3 BRUTUS TLP | 47 |
| 4.4 GENESIS SPAR | 48 |
| 5. ANALYSIS OF MONITORING DATA FOR BRUTUS TLP | 51 |
| 5.1 INTRODUCTION..... | 51 |
| 5.2 GLOBAL PERFORMANCE..... | 52 |
| 5.3 COMPONENTS OF THE DESIGN RECIPE – TENDON TENSION EXTREMES..... | 57 |
| 5.4 DESIGN RECIPE – NATURAL FREQUENCIES AND ENERGY CONTENT | 63 |
| 5.5 DESIGN RECIPE – DAMPING | 67 |
| 5.6 DESIGN RECIPE – OVERALL BIAS..... | 68 |
| 5.7 VORTEX SHEDDING EFFECTS | 72 |
| 6. RESULTS FROM MONITORING DATA FOR TYPHOON AND ALLEGHENY | 75 |
| 6.1 INTRODUCTION..... | 75 |
| 6.2 TYPHOON - GLOBAL PERFORMANCE | 75 |
| 6.3 TYPHOON DESIGN RECIPE – OVERALL BIAS | 77 |
| 6.4 TYPHOON DESIGN RECIPE – TENDON TENSION EXTREMES | 77 |
| 6.5 TYPHOON - VORTEX SHEDDING EFFECTS..... | 79 |
| 7. CONCLUSIONS AND RECOMMENDATIONS | 81 |
| 7.1 PRINCIPAL CONCLUSIONS..... | 81 |
| 7.2 DESIGN ENVIRONMENTAL CONDITIONS | 83 |
| 7.3 TLP GLOBAL PERFORMANCE AND DESIGN RECIPE | 83 |
| 7.4 RECOMMENDATIONS | 85 |
| 8. REFERENCES..... | 87 |
| ACKNOWLEDGEMENTS | 92 |

LIST OF FIGURES

Figure 1 –Hurricane Andrew (from National Climatic Data Center)
Figure 2 – Sample Design Current Profiles
Figure 3 – Loop and Eddy Currents
Figure 4 –Hurricane Lili Track (National Hurricane Center’s Best Track)
Figure 5 – Hurricane Lili, October 2nd 2002
Figure 6 – Fixed Platform Damaged by Hurricane Lili
Figure 7 –Deep Water Platforms in Lili’s Vicinity
Figure 8 –Buoys near Lili’s Track
Figure 9 –Brutus TLP
Figure 10 –Data for Buoy 42041
Figure 11 – Time Series, Wind Speed, Anemometer 21 (from 0:00 am GMT to 6:00 am GMT)
Figure 12 – Summary of Hindcast Peak Winds and Seastates for Typhoon
Figure 13 - Half-hour Wind Velocity at Anemometer 21 during Hurricane Lili
Figure 14 - Half-hour Wind Velocity at Anemometer 31 during Hurricane Lili
Figure 15 - 1hr Mean Wind Velocity Brutus Anemometer 21
Figure 16 - 1hr Mean Wind Velocity Brutus Anemometer 31
Figure 17 – Wind Direction, Raw Data from Brutus
Figure 18 – Mean Overturning Moment, inferred from Tendon Tensions
Figure 19 - Current Measurements during Lili (CST Date and Time on Horizontal Axis)
Figure 20 - The geometry of Profiler Sidelobe Interference
Figure 21 – Current Profiles at the Time of Hindcast Peak Wind (October 3rd 3:40 AM GMT)
Figure 22 – Inertial Current Profile (October 4th 6:50 AM GMT)
Figure 23 – Allegheny TLP (Payload 4,000 tonnes, Water Depth 3,300ft)
Figure 24 – Damage to Allegheny during Lili (Caged Ladder)
Figure 25 – Damage to Allegheny during Lili (Handrails)
Figure 26 – Typhoon TLP (Payload 5,000 tonnes, Water Depth 2,100ft)
Figure 27 – Location of Lifeboats at Typhoon
Figure 28 – Damage to Lifeboats at Typhoon
Figure 29 – Damage to Lifeboats at Typhoon
Figure 30 – Damage to Lifeboats at Typhoon
Figure 31 – Prince TLP (Payload 4,000 tonnes, Water Depth 1,490ft)
Figure 32 – Location of Decks on Prince TLP
Figure 33 – Genesis Spar
Figure 34 – Location of Instrumented Brutus TLP Tendons
Figure 35 - Brutus’ Offset during Hurricane Lili
Figure 36 - Maximum Tendon Tensions
Figure 37 - Minimum Tendon Tensions
Figure 38 - Probability of T2 Peak Tension for TI 12
Figure 39 - Probability of T5 Peak Tension for TI 12
Figure 40 - Probability of T8 Peak Tension for TI 15
Figure 41 - Probability of T11 Peak Tension for TI 18
Figure 42 - Probability of T2 Minimum Peak Tendon Tension for TI 15
Figure 43 - Probability of T5Minimum Peak Tendon Tension for TI 15
Figure 44 - Probability of T8 Minimum Peak Tendon Tension for TI 18

Figure 45 - Probability of T11 Minimum Peak Tendon Tension for TI 15
Figure 46 – Example Surge PSD
Figure 47 – Example Surge PSD
Figure 48 – PSD for Tendon Tension (T2)
Figure 49 - Coherence between Tendons T5 & T11
Figure 50 - Coherence between Surge and T2 & T5 Average
Figure 51 - Surge Response Comparison
Figure 52 - Sway Response Comparison
Figure 53 - T2 Response Comparison
Figure 54 - T5 Response Comparison
Figure 55 - T8 Response Comparison
Figure 56 - T11 Response Comparison
Figure 57 - Spectrogram for T2 Tendon Tension
Figure 58 - T2 PSD including High Frequency Response
Figure 59 - Time Series of Tension Statistics
Figure 60 - T1 Peak Tension Distribution
Figure 61 - T5 Peak Tension Distribution
Figure 62 - Spectrograms for Typhoon's Tendons during Lili
Figure 63 - Spectrograms for Allegheny's Tendon Tensions during the Millennium Eddy

LIST OF TABLES

Table 1 – Floating Production Units near Lili's Track
Table 2 – Hindcast Environmental Conditions
Table 3 – Design Hurricane Environmental Conditions
Table 4 - Available Measured Data from Floating Production Units
Table 5 – Typhoon Equipment Damage during Lili
Table 6 – Genesis Equipment Damage during Lili
Table 7 - Brutus Instrumentation
Table 8 - Motion Statistics (Complete Time-Series)
Table 9 - Motions Statistics for 3 Hour TI
Table 10 - Tendon Tension Statistics (Complete Time Series)
Table 11 - Tendon Tension Statistics for 3 Hour TI
Table 12 - Measured Γ Values
Table 13 - Natural Periods at Relevant Load Condition
Table 14 - Wave Frequency Surge and Sway % Damping
Table 15 - Resonance Roll and Pitch % Damping
Table 16 - Tendon Tension Statistics for ETS

1. INTRODUCTION

1.1 Instructions

1.1.1 In response to Solicitation 1435-01-03-RP-70926 entitled 'White Papers – Hurricane Lili Impact on Offshore Operations', Global Maritime (GM) submitted to the Minerals Management Service (MMS) a White Paper entitled 'Assessment of Performance of Deepwater Floating Production Facilities'. In a letter dated January 27, 2003, the MMS requested GM to develop the work scope further and submit a proposal¹ for the work. The proposal was accepted and GM was instructed to proceed with the work on May 5, 2003.

1.2 Aims and Objectives of the Project

1.2.1 Several deep water floating production facilities are currently in operation in the Gulf of Mexico, with many more planned for the future. In general, the performance of such units has been adequate but some facilities in the Gulf of Mexico have experienced operational issues. Hurricane Lili provided an opportunity to verify the performance of deep water floating production units in the field during a major environmental event.

1.2.2 The present study collected and assessed information on the performance of deepwater production facilities that were impacted by Lili. The following specific objectives were pursued:

- Identify the units that were closest to Lili's track and most likely to be impacted by it.
- Collect information on any observed damage to such units and assess its significance. If significant structural damage was observed, identify potential abnormal loading (such as loss of air gap or collision) and failure mechanisms.
- Assess the environmental conditions during Lili and if these were of a sufficiently large magnitude to provide a meaningful test of the design of the units affected. Identify and collect any measured data that would assist in assessing the performance of the units. Verify if the performance of the units during Lili stayed within their design limits.
- Verify the data collected against current knowledge from the point of view of design environmental conditions and assess any safe / unsafe bias.
- Verify the data collected against current knowledge from the point of view of design response / performance models and assess any safe / unsafe bias.
- Review past operational experience and briefly document key issues of concern to the industry. These are understood to be prediction of meteorological data, its translation into design bases, and the impact of vortex shedding effects on the behavior of risers and TLP tendons as well as on the motions and therefore global performance of deepwater floating production installations. Assess if the data collected during Lili sheds new light into these issues.

1.2.3 Overall, the present study aims to provide further insight into these critical issues and develop recommendations for improvement in design and operation of deep water floating production installations.

1.3 Scope of Work

1.3.1 The approach taken in this project consists of the following tasks:

1.3.2 **Task 1 – Data Collection.** This task involves gathering available information on the performance of the relevant installations during Hurricane Lili including:

- a) Monitoring data such as environmental data, motions, tendon tensions (for TLPs), etc.
- b) Inspection reports and any other information concerning damage observed due to Lili.

1.3.3 **Task 2 – Review of Collected Data.** This task includes an evaluation of the information gathered for use in the assessment of the performance of the systems considered.

1.3.4 **Task 3 – Review of Monitoring Data.** This task covers an evaluation of the cases where good quality monitoring data was recorded for further analysis and interpretation. Also gather more detailed information on the installations considered to permit such an analysis.

1.3.5 **Task 4 – Analysis of Monitoring Data.** For the cases considered in Task 3, perform analyses of the monitoring data to verify measured global performance against expected performance based on design results. Verify design approximations and identify areas where further work would be recommended such as in validating computational analyses and other design procedures.

1.3.6 **Task 5 – Guidelines and Procedures.** Based on the previous tasks, propose modifications to current design / assessment guidelines. Also suggest monitoring, inspection, refurbishment and maintenance options that would contribute to improve future performance.

1.3.7 Task 6 – Meetings.

1.3.8 **Task 7 – Model Validation.** This task will develop global performance computer models for the cases considered in Tasks 3 and 4 and compare numerical predictions with the actual performance of the installation. The results from such comparison will be used to help indicate modifications in analytical procedures that would improve their abilities to determine realistic performance characteristics.

1.3.9 **Task 8 – Revisit Guidelines and Procedures.** Revisit the results and conclusions of Task 5 based on the results and conclusions of Task 7.

1.3.10 The project will consist of two phases. This report corresponds to Phase 1 which has been sponsored by the MMS and covers Tasks 1 to 6 above.

1.3.11 Phase 2 will cover Tasks 7 and 8 and will require additional funding, perhaps on a joint

industry project (JIP) basis. The scope of work for this phase will be developed further once data from Phase 1 has been collated and reviewed.

1.4 Outline of the Report

- 1.4.1 Section 2 gives the background to the present study in terms of similar work carried out in the past for fixed platforms under hurricane conditions and in terms of the design standards and operational issues for floating production units that motivated the present study.
- 1.4.2 Section 3 covers the environmental conditions during Lili and comparisons with environmental design criteria. Section 4 gives some of the main particulars of the units and summarizes the results of the post-hurricane inspections of such units. Sections 5 and 6 cover the analysis of monitoring data for the Brutus and Typhoon units. Section 7 gives conclusions and recommendations.

2. BACKGROUND

2.1 Historical Perspective

2.1.1 The Gulf of Mexico pioneered offshore exploration and production with offshore platforms installed as early as the 1940's and now hosts over 4,000 offshore platforms. Operations in the Gulf of Mexico are, from time to time, challenged by hurricanes. Notable major events that had an impact on the offshore industry were hurricanes Hilda (1964) and Camille (1969), followed by more recent events such as hurricanes Juan (1984), Andrew (Figure 1, 1992) and now Lili (2002). Hurricane Roxanne (1994) had a major impact on operations offshore Mexico.

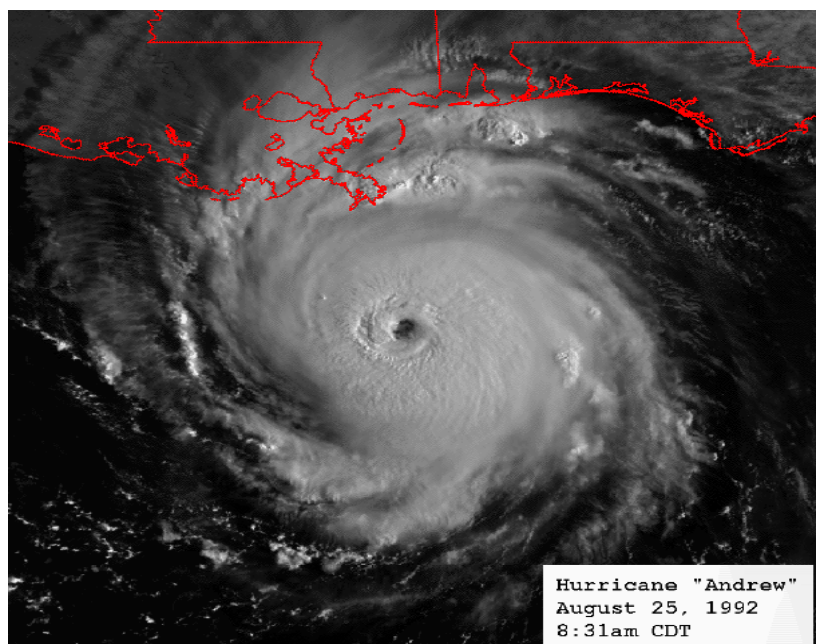


Figure 1 –Hurricane Andrew (from National Climatic Data Center)

2.1.2 The cooperative efforts of government and industry over the past 35 years permitted dramatic improvements in the modeling of the surface marine meteorological characteristics of Gulf of Mexico hurricanes and the corresponding ocean response to their passage. Such studies took advantage of measurements taken during the above mentioned events as well as during other events such as Audrey (1957), Bertha (1957), Carla (1961), Edith (1971), Delia (1973), Frederic (1979), Danny (1985) and Georges (1998). A summary of such work is given by Cardone et. al.² discussing major programs such as the 1969-1971 Ocean Data Gathering Program³ (ODGP) for winds and waves, the 1974-1977 Ocean Current Measurement Program (OCMP) for continental shelf currents, the Hurricane Andrew hindcast study⁴ and the GUMSHOE JIP⁵.

2.1.3 The effect such events had on offshore operations was also studied and improvements to design standards were developed. In the US, the industry responded to such events with

significant work⁶⁻⁹ carried out by JIPs, Universities, R&D work within the oil companies and by studies and workshops supported by the MMS, API and other organizations. Hurricane Andrew, in particular, spurned a great deal of performance studies since it was a large storm which in some regions exceeded the API RP 2A¹⁰ recommended design wave criteria for new structures (based on a 100-year return period load which, by definition, has a 1% probability of exceedance in every given year). As a consequence, 27 steel jackets either failed or were damaged and 43 caissons either toppled or were damaged.

- 2.1.4 Significant improvement in design and assessment standards accrued from such studies. The first Edition of API RP 2A was issued in 1969 and its ninth Edition in 1978. Hurricane Andrew provided evidence¹¹ of the increased reliability of fixed platforms designed after the mid-seventies. The latest Edition of API RP 2A (21st) was issued in 2000 incorporating consequence-based criteria for the design of new structures.
- 2.1.5 The assessment of existing fixed structures has also benefited from these studies. This is an important development as there are now over 1,200 of such platforms exceeding 20 years of age. These units were designed according to the practices of their time which were different from the improved standards adopted in the design of new structures. Re-assessment and re-qualification criteria were incorporated into API RP 2A in 1997 in Supplement 1, Section 17 for re-assessment of existing structures. The industry continues to work on these issues as shown in the recent MMS Workshop on Assessment of Existing OCS Platforms¹² and the recent formation of an API Committee to improve Supplement 1, Section 17 of API RP 2A.
- 2.1.6 The overall result of such efforts has been an improvement in the reliability of platforms designed after the mid-1970s and a more rational risk-based approach to the integrity management of older platforms designed prior to the mid-1970s.
- 2.1.7 Significant work^{11,13-16} along the same lines was carried out in other countries such as Mexico, UK and Norway which has also given a significant contribution to the improvement of design and assessment standards. Draft ISO standards now exist for metocean conditions (19901-1) and for the design of fixed steel platforms (19902) with completion scheduled for early 2005 and early 2006 respectively.
- 2.1.8 In recent years exploration and production has been steadily moving into deep water. In the Gulf of Mexico there are currently 30 production units in over 1000ft of water depth, with many more to be added in the future. It has been widely reported (e.g. Houston Chronicle, 03/14/04, Business, page 7D) that, according to the MMS, a record number of drilling rigs were working in ultra-deep water in the Gulf of Mexico. For the first time, a dozen rigs were drilling for oil and gas in 5,000ft of water or greater. Deepwater production rose 535 percent between 1995 and 2002, while deep water gas production rose 620 percent in those same years. Several oil and gas discoveries have been announced in water depths greater than 5,000ft, including five in 2001, three in 2002 and six in 2003.
- 2.1.9 The same trend for deep water exploration and production can be seen on a worldwide basis, particularly in Brazil and West Africa. PEMEX, Mexico's state energy company, is seeking technology alliances that could help it explore its reserves in deep water in the near future (Houston Chronicle, 03/14/04, Business, page 7D). Such worldwide developments

are significant for the U.S. both as a consumer of oil and natural gas from worldwide markets and as a provider of know-how, equipment and services for international oil and natural gas exploration and production.

2.1.10 It is therefore important that the combination of government and industry sponsored programs that had a significant impact on improving the reliability of shallow water production platforms is continued and improved for the developments in deep water.

2.2 Performance and Reliability of Floating Production Facilities

2.2.1 The global performance of the early TLP structures (Hutton, Heidrun and Snorre) was investigated¹⁷⁻²⁰ under operating conditions and winter storms and concluded to be within design expectations. On a worldwide basis the reliability of TLPs has been extensively investigated and many publications by well-known experts in the field of structural reliability can be found in the open literature²¹⁻⁴⁰. Hurricane Lili provided a unique opportunity to investigate the response of such structures to a major event such as a hurricane.

2.2.2 A pioneering effort in standard development for deepwater structures was the TLP Model Code⁴¹, which was a JIP organized in early 1991 and managed by Conoco which investigated several global response and local structural failure modes, their corresponding load effects and design reliabilities. Follow up work led to the early development of the API Bulletins 2U⁴² and 2V⁴³ which address stiffened cylinders and stiffened plates respectively and have recently upgraded^{44, 45}. Such work provided a useful input to the development of standards for TLP design such as API RP 2T⁴⁶. The development of a separate ISO standard (19904-2) for TLPs is presently under consideration.

2.2.3 API has devoted a significant effort to the development of standards for deep water floating production systems and components such as API RP 2FPS⁴⁷ for floating production systems (ship-shaped, semi-submersibles and spars), API RP 2SK⁴⁸ for station-keeping systems and API RP 2RD⁴⁹ for production risers in floating production systems and TLPs. Significant work has also been carried out at an international level and ISO standards are currently being drafted for Stationkeeping (ISO 19901-7) and Floating Production Systems (ISO 19904-1).

2.2.4 Despite such advances, it is noted that deepwater production facilities in the Gulf of Mexico have experienced operational issues and there is concern over the prediction of meteorological data and its translation to design bases. There is also concern over vortex shedding effects on the behavior of risers, tendons and pipelines as well as on the global motions and therefore global performance of deepwater structures. These are complex issues that affect different platforms in different ways as discussed in the next sections.

2.3 Meteorological Data

2.3.1 The development of accurate design current profiles is of key importance for deep water floating production systems.

2.3.2 Hurricanes have traditionally governed the design of production units in the Gulf of Mexico in shallow waters. These are tropical revolving storms, which may hit the Gulf coast between June and November. The forcing from the hurricane wind fields produce random waves as well as wind-driven surface currents. The surface currents dominate over the top mixed layer near the surface, which then transitions into lower layers with reduced current velocities.

2.3.3 Figure 2 shows typical design current profiles. A slab-type profile such as Design Profile 2 in Figure 2 is given by API RP 2A¹⁰ and has been applied in comparative studies⁵⁰ and also extensively used in the design of platforms in the Gulf of Mexico. The mixed layer depth (of the order of 250 ft) and current velocity (of the order of 1.9-2.0 knots) are based^{51,52} on regression statistics applied to results of numerical models calibrated against major events such as Betsy, Camille and Carmen. A sheared profile such as Design Profile 1 has been applied to response-based studies⁸⁷ and preferred in more recent platform designs.

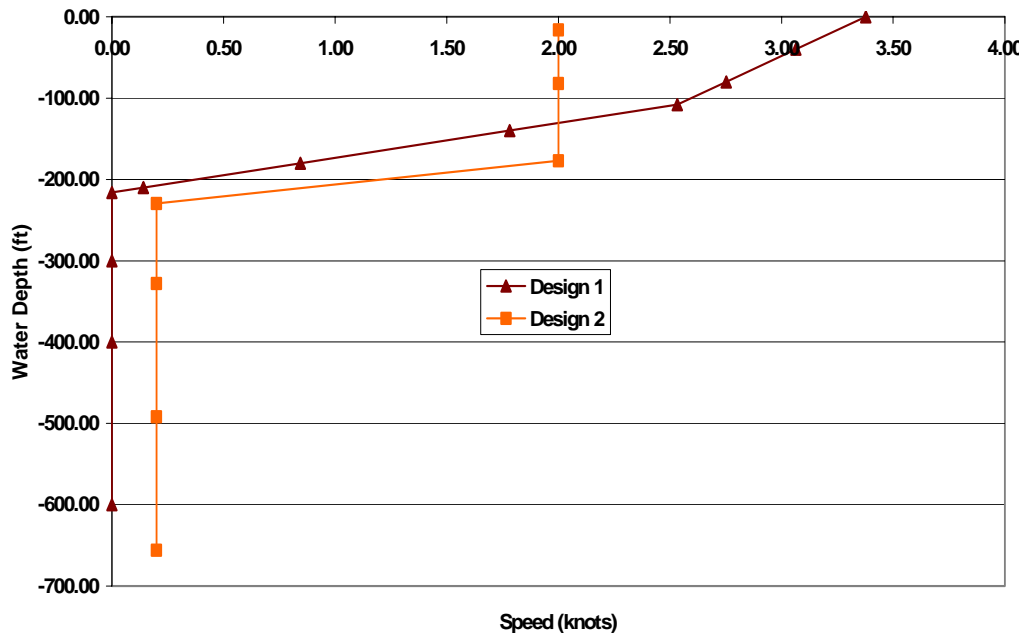


Figure 2 – Sample Design Current Profiles

2.3.4 The analysis of time-series of data from hurricanes indicates^{51,67} that current oscillations of an inertial nature will result from the hurricane's peak wind forcing. The first peak in mixed layer current velocity occurs some hours after the passage of the hurricane but a second peak occurs some 24 hours later. It has been stated⁵⁰ that, for a spar that experienced VIM under hurricane currents in the Gulf of Mexico, the largest VIM occurred only after waves and winds had subsided significantly.

2.3.5 Loop and Eddy currents are also of primary importance to the design of deep water floating production facilities. These are illustrated in Figure 3.

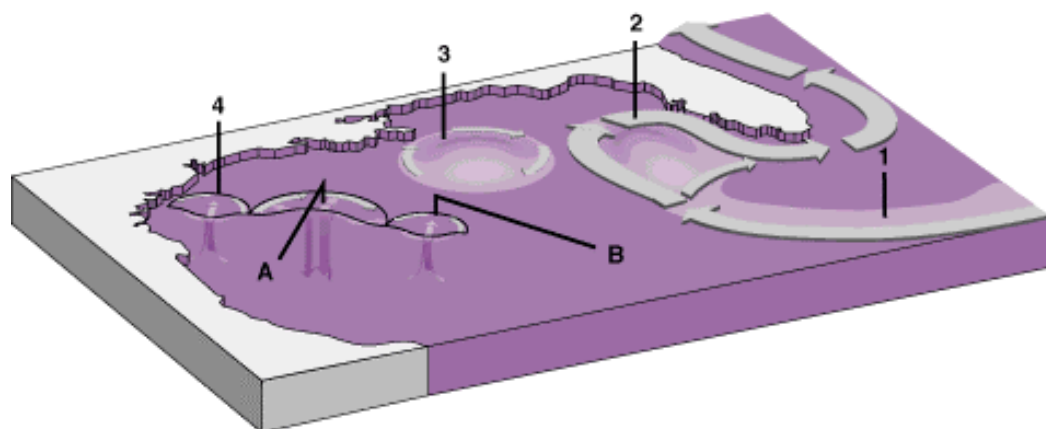


Figure 3 – Loop and Eddy Currents⁵³

2.3.6 Loop and Eddy currents form as follows:

1. Warm water from the Caribbean Sea enters the US Gulf of Mexico through the Yucatan Strait and exits by the Florida Strait.
2. A clockwise flow called Loop Current gradually forms in the Eastern US Gulf of Mexico. Eventually, the loop breaks off and forms an eddy.
3. The eddy has a core of warm water that rotates clockwise as it moves west across the gulf. Clockwise-rotating eddies in the northern hemisphere are called anticyclones (see 'A' in Figure 3).
4. Smaller Eddies spin off the warm anticyclones. These rotate in the opposite direction, attract cooler water from the deep Gulf and are called cyclones (see 'B' in Figure 3).

2.3.7 The Loop / Eddy currents persist for long periods of time and may have high surface current velocities which extend deep into the Gulf. It is not uncommon that surface current velocities of 5 knots are reported from visual observations. However, visual observation are prone to error and it is understood that reliable measurements⁵⁴ as well as analyses⁵⁵ based on measured TLP offset and setdown tend to support values in the range of 3.5 - 4.0 knots.

2.3.8 **Effect of Eddies on Hurricanes.** A warm eddy such as the ones present in the Gulf can be a major source of energy to a storm that passes over it. Normally, hurricane winds draw the heat stored in these pockets of ocean water to fuel the storm. At the same time the winds may also mix the warm surface water with cooler water below as the storm passes by and the upwelling of cool water by the wind can weaken slow-moving storms. However, the layer of warm water in the eddy is so thick that the ocean surface is less susceptible to storm-induced cooling than it is outside the eddy.

2.3.9 The extra heat often gives hurricanes a burst of energy that can lead to rapid intensification. This is believed⁵⁶ to have happened in early October 1995, when Hurricane Opal intensified over the central Gulf of Mexico from a 95-mph Category 2 hurricane to a Category 4 hurricane with 150 mph winds in only 14 hours. This effect has led to the postulated

‘Hurricane Alleys’, or areas that would be more prone to the formation of more intense hurricanes as these pass over warm eddies⁸⁸.

2.4 Impact of High Currents on Deep Water Operations

2.4.1 High currents are known to have impacted Gulf of Mexico operations in the following areas: station keeping, running of riser / BOP / ROV, offshore installation, riser flex joint angle, pipelaying, mooring / riser loads, fatigue / VIV of offshore components.

2.4.2 The potential impact of current velocities of 3 - 4 knots can be seen from the typical figures below concerning limits for marine operations⁵⁷:

- Drilling riser running and retrieval are usually limited to about 1 knot (without fairings)
- Production riser running and retrieval typically limited to 0.6 – 0.9 knots
- Platform installations such as deck mating limited to less than 0.6 knots
- Installation of TLP tendons may be limited to 0.6 knots unless surface roughness is sufficiently low
- Diving operations are limited to 0.5 knots⁵⁸.

2.4.3 Reporting of costs due to downtime in such operations are not common in the open literature but the following was found:

- British Borneo reported⁵⁴ the shutdown of deepwater operations at Ewing Bank 965 due to a Loop Current event contributed to a US \$20 million increase in development costs for the Morpeth field.
- Riser VIV was observed⁵⁹ in the Prince TLP during a Loop Current event on March 2002 with some damage to the passive riser tensioning system for one of the wells.
- The Millennium Eddy in 2001 induced VIV on the tendons of the Allegheny mono-column TLP, which caused vibrations on the entire structure for several weeks⁵⁵. Some structural details were reinforced⁶⁰ to preserve the fatigue life. There was also damage to the riser suppressors. Indication of riser clashing was found in inspections after Hurricane Lili but it is unclear if the damage took place during Lili or during the Millennium Eddy as no inspections had been carried out between these events.
- It has been reported⁵⁸ that in 2003 the loop current shed an eddy that, in conjunction with other events such as Tropical Storm Bill and Hurricane Claudette, affected six major deepwater installation projects. The main problem caused by the eddy was the inability of the installation equipment to operate in the high current, specifically remote operated vehicles (ROVs) and in some cases heavy lift vessels. Some of the reported side-effects included:
 - Installation work on BP’s NaKika was delayed a week while waiting for more

moderate currents and hurricane Claudette to pass by.

- Completion of the tendon installation for Total's Matterhorn TLP was delayed six weeks due to strong eddy currents and the impacts of tropical storm Bill and hurricane Claudette.
- During a storm evacuation caused by tropical storm Bill, the high currents contributed to the parting of a tug tow line on Dominion's Devils Tower spar causing the unit to drift under control of two tugs off location. Once the hull returned to the installation site, the current caused the spar to list 8° from vertical and installation was further delayed until currents subsided.
- Heerema's Balder experienced several delays while waiting to complete BP's Mardi Gras pipeline, in turn delaying other operations scheduled for the deepwater construction vessel on projects such as NaKika, Matterhorn, Kerr-McGee's Gunnison spar and Anadarko's Marco Polo TLP.
- It has recently been reported⁶¹ that, in a 24-day operation, Shell Global Solutions (US) Inc. has recently completed the industry's first replacement of vortex-induced vibration (VIV) helical strakes with patented ROV retro-fit fairings along a 595-ft. stretch of catenary pipeline riser on Murphy Oil Corporation's Medusa SPAR, located at 2250 ft water depth in the Gulf of Mexico.
- A line tensioning procedure⁹¹ had to be developed to mitigate the effect of Vortex Induced Motions (VIM) on ChevronTexaco's Genesis spar.

2.5 Vortex Shedding Effects and Vortex Induced Vibration (VIV)

2.5.1 As the fluid flowing around a bluff (non-streamlined) body intensifies (increased Reynolds number) the phenomenon of vortex shedding takes place, where vortices form downstream of the body. The non-dimensional shedding frequency (or Strouhal number) is simply described as follows:

$$St = f_v D / U \quad (1)$$

Where f_v is the frequency of vortex shedding, D is the body's diameter and U is the mean fluid velocity.

2.5.2 Early experiments⁶² have shown that the Strouhal number tends to remain constant at a value of 0.2 for a Reynolds number in the range of 300 to 200,000. It follows that vortex shedding will induce harmonic loading normal to the direction of the current flow at a frequency $f_v = 0.2 U / D$. For lightly damped or flexibly mounted bluff bodies in a flow, resonance may occur when the frequency of excitation f_v approaches the natural frequency of the body and its mountings as well as sub-harmonics associated with such frequency.

2.5.3 As a consequence of vortex shedding induced resonance, the body oscillations can reach sufficient amplitude such that the body and wake oscillation frequency take on the same

value (lock in phase). Large amplitudes of oscillation may be induced when interaction between the fluid flow and the structural motion cause such a 'lock-in' effect.

2.5.4 For a circular cylinder lock-in effects produce a substantial increase in not only the oscillatory lift force, but also in the mean drag force. Such increased drag and high-amplitude resonant behavior can have a significant impact on the fatigue and failure of a structure.

2.5.5 The most common offshore structural components subject to VIV are marine production and drilling risers, steel catenary risers (SCR) and top tension risers in particular. In flexible risers, the inherent damping of the composite cross section may reduce problems associated with VIV.

2.5.6 There are added complexities for deep water risers where VIV may excite high structural modes which are associated with higher curvature. For SCRs, the critical point for VIV induced fatigue failure may be the seabed Touch Down Point (TDP) where the interaction of the SCR with the seabed is highly non-linear.

2.5.7 VIV is a key design aspect in regions of high current (in excess of 2 knots) such as the Gulf of Mexico, Campos Basin offshore Brazil, the northern region offshore Brazil exposed to the Guyana current, West Africa and West of Shetlands. The Eddy currents that form in the Gulf of Mexico may extend deep into the water column and can be a matter of concern.

2.5.8 At present riser VIV tends to be mitigated using VIV-suppressors such as fairings and helical strakes that are attached to the riser and provide some control over the vortex shedding process. However, such suppressors may also increase drag.

2.5.9 Avoidance of VIV in risers and other structures such as TLP tendons has been an elusive target for designers, especially in deepwater environments where the effects are particularly complex. The main factors that contribute to the uncertainties in design include:

- Long-term measurements are necessary to validate current profiles extending deep into the water column for VIV prediction.
- Empirical or semi-empirical solutions based on modal analysis are often used to predict VIV and may not fully capture the complex interaction between fluid loading and structural response.
- Interpretation of scaling effects on model test data and the effects of small geometrical imperfections are also complex issues.
- Adjacent risers interact when subject to current and may oscillate and collide.
- Fatigue damage and failure in itself is an area prone to uncertainty.

2.5.10 It is clear from Equation 1 that, as fluid velocities increase, larger diameter structures also become prone to vortex shedding effects. On a larger scale, spar hulls have been subject to VIM that was not fully anticipated in design with knock-on effects on their global

performance including structure, mooring system and risers. VIM has been the subject of intense research and the MMS has recently sponsored a seminar⁶³ and on going work on the subject.

2.6 ‘Traditional’ Global Performance Analysis of Floating Systems

2.6.1 The issues of current prediction, VIV and VIM have gained much attention during recent years. However, as previously noted, Lili provided a unique opportunity to verify the more traditional but equally important aspects of Global Performance Analysis (GPA) which forms a significant part of the design process for floating systems. GPA permits design estimates of the following:

- Maximum Motions, Offset, Set-Down
- Minimum Air Gap
- Maximum Inertial Loads
- Maximum and Minimum Tendon Tensions
- Mooring Line Loads
- Riser Loads
- Tendon Fatigue Life
- Global Loads for Structural Assessment

2.6.2 In developing a GPA, design approximations need to be made to model critical aspects of the response of such structures. Monitoring data provides an opportunity to benchmark such design assumptions against data on the field for a major environmental event.

3. ENVIRONMENTAL CONDITIONS DURING HURRICANE LILI

3.1 Hurricane Lili's Track and Intensity

3.1.1 Hurricane Lili's best track is shown in Figure 4. It was the most intense hurricane of the 2002 season and developed in late September, though it did not reach peak intensity until early October. It began as a tropical depression on September 13th, 2002 approximately 1,000 miles west of the Lesser Antilles. By the 23rd, Lili had moved across the Windward Islands as a tropical storm. As it moved across the Caribbean, Lili fluctuated in intensity and was a Category 1 hurricane near western Cuba on October 1st. It came ashore on Thursday 3rd October in southwest Louisiana (on the west side of Vermillion Bay) as a Category 2 hurricane.

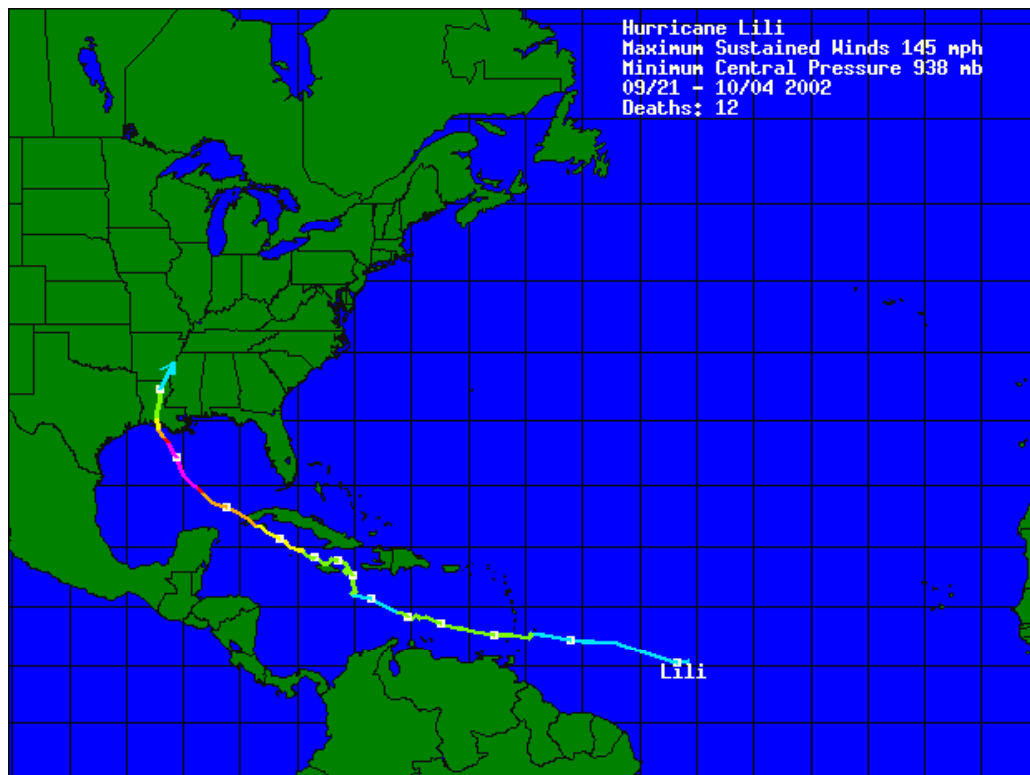


Figure 4 –Hurricane Lili Track (National Hurricane Center's Best Track)

3.1.2 After reaching wind speeds of 145mph (Category 4) on the 2nd (Figure 5, from the National Oceanic and Atmospheric Administration Website) and maintaining intensity into the 3rd, it suddenly lost intensity and was a much weaker hurricane by landfall. Still a powerful storm, it led to widespread damage, flooding and power outages. At least 13 deaths have been attributed to Lili, most of them occurring as it crossed the Caribbean. Four people died in Haiti as Lili's outer rain-bands caused torrential rain and mudslides, while seven victims were reported in Jamaica and one death each in Cuba and the United States have been blamed on the storm. Damage costs for Louisiana alone have been estimated at approximately \$170 million.

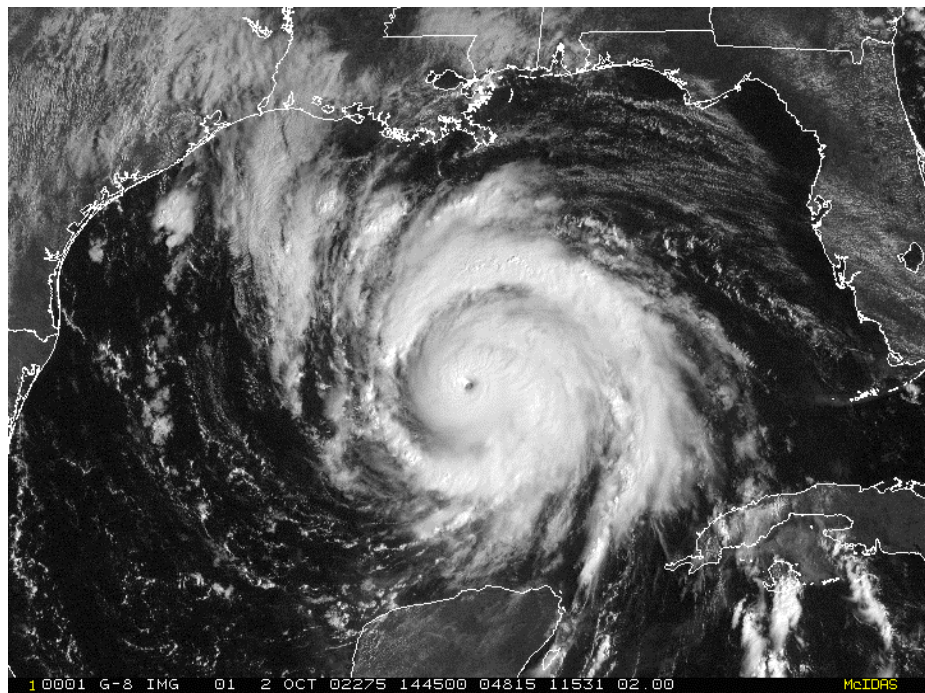


Figure 5 – Hurricane Lili, October 2nd 2002

3.1.3 Hurricane Lili caused significant damage to some fixed offshore production platforms, Figure 6, as well as to mobile drilling units.

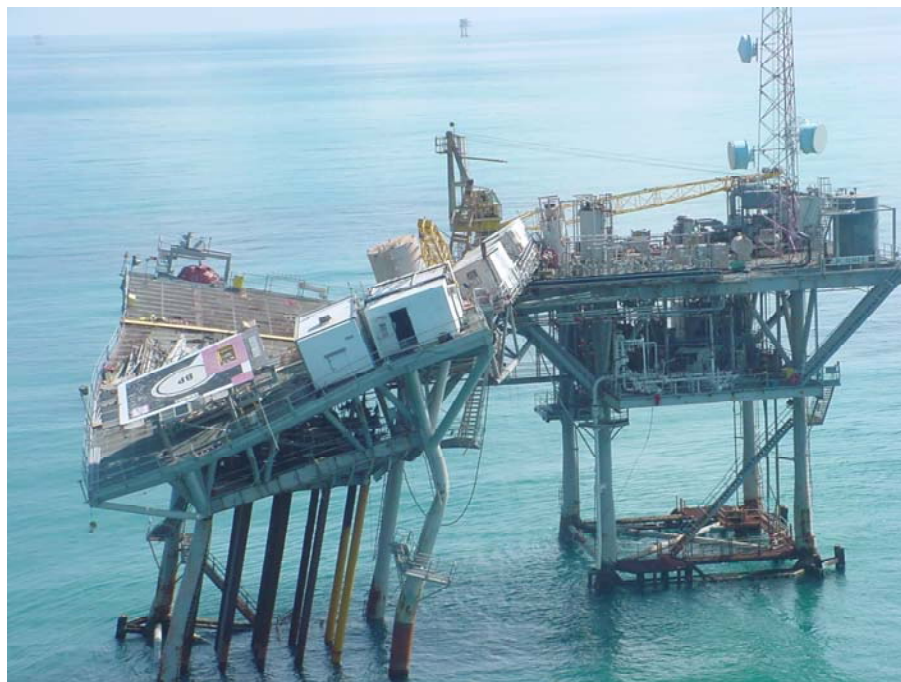


Figure 6 – Fixed Platform Damaged by Hurricane Lili

3.1.4 Lili was still a Category 4 hurricane while over the north-central Gulf of Mexico and during the early hours of October 3rd, 2002 it passed through the Green Canyon and Eugene Island areas, impacting several Tension Leg Platforms (TLPs) and a Spar, Figure 7 and Table 1.



Figure 7 –Deep Water Platforms in Lili’s Vicinity

Table 1 – Floating Production Units near Lili’s Track

| Floating Production Unit | Type | Operator |
|--------------------------|-----------------|---------------|
| Typhoon | Mono-Column TLP | ChevronTexaco |
| Morpeth | Mono-Column TLP | ENI Petroleum |
| Allegheny | Mono-Column TLP | ENI Petroleum |
| Jolliet | 4-Column TLP | Conoco |
| Genesis | Spar | ChevronTexaco |
| Brutus | 4-Column TLP | Shell |
| Prince | MODEC TLP | El Paso |

3.1.5 A hindcast study² permitted the maximum environmental conditions such units were exposed to be estimated and the results are given in Table 2.

Table 2 – Hindcast Environmental Conditions²

| Hindcast | | | |
|---------------|---------------|-----------------------|-----------------|
| Floating Unit | Wind* (knots) | Sig. Wave Height (ft) | Current (knots) |
| Typhoon | 71.22 | 37.04 | 2.15 |
| Morpeth | 43.17 | 30.11 | 1.98 |
| Allegheny | 50.13 | 33.30 | 1.83 |
| Jolliet | 50.30 | 30.97 | 1.53 |
| Genesis | 54.46 | 35.11 | 2.50 |
| Brutus | 59.83 | 36.75 | 1.80 |
| Prince | 46.13 | 32.09 | 2.00 |
| Buoy 42041 | 64.98 | 37.73 | - |

*1/2-hour mean at 10m above sea level

3.1.6 The values in Table 2 were obtained from the hindcast gridpoints considered to be closest to the position of the production units. It is noted that the location of the units do not necessarily match the location of the hindcast gridpoints and the values in Table 2 are subject to some interpretation and uncertainty. For example, the peak environmental conditions for Typhoon in Table 2 correspond to a gridpoint at 27.75 N & 91.10 W. For a gridpoint at 27.75 N & 91.125 W, the corresponding environmental conditions are 75.10 knots wind, 38.60 ft significant wave height and 1.84 knots surface current.

3.1.7 Table 3 gives sample design hurricane environmental criteria for different return periods based on two production units in relatively close proximity. The 25-year return period value, by definition, has a 4% (1/25) probability of exceedance in every given year.

Table 3 – Design Hurricane Environmental Conditions

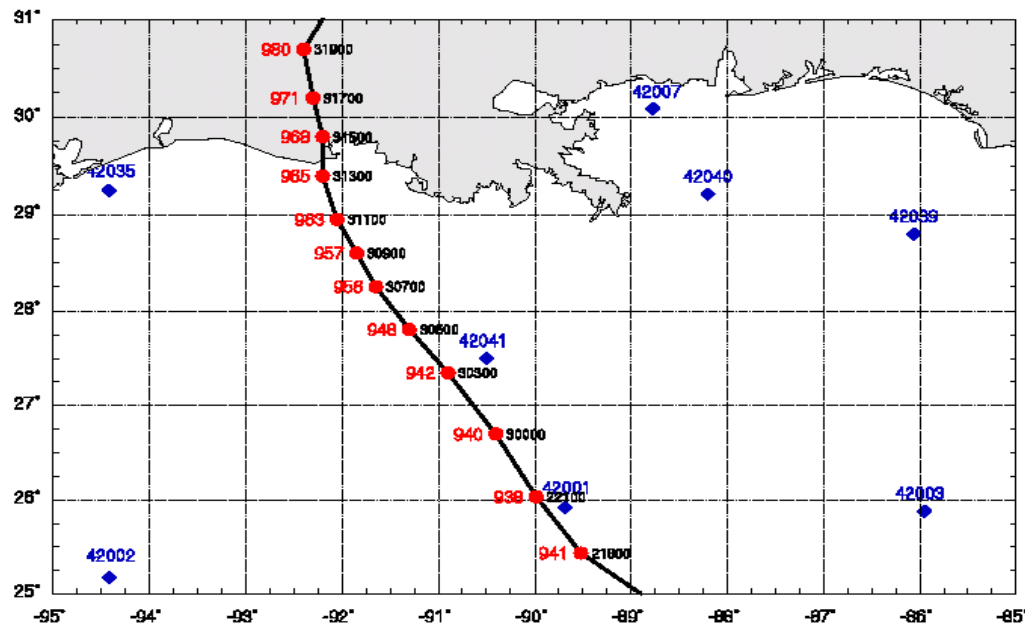
| Return Period (Years) | Wind* (knots) | Signif. Wave Height (ft) | Associated Surf. Current (knots) |
|-----------------------|---------------|--------------------------|----------------------------------|
| 10 | 49.2 | 25.6 | 1.2 |
| 25 | 55.7 | 31.0 | 2.6 |
| 100 | 71.0 - 72.9 | 39.0 - 40.0 | 2.0 - 3.4 |
| 1000 | 83.0 - 83.6 | 47.0 - 48.5 | 2.3 - 4.1 |

*1-hour mean at 10m above sea level

- 3.1.8 The Typhoon Mono-Column TLP was in close proximity of Lili's track and the hindcast environmental conditions for this unit were fairly close to typical 100-year design values of wave, wind and current.
- 3.1.9 The hindcast values also suggest that the environmental conditions during Hurricane Lili were sufficient to test the response of both the Brutus TLP and the Genesis Spar vis-a-vis their relevant design events.

3.2 Hindcast Study by Oceanweather Inc.

- 3.2.1 It is noted that the data in Table 2 is based on the hindcast study² by Oceanweather Inc. The hindcast model took advantage of considerable experience from previous projects as outlined in Section 2.1 and discussed in more detail in the literature².
- 3.2.2 The ocean response modeling used rests critically on the accuracy of the wind fields that force the models (and thus generate waves and current). As far as winds and waves are concerned, the hindcast study collected a wealth of data² ranging from aircraft reconnaissance to measurements from the buoys of the National Data Buoy Center (NDBC) which provided unique measurements of the profile of surface winds and sea state in the inner core of Lili.
- 3.2.3 Hurricane Lili's track relative to the NDBC buoys is shown in Figure 8. One of such buoys (42041) is included in Figure 7 and Table 2. This buoy was approximately 15 nautical miles of the northeast side of Lili's track and some 16-17 nautical miles from both the Genesis spar and the Allegheny mono-column TLP. Overall the hindcast model was able to accurately predict winds and waves during Lili²: at the two buoys near the track the bias in significant wave height and period was 0.1m and 0.2 sec respectively and the correlation coefficient was 0.95 and 0.98 respectively.



Track of Lili in Northern Gulf with fix time (black, GMT, DDHHMM format), central pressure (red, mb) and NDBC buoy locations (blue).

Figure 8 –Buoys near Lili’s Track²

3.2.4 A state-of-the-art model was used to hindcast currents but there were no public domain measurements of currents during the passage of Lili to validate it to the same extent that was possible for winds and waves. The hindcast study did not have access to the field measurements taken at the production units and made available to this project, Table 4. The implications of such measurements are discussed in the following Section.

Table 4 - Available Measured Data from Floating Production Units

| FPU | Wind | Wave | Current | Motions | Tendon Tension |
|---------|------|------|---------|---------|----------------|
| Typhoon | - | - | | - | Yes |
| Genesis | - | - | Yes | - | - |
| Brutus | Yes | - | | Yes | Yes |

3.2.5 It is noted that no monitoring data was available for Joliet as the monitoring system was not operational during Lili. This also happened for the Allegheny and Prince TLPs and for the Genesis Spar. Unfortunately valuable monitoring data was not recorded when such platforms were subject to a significant design event. A contributing factor for this occurrence was that these units were evacuated during Hurricane Isidore and powering of the monitoring system had not been restored (or failed) during Lili. It is understood that some units are currently upgrading the batteries that power their monitoring systems.

3.3 Maximum Winds and Seastates

- 3.3.1 Direct wind measurements for Lili were available from the Brutus TLP as well as from the National Data Center Buoys. The buoys, 42001 and 42041, measured the winds 10 and 5 meters above the sea surface respectively. As previously discussed, buoy 42041 was approximately 15 nautical miles of the northeast side of Lili's track and some 16-17 nautical miles from both the Genesis spar and the Allegheny mono-column TLP.
- 3.3.2 At Brutus, winds were measured with two anemometers: Anemometer 21 which is mounted at the boom rest of crane number 3 and Anemometer 31 which is mounted on the derrick crown. Anemometers 21 and 31 are located at 278 and 350 feet above the keel, Figure 9 (188ft and 260ft respectively above the sea surface based on the nominal draft of 90ft).
- 3.3.3 The time-series of wind measurements from Anemometers 21 and 31 was processed in MATLAB to obtain ½-hour and 1-hour mean wind velocity values. For comparison with the hindcast data and with design data the results were converted to ten meters above mean sea level based on the 'API' wind profile (which is the wind profile contained in API RP 2A up to the 20th Edition and used on a large number of existing platforms). The maximum values were also evaluated based on the 'NPD' wind profile (which refers to the Norwegian Petroleum Directorate and was incorporated on the 21st Edition of API RP 2A).
- 3.3.4 Figure 10 shows good agreement between the hindcast and the measurements for Buoy 42041 in terms of winds and seastates. The results of the hindcast model for the Buoy 42041 location show the maximum wave height and wind speed at that location during the early hours of October 3rd, 2002 at around 3:00am GMT. A peak significant wave height of 33.1ft was measured at 1:00am GMT. A larger significant wave height of 40.4ft was measured at 3:00 GMT but later dropped by NDBC due to quality control concerns. Further contact with NDBC indicated that this higher significant wave height value is reasonable but was not considered 100% reliable due to signal parity problems.



Figure 9 – Brutus TLP

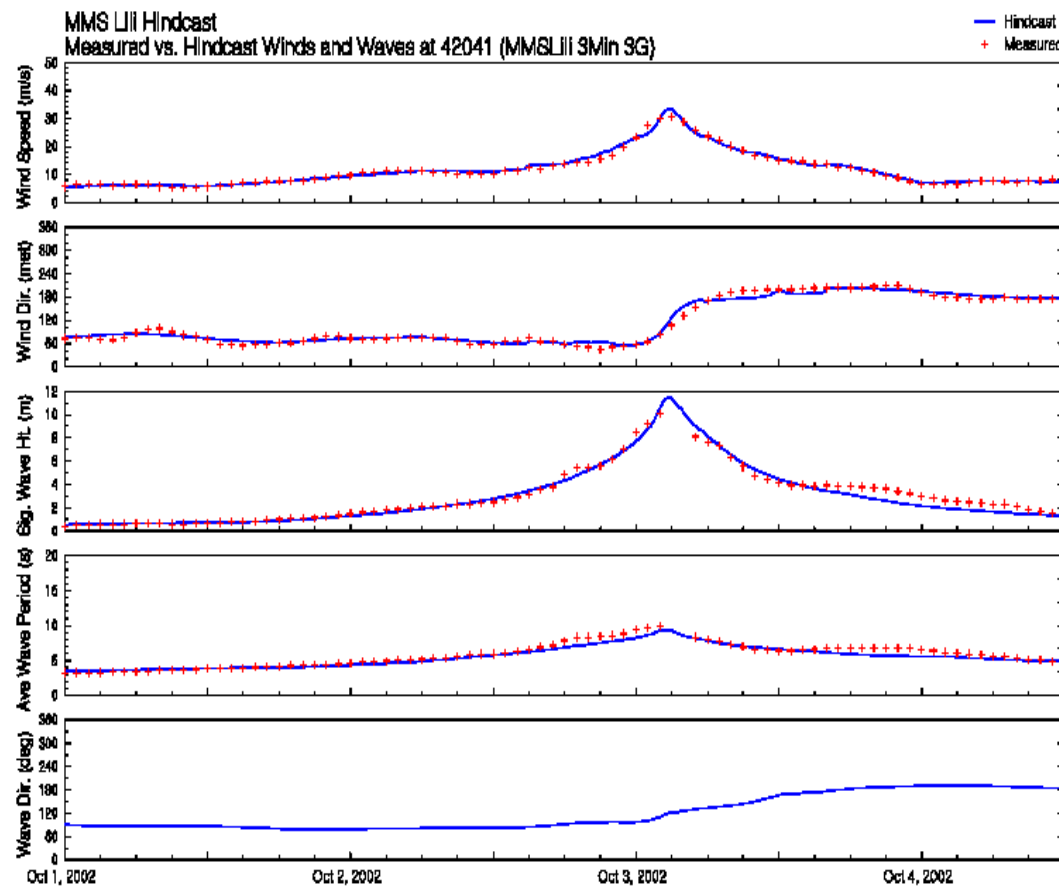


Figure 10 –Data for Buoy 42041²

3.3.5 Unfortunately, lightning damaged the wave probe at Brutus and no measured wave data is available from any of the floating production units.

3.3.6 The wind measurements at Brutus (recorded according to Central Standard Time) indicate peak winds occurring at around 4:00 am GMT (22:00 pm CST). It can be observed that peak wind speeds were only sustained for a period of about 2.0 hours as shown in Figure 11 and not 3.0 hours as usually adopted in design.

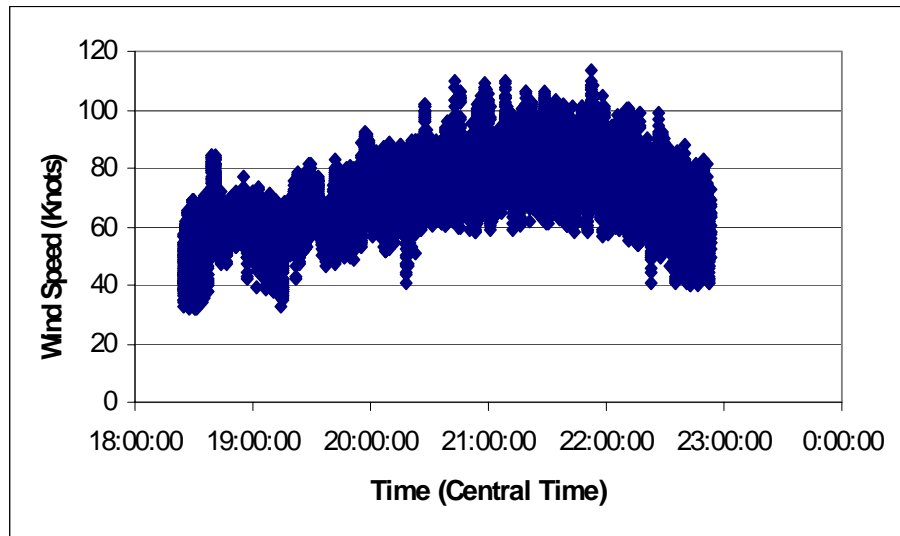


Figure 11 – Time Series, Wind Speed, Anemometer 21 (from 0:00 am GMT to 6:00 am GMT)

3.3.7 According to the hindcast, Lili passed almost directly over Typhoon, with peak winds at around 5:00am GMT. The blue arrows in Figure 12 correspond to wind and the red arrows correspond to waves. It is understood⁶⁴ that the platform data (not shown in Figure 12 but discussed further in this report) was recorded in Central Daylight Time (GMT – 5 hours).

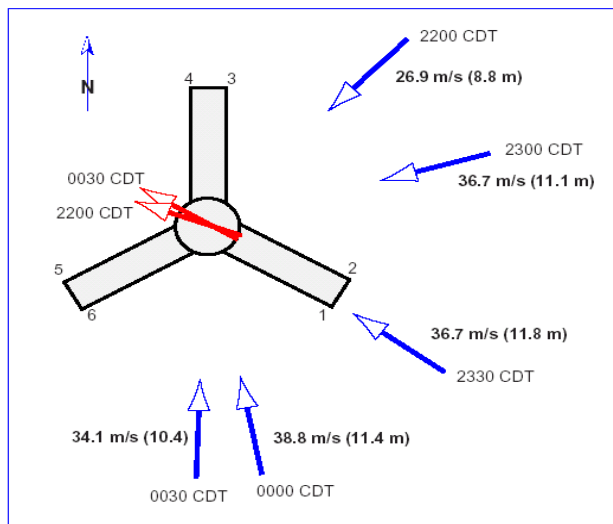


Figure 12 – Summary of Hindcast Peak Winds and Seastates for Typhoon⁶⁴

3.3.8 The 1/2-hour mean wind velocity at ten meters above sea level was estimated from the wind velocities measured by the anemometers at Brutus based on the 'API' wind profile. The results are given in Figures 13 and 14 and the hindcast wind velocities were lower than those calculated from the measurements. The maximum 1/2-hour mean wind velocity at 10m above sea level calculated from the measurements reduced by 5% when adopting the 'NPD' wind profile⁹⁰ thus reducing the discrepancy.

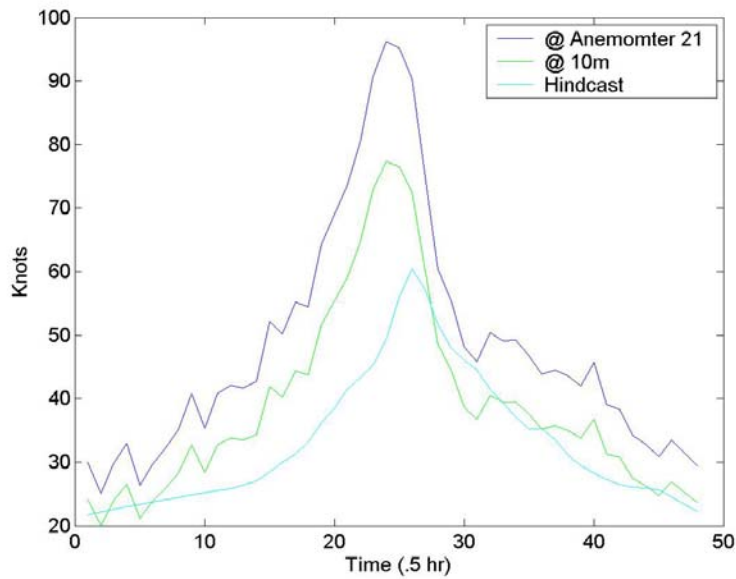


Figure 13 - Half-hour Wind Velocity at Anemometer 21 during Hurricane Lili

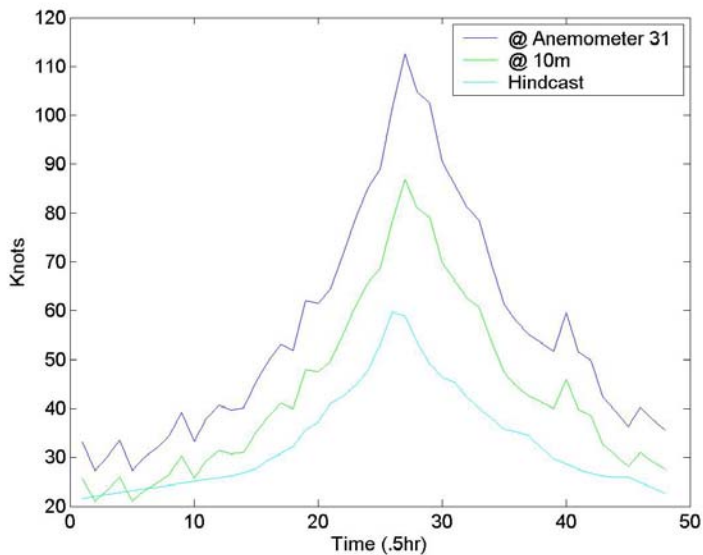


Figure 14 - Half-hour Wind Velocity at Anemometer 31 during Hurricane Lili

3.3.9 The following should be noted concerning such discrepancy:

- Winds measured from large offshore platforms may be biased due to topsides induced flow distortion effects and this could have affected the measurements for Anemometer 21. Anemometer 31 was mounted at the crown of the derrick and less likely to be affected by flow around the topsides. Anemometer 31 was mounted at a height significantly greater than the standard reference 10m level and simple wind profile factors may not apply very well in this case.

- According to Oceanweather⁶⁵ if the Brutus measured wind data were to be incorporated into the hindcast wind field, the resulting hindcast wave heights would have become seriously biased high in relation to the measurements taken at the buoys. The wind measurements taken at the buoy were at 5m and 10m above sea level and thus much closer to the standard reference 10m height.

3.3.10 For comparison to design wind velocities, the one-hour mean wind velocity at 10m above sea level was estimated from the wind velocities measured by the anemometers at Brutus based on the 'API' recommended wind profile. The results are given in Figures 15 and 16 where the upper curve gives the direct measurement results and the lower curve gives the results calculated at 10m above sea level. The horizontal lines show the different design environmental conditions used for the different design load cases (25-years return period summer reduced event, 100-year extreme design storm, 1,000-year survival condition). It can be seen that the 1-hour mean wind velocity values obtained from the measurements were of similar levels to those expected from a 100-year event.

3.3.11 The maximum 1-hour mean wind velocity at 10m above sea level calculated from the measurements reduced by 3% when adopting the 'NPD' wind profile.

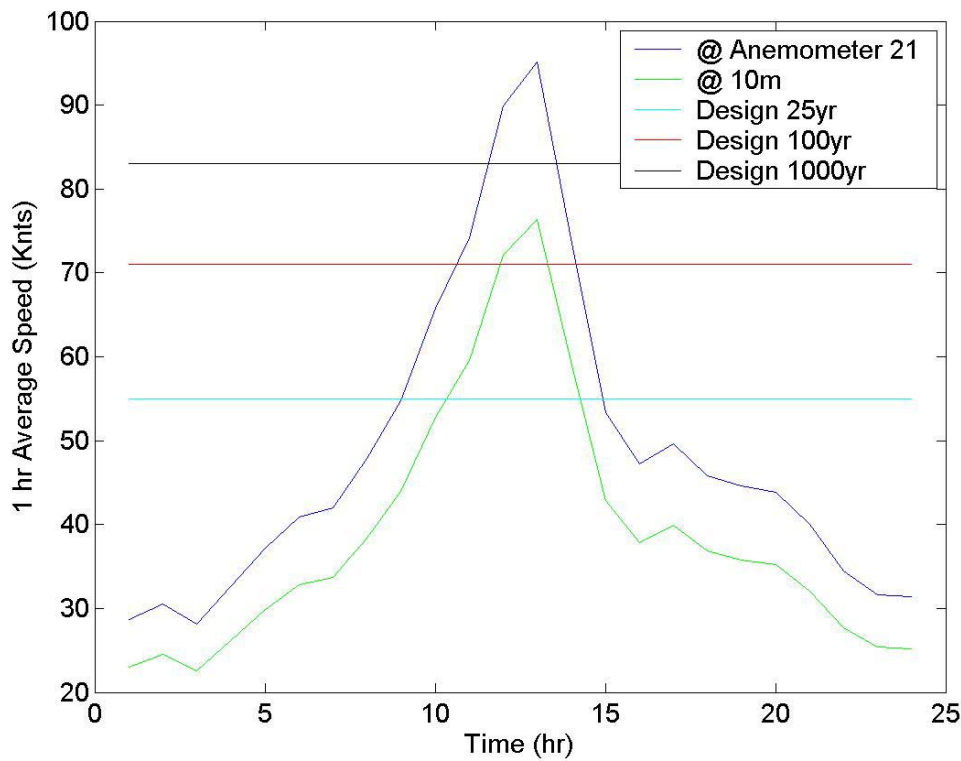


Figure 15 - 1hr Mean Wind Velocity Brutus Anemometer 21

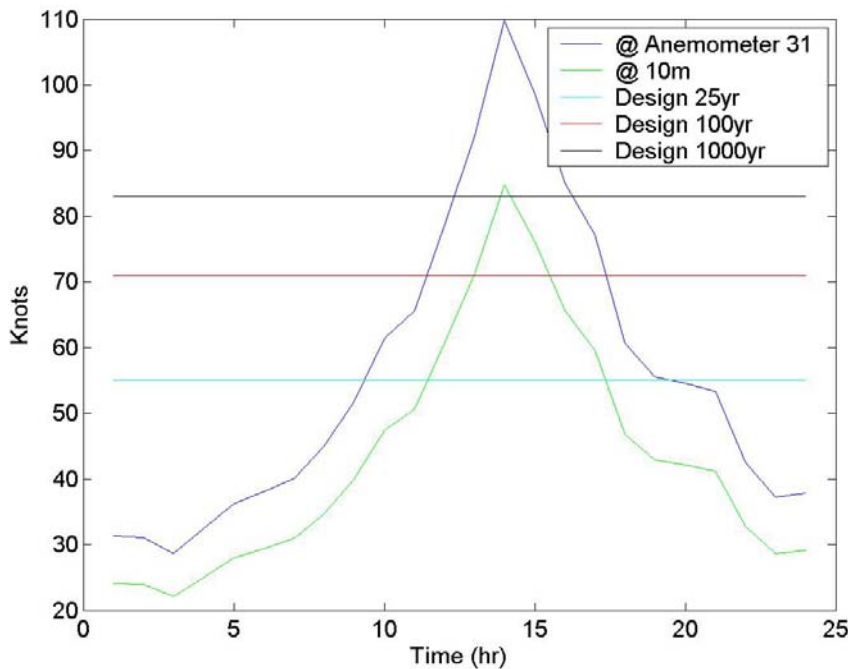


Figure 16 - 1hr Mean Wind Velocity Brutus Anemometer 31

3.4 Directionality of Winds and Seastates

- 3.4.1 The measurements and the hindcast data from Buoy 42041 showed that winds changed their mean direction as the hurricane developed its peak intensity. Over a period of 3 hours that contained the peak wind velocity, wind direction changed from approximately 80 degrees to 200 degrees, Figure 10. These values refer to the direction the wind is blowing from, measured clockwise from North.
- 3.4.2 The mean wave direction also changed but at a much more gradual rate than that observed for the mean wind direction, Figure 10.
- 3.4.3 The change in wind direction was also observed in the Brutus measurements from approximately 50 degrees to approximately 240 degrees, Figure 17. It is noted that Figure 17 gives the raw data measured and therefore includes fluctuations.

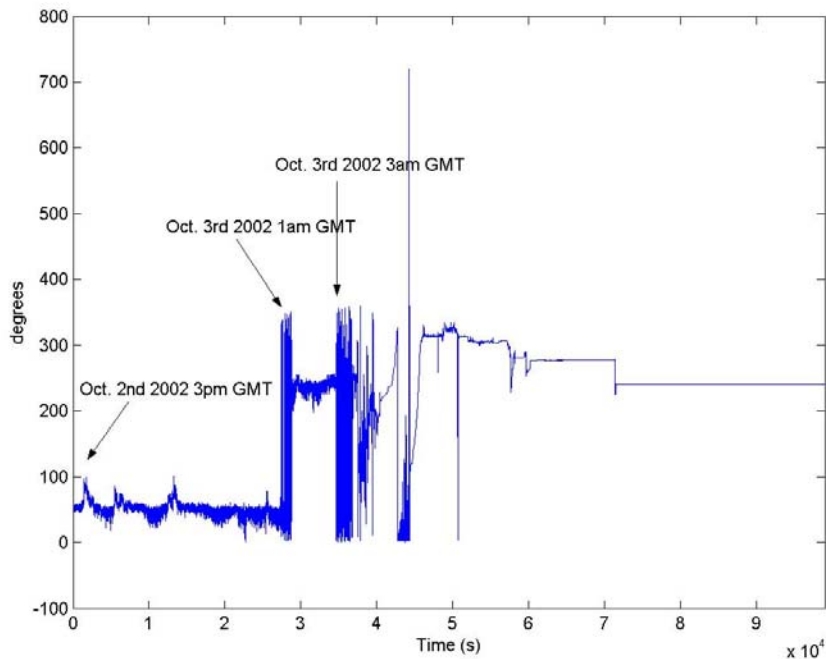


Figure 17 – Wind Direction, Raw Data from Brutus

3.4.4 A similar change in wind direction was also inferred from the mean moment on Typhoon calculated from the measured tendon tensions⁶⁴, Figure 18.

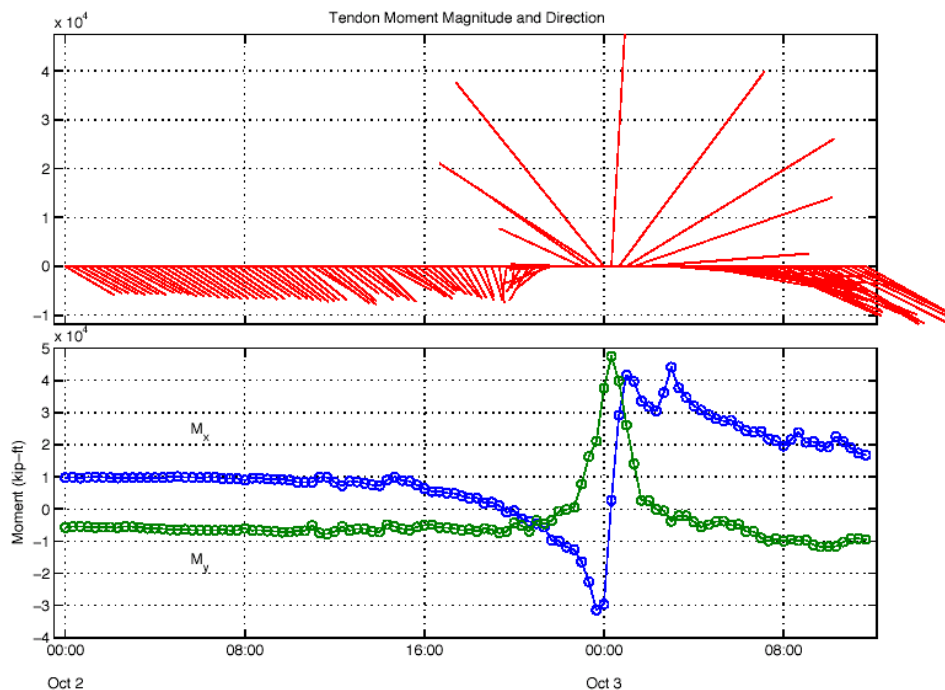


Figure 18 – Mean Overturning Moment, inferred from Tendon Tensions⁶⁴

3.5 Current

3.5.1 It can be observed from Table 3 that hurricane surface current values used by designers differ between themselves more than the values used for winds and waves.

3.5.2 There are at least two models that have been used extensively to predict currents during hurricanes: a Turbulence Closure model⁶⁶ and a mixed layer model⁶⁷. Both models have given similar mixed-layer averages for some platform designs⁶⁸ but the Turbulence Closure model tends to give higher surface current velocity values.

3.5.3 The hindcast model for Lili was based on validating a state-of-the-art model (HYCOM⁶⁹) against measurements from Hurricane Andrew and then run such model for Lili with the inclusion of satellite-derived sea surface stratification data. HYCOM⁶⁹ (Hybrid Coordinate Ocean Model) combines advantages of the different current models in optimally simulating coastal and open-ocean circulation features.

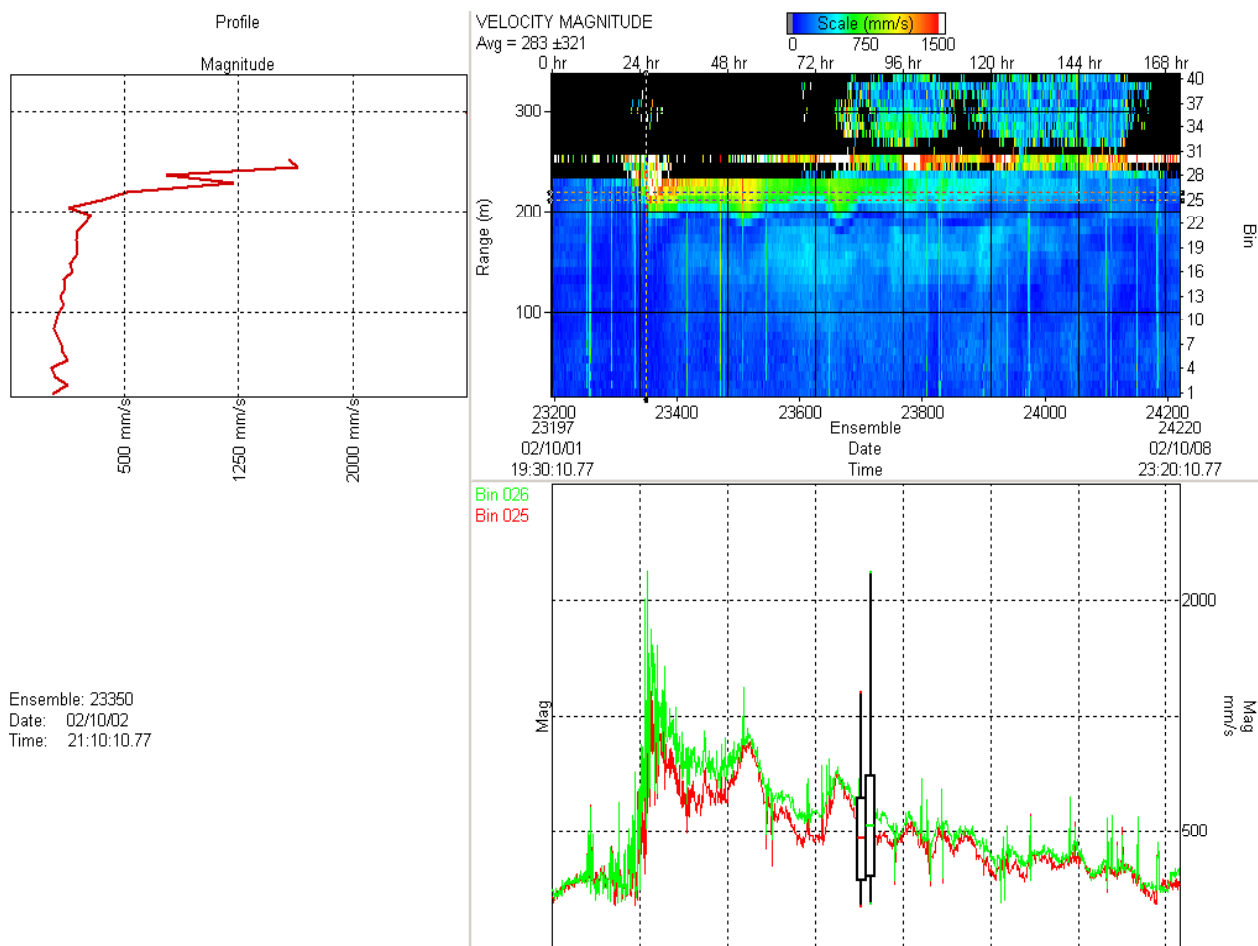
3.5.4 As far as measurements are concerned, the only relevant current data for Lili were those recorded by an Acoustic Doppler Current Profiler (ADCP) unit near the Genesis spar and made available by ChevronTexaco to this project⁷⁰. The 75 kHz ADCP unit was located about ¼ of a mile from the Genesis Spar at a depth of 250m (820ft) below the mean sea surface. The magnitudes of the 10-minute average current were profiled from September 26th to October 15th. Such current measurements were not available to Oceanweather's hindcast study.

3.5.5 Figure 19 shows the current profiles measured, with an emphasis on the period from October 2nd to October 4th (data was recorded in CST). The time of the peak winds due to Lili at Genesis based on the hindcast is included in the bottom part of Figure 19.

3.5.6 On a more rigorous examination, the data from the ADCP unit in this upper portion of the water column was considered questionable due to contamination from the acoustic side lobe from the surface. ADCP units⁷¹ use the Doppler Effect to measure current velocity by transmitting a short pulse of sound, listening to its echo and measuring the change in pitch or frequency of the echo. Doppler current sensors use large transducers (relative to the wavelength of the sound) to obtain narrow acoustic beams. Since each beam measures velocity parallel to the beam and does not sense the velocity perpendicular to the beam at all, three or four beams are used, all pointed in different directions.

3.5.7 ADCP units looking up or down typically lose data near the surface or bottom. This loss is caused by contamination of the near-surface data by side lobe echoes. The acoustic beams focus most of the energy in the center of the beams, but a small amount leaks out in other directions. Because sound reflects much better from the water surface than it does from the water, the small signals that travel straight to the surface can produce sufficient echo to contaminate the signal from the water.

3.5.8 This is illustrated in Figure 20 where D represents the true range from the ADCP to the surface and α represents the ADCP beam angle.



Lili Peak Waves at Genesis, October, 3rd 3:40 AM GMT (21:40 CST)

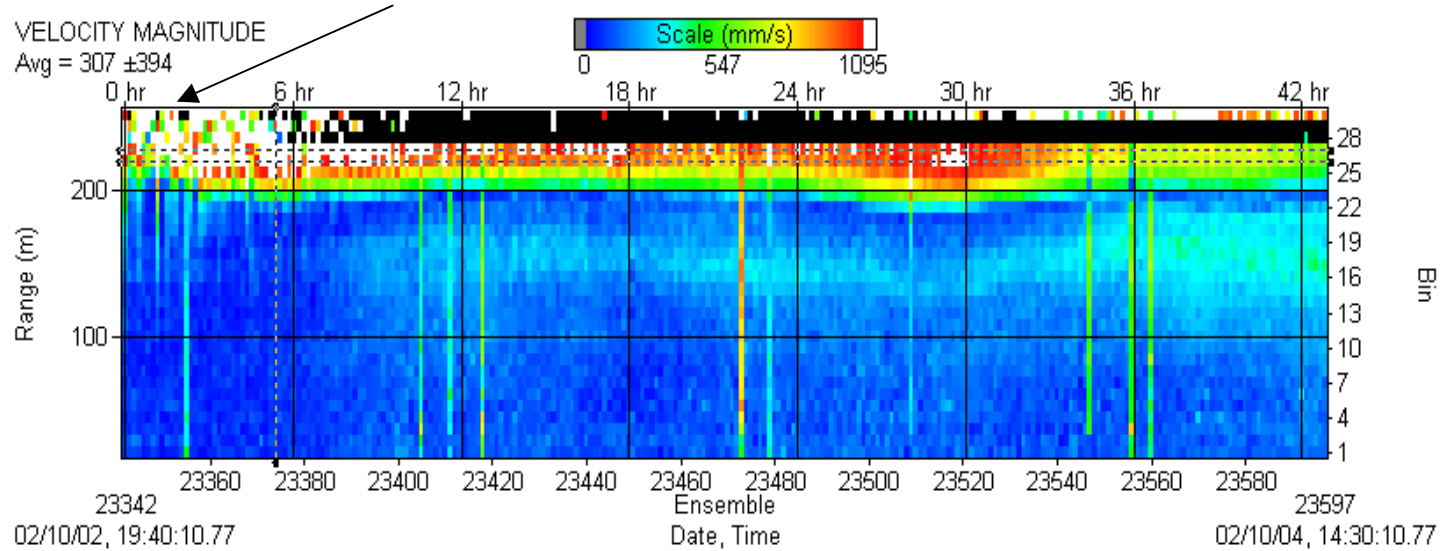


Figure 19 - Current Measurements during Lili (CST Date and Time on Horizontal Axis)

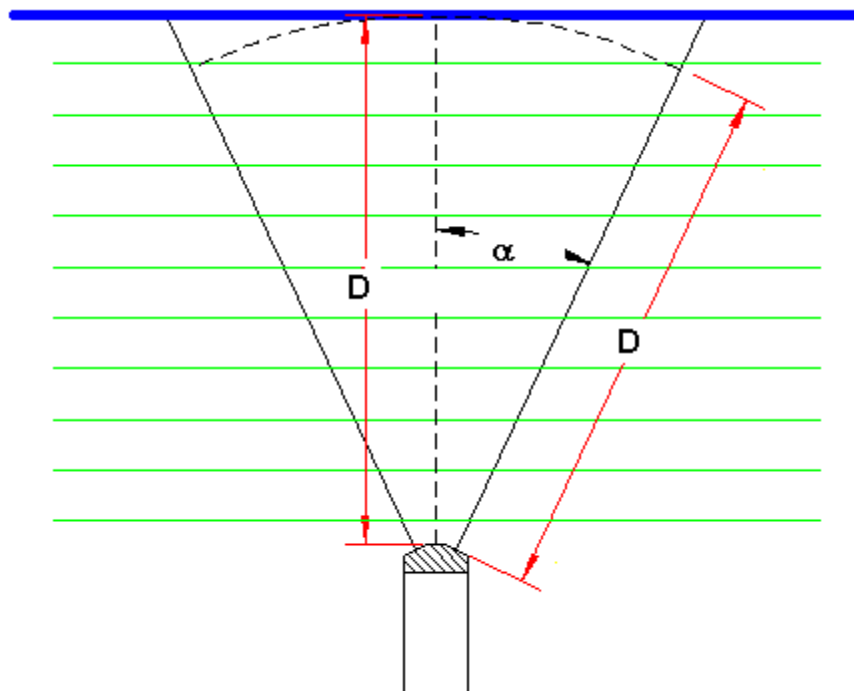


Figure 20 - Geometry of Profiler Sidelobe Interference⁷¹

3.5.9 According to information from the ADCP unit manufacturer⁷², the ADCP unit used for Genesis is made to have very low side lobes (<60dB 2-way at 30-40 degrees from the main lobe). However, even with these low side lobes the combined energy from the side lobes of all its 4 beams will cause bias in the data near the sea surface or bottom. The rule of thumb for cut off of a data set is:

$$\text{Cut Off Depth} = D * (1 - \cos(\alpha)) + \text{Cell Depth} \quad (2)$$

3.5.10 For a 75kHz ADCP (which have 20 degree beam angles), the 250m (820ft) of range to the surface and a 16m depth cell then a minimum depth of $250 * (1 - \cos(20)) + 16 = 31m$ (102ft) should be excluded. A conservative estimate⁷¹ would extend the depth of data to be excluded by another cell depth, leading to a depth of 47m (154ft).

3.5.11 The current measurements for Genesis nearest to the surface with a complete time trace during the peak of the storm were at 45m (148ft) below the surface (at Bin 24, Figure 19). Current measurements at 37m (121ft) below the surface (at Bin 25, Figure 19) had short drop-outs at the peak of the storm. Current measurements at 29m (95ft) below the surface (Bin 26, Figure 19) seemed to be returning reasonable data almost all the time. Such results were more positive than indicated by the rule of thumb values in the previous paragraphs. A current value of 1250 mm/sec (2.4 knots) was measured at Bin 26.

3.5.12 Inspection of Figure 19 indicates that markedly sheared current profiles were observed with current magnitudes exceeding 1 knot limited to a depth of approximately 200ft. Such

current values lasted for a period of approximately 30 hours after the peak waves due to the inertial oscillation of currents, which typically correspond to a period of about 24 hrs in the Gulf of Mexico.

3.5.13 Figure 21 shows the current profile measured by the ADCP unit (excluding data above 29m below the surface) in comparison with sample design current profiles and the hindcast current profile at the time of the peak hindcast waves at Genesis.

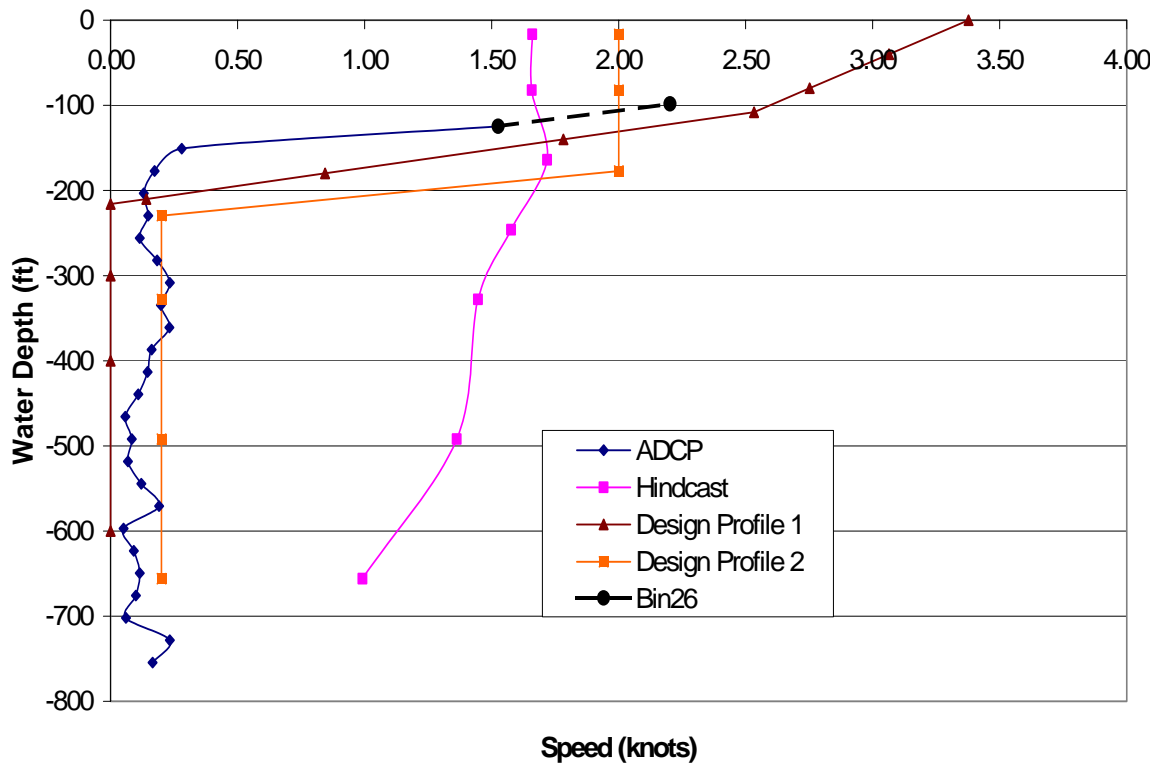


Figure 21 – Current Profiles at the Time of Hindcast Peak Waves (October 3rd 3:40 AM GMT)

3.5.14 Figure 22 shows the same comparison for 27 hours after the occurrence of the peak hindcast winds at Genesis. The seastates here have subsided to a significant wave height of less than 13ft.

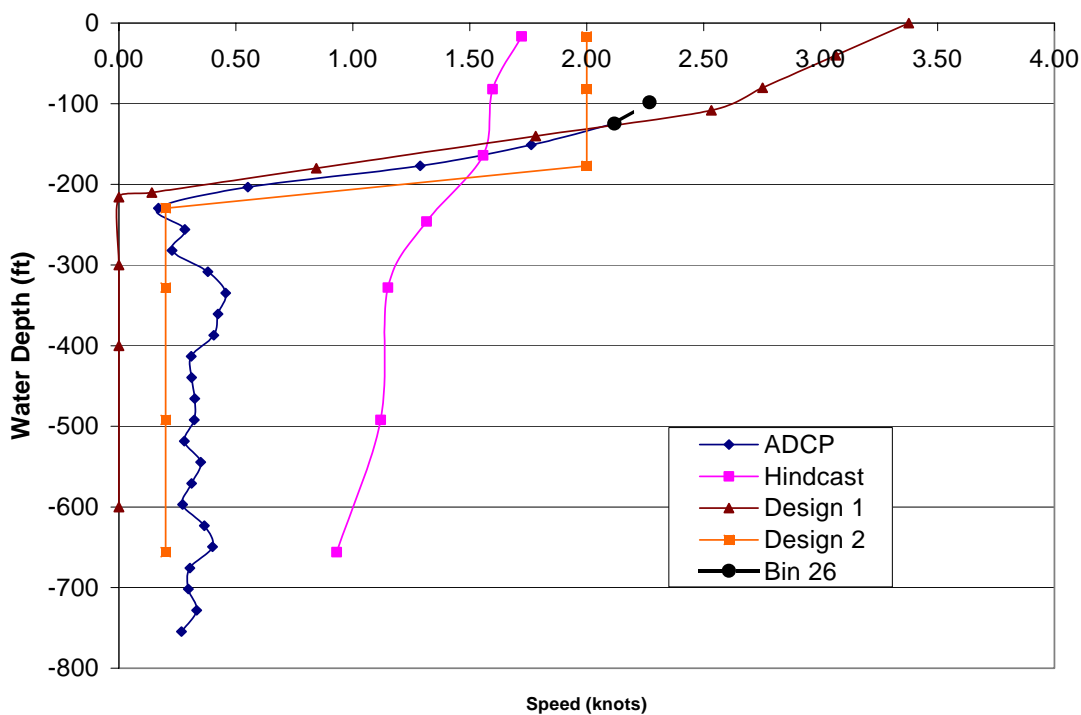


Figure 22 – Inertial Current Profile (October 4th 6:50 AM GMT)

3.5.15 Given the complexity of modeling hurricane currents, the design current profiles examined achieved a reasonable level of competence in terms of capturing the global current loading. Relative to the measurements, the hindcast model under-predicted the surface currents and over-predicted deep currents.

3.5.16 A validated Turbulence Closure model⁶⁸ applied to the Genesis location in conjunction with those current measurements considered to be reliable predicted maximum surface current velocity values that were not a matter of concern vis-à-vis the unit's continuing operations.

4. INSPECTION RESULTS FOR INSTALLATIONS AFFECTED BY LILI

4.1 Allegheny and Typhoon - SeaStar® Mono-Column TLP Designs

4.1.1 Typhoon, Morpeth and Allegheny are of Atlantia Offshore's wet tree SeaStar® design⁷³⁻⁷⁵, consisting of a mono-column hull that includes tendon porches extending radially outward, a conventional trussed deck structure and a tubular structure for the deck to hull transition. It provides a stand-alone production facility to support a number of subsea wells. Wells are tied-back to the platform via flexible production risers or steel catenary risers (SCRs).



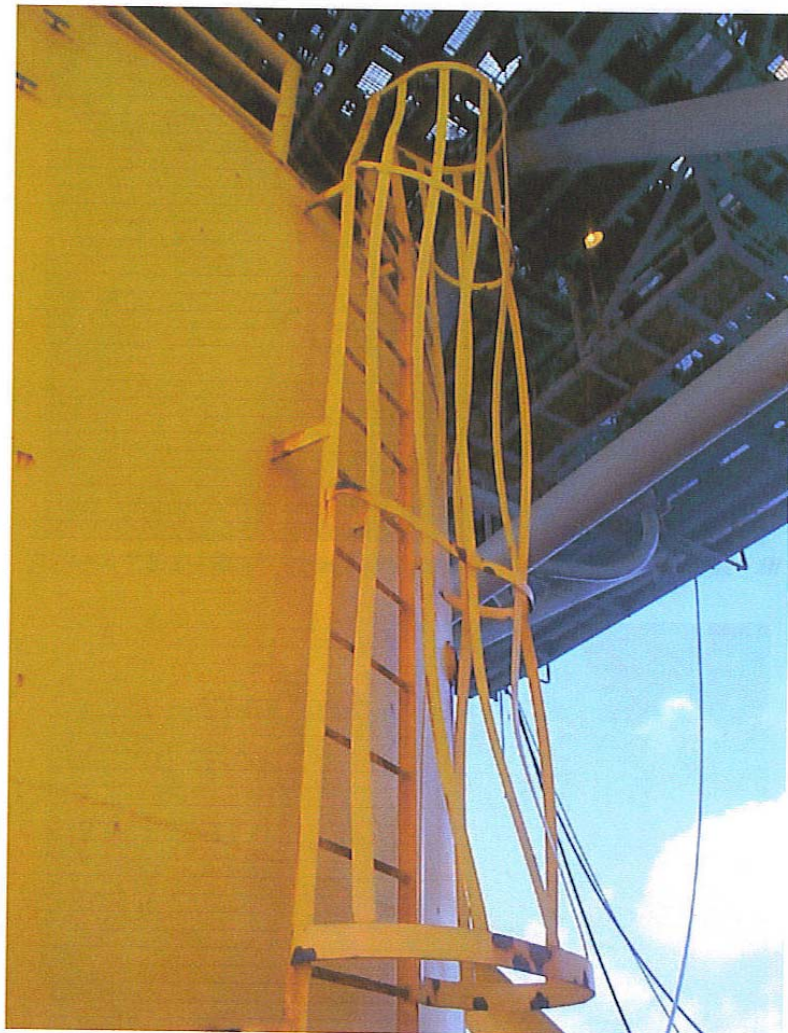
Figure 23 – Allegheny TLP (Payload 4,000 tonnes, Water Depth 3,300ft)⁷³

4.1.2 An inspection report⁶⁰ for Allegheny was provided by Atlantia Offshore covering:

- Visual inspection of the critical internal areas
- Visual inspection of the critical external hull areas above the waterline
- General internal inspection of the primary hull structure
- External visual inspection of the hull and tendons with the use of an ROV
- Cathodic Protection (CP) voltage measurements on the hull and tendons using ROV
- Visual inspection of the deck critical and primary structural areas

4.1.3 Overall, the platform was found to be structurally sound with no structural failures or cracks. Inspection of the underwater portion of the hull, appurtenances, top connectors, tendon porches, tendons and pile connector did not indicate any damage. No signs of scour in the seabed were found.

4.1.4 Minor damage was observed to ladders, ladder cages and handrails due to Lili, Figures 24 and 25.



Picture 2.6-1 – Bent Caged Ladder due to Hurricane Lili

Figure 24 – Damage to Allegheny during Lili (Caged Ladder)⁶⁰



Picture 2.6-3 – Missing or Bent Handrails due to Hurricane Lili



Picture 2.6-2 – Missing or Bent Handrails due to Hurricane Lili

Figure 25 – Damage to Allegheny during Lili (Handrails)⁶⁰

4.1.5 It was observed that a previous major loop current event had a substantial impact on Allegheny. The VIV induced on the tendons by such current caused vibrations on the entire structure for several weeks^{55,60}. Some structural details were reinforced to preserve the fatigue life. There was also damage to the riser suppressors and indication of riser clashing. However the risers were not inspected between the Loop Current Event and Hurricane Lili and it is not possible to determine which event had the most effect on the risers.



Figure 26 – Typhoon TLP (Payload 5,000 tonnes, Water Depth 2,100ft)⁷⁴

4.1.6 Hurricane Lili passed almost directly over Typhoon. An inspection report⁷⁶ was provided by Atlantia Offshore covering the following:

- Visual inspection of the underwater portion of the hull, appurtenances, top connectors, tendon porches, the tendons and the pile connector.
- Potential readings along the length of the tendons and on the underwater portion of the hull.

4.1.7 No signs were found of hull damage, tendon damage, tendon porch damage or seabed scour. ChevronTexaco provided additional information⁷⁷ concerning damage to equipment and a summary list is given in Table 5.

Table 5– Typhoon Equipment Damage during Lili

| | |
|-----------------------------------|---------------------------|
| Lifeboat # 1 | Capt. Area roof damage |
| Lifeboat # 1 | Aft window broken |
| Lifeboat # 1 | Self Righting bag damaged |
| Fire Hose Station # 17 | Broken Off mounts |
| Fire Hose Station # 17 | Broken Off mounts |
| Satellite dish | Mount bent |
| Temp. Building Plumbing | PVC Broken |
| Both Life Rafts | Missing |
| HUS Ladders | Back scratches flatten |
| Hand rails on HUS | two sections missing |
| Hand rails on HUS | One section damaged |
| HUS A/C | Damaged |
| Cable trays under Production Deck | Damaged |
| Heliport Skirting | Damaged |
| Radio Chargers | Damaged |
| Control Room CD/Radio player | Damaged |
| Bunn Coffee Pot (control rm) | Damaged |
| Printer Control Rm | Damaged |
| Cannon Copier | Damaged |
| Fax Machine Control Rm | Damaged |
| Lights | Damaged |
| Numerous Signs | Damaged or Missing |
| Fire extinguishers | |
| Walls in two bedrooms | Damaged |
| Crane Cab | Damaged |
| Air Compressor Panel | |
| Battery Box for fire pump | Damaged |
| Life Rings | |
| Life Jackets & Boxes | |
| Fog Horn | |
| Weight Room | |
| Scaffolding | Damaged |
| Laptop Computer | Damaged |
| OA's Computer Monitor | Damaged |
| Pipeline Pump Panel | Damaged |

4.1.8 Lifeboats were damaged possibly due to failure of its securing equipment, Figures 27 to 30.

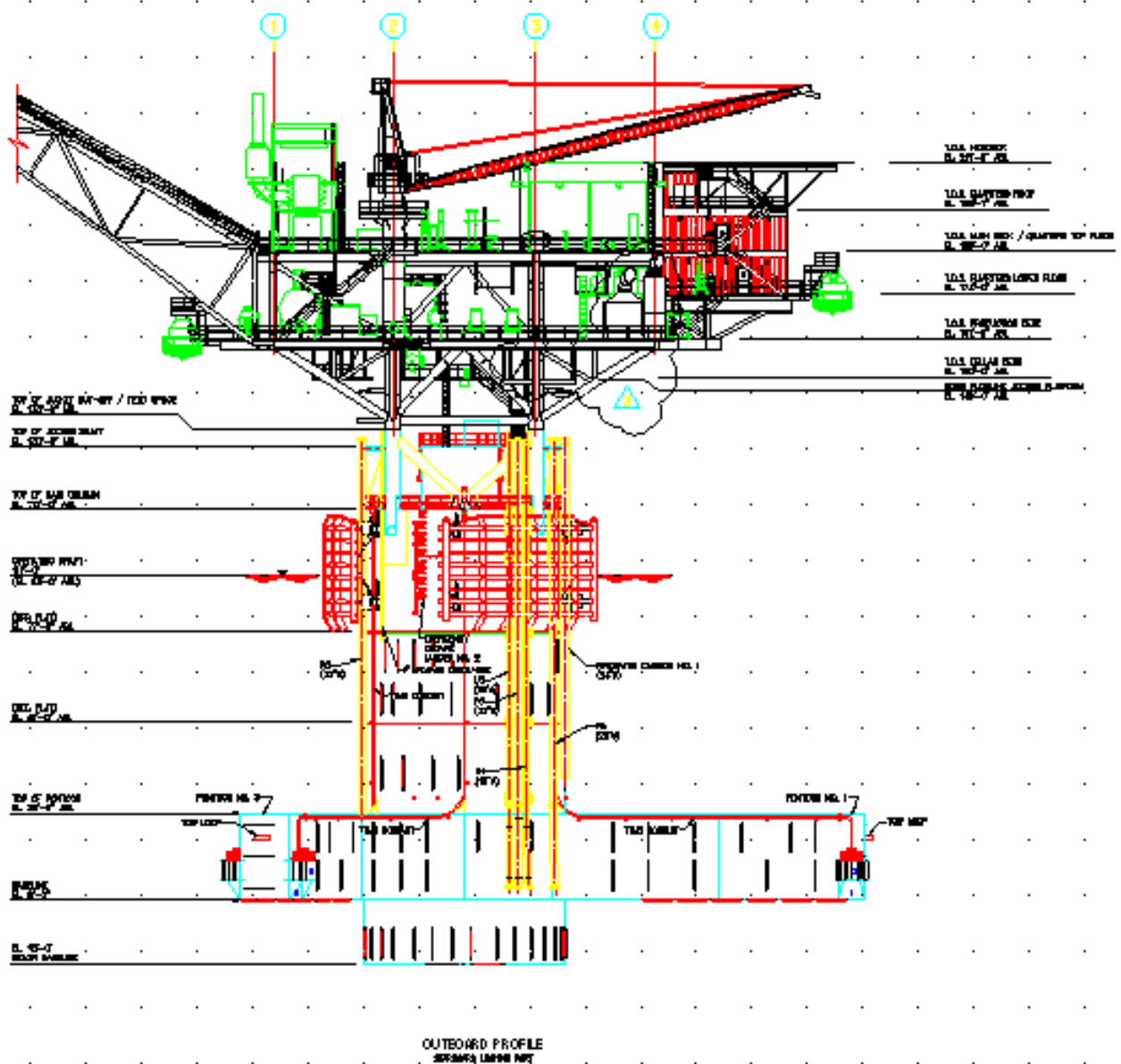


Figure 27 – Location of Lifeboats at Typhoon



Figure 28 – Damage to Lifeboats at Typhoon



Figure 29 – Damage to Lifeboats at Typhoon



Figure 30 – Damage to Lifeboats at Typhoon

4.2 Prince - MODEC TLP Design

4.2.1 The first MODEC TLP, Figure 31, was installed⁷⁸ on El Paso's Prince field in the Gulf of Mexico in 454m (1,490 ft) water depth. The Prince TLP is a small multi-purpose tension leg platform with a displacement of 13,100 tonnes and is moored to the seabed by eight-24 inch diameter tendons. The Prince deck is a three level deck and has a structural weight of 1,550 tonnes. The topside payload is 4,00 tonnes. Gas produced from the facility is exported via a 12" line to the El Paso Energy Partner's South Timbalier Block 292 platform located approximately 14.2 miles north/northwest of Prince.

4.2.2 Prince follows the MOSES design concept⁷⁹. Rather than using a single central column, its hull consists of four slender steel columns rising from a submerged buoyant base, which was designed to carry much of the buoyancy deep in the water to improve the hydrodynamic performance of the hull. The spacing of the columns adds additional support for the topsides, thus reducing the deck weight and making the topsides easier to build.

4.2.3 Another key feature of the design is that the risers do not come up thought the center of the structure as in other systems, but are routed along the outside of the hull to a wellbay positioned at one end of the platform. The wellbay is located as far away as possible from the quarters and the need for having a moonpool is removed. Further, to reduce clashing, the risers are supported laterally at the keel using a keel guide that allows the riser to slide vertically while being restrained laterally.

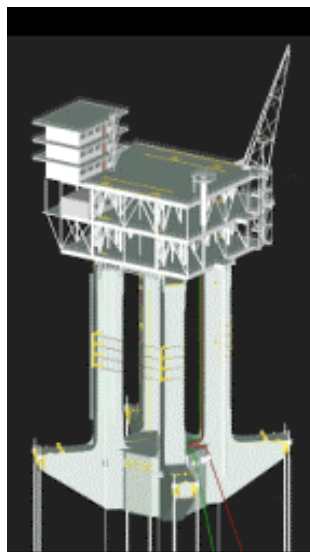


Figure 31 – Prince TLP (Payload 4,000 tonnes, Water Depth 1,490ft)^{77, 78}

4.2.4 The main following information was provided by El Paso concerning the effects of Lili on the Prince TLP⁵⁹:

- The unit was subjected to severe motions as indicated by equipment displaced on board but the magnitude cannot be determined because no tension data logging could take place as power was down and systems shut down.
- The only damage observed was a piece of fiber glass grating on a deck 45 ft from the water that was pushed up. This grating was located 12 ft under the cellar deck, Figure 32. This could have been due to wave run-up.
- Water entered vents located 30-35 ft from the water line.
- Riser VIV was observed during the loop current event on March 2002 with some damage to the passive riser tensioning system for one of the wells. However, no damage or VIV was observed during Lili.
- It was not considered necessary to perform underwater inspections after Lili.

JUL-17-2003 02:35P FROM: T0:912915590541 P:3/1

Figure 3: TIP 3-D Rendition (South Face)

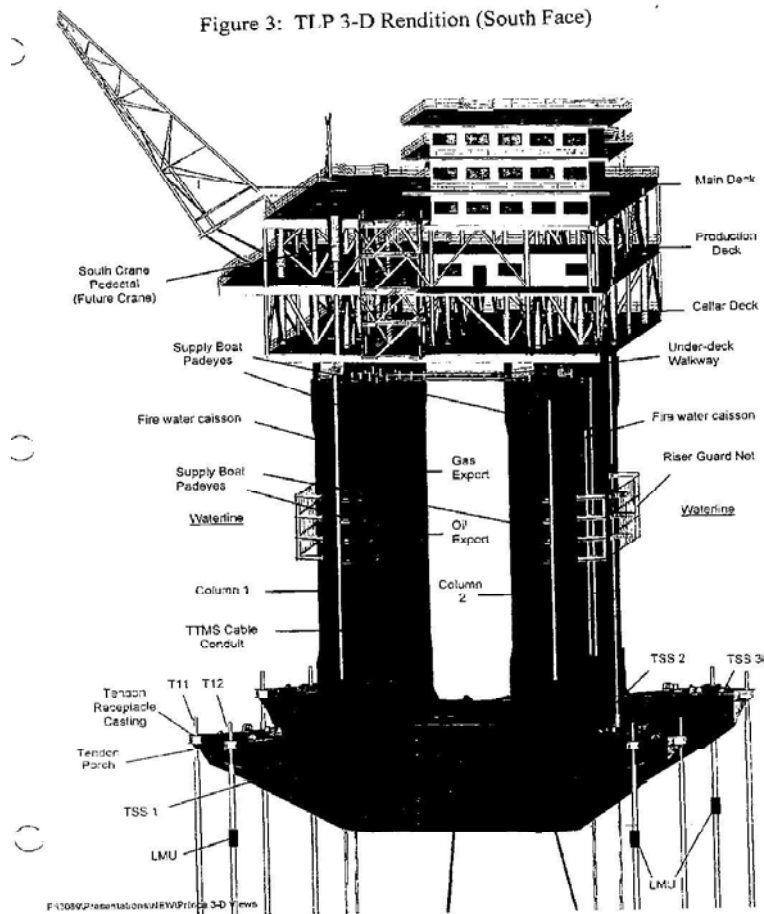


Figure 32 – Location of Decks on Prince TLP

4.3 Brutus TLP

4.3.1 Brutus is an eight-slot TLP specifically designed to serve as a hub for future subsea developments in the surrounding area and was Shell's fifth TLP to be installed in the Gulf of Mexico. The TLP is 3,250 feet high, from the seafloor to the crown block of the drilling rig.

4.3.2 The Brutus TLP was installed in June 2001 and is operated by Shell in Green Canyon block 158 in 2958 ft of water. Brutus is a TLP design consisting of four columns and four pontoons with a total of twelve tendons and shares much in common with its predecessor and sister vessel, the Mars TLP. The design of Brutus relied heavily on knowledge gained from the MARS design process.

4.3.3 Although similar in size and configuration to its sister platforms Mars and Ram Powell TLPs, Brutus⁸⁰ was designed with increased displacement to handle subsea tiebacks and with dual processing systems for its role as a hub. Its hull was designed to reduce weight, include additional subsea riser baskets and umbilical pull tubes, and to incorporate a 10m

central access shaft in the columns. Reduced hull weight and fewer platform wells allowed for significant expansion of the topsides facilities to accommodate the processing trains required for metering and producing from multiple satellite fields. Larger and more buoyant tendons were designed for Brutus to accommodate potential increases in dynamic tendon loads due to the higher centre of gravity of the payload.

4.3.4 Detailed monitoring data was provided⁸¹ by Shell for Brutus during Lili which is covered in detail in Section 5.

4.4 Genesis Spar

4.4.1 The Genesis spar production facility is moored in 2,600ft of water. Its hull is 122ft in diameter and the length of its buoyant section is 295 ft yielding a 55 ft freeboard and a 650 ft draft. It is 705ft tall and incorporates a 58ftx58ft well bay at its centre, which is enough for 20 well slots. The riser system consists of the production, export and drilling risers, all run with a platform drilling rig.



Figure 33 – Genesis Spar

4.4.2 The spar can support up to 20 production risers, two export pipeline risers and one drilling riser. Each is approximately 2,650ft long up to the span, from seafloor wellheads to the topsides. The 20 subsea wellheads and two export riser bases on the seafloor are arranged in a 140ft-diameter circle, with 20ft of spacing.

4.4.3 ChevronTexaco provided information⁷⁷ on equipment damage during Lili summarized in Table 6. No significant damage to the structure or risers was reported.

Table 6 – Genesis Equipment Damage during Lili**Number 5, 6 and 7 chain jacks**

grating (10)
aluminum drip pans with drain pipe (3)
straighten I-beams
revise deck backdown rope
replace backdown ropes

Number 8, and 9 chain jacks

grating (4)
aluminum drip pans with drain pipe (2)

Mooring inspection ladder cages

full length (3) (new two sections)
half length - repair

West landing and steps

grating (2)

Misc. costs (for above repair work)

boat costs
crew mob and demob
helicopter
misc.

ADCP electrical cable severed at waterline**Bunkhouse ceiling tiles****Deck 10 grating****Boat landing stairs****Twila's office stuff****Cover on A air compressor****lifevests and box****Misc. food****FRC sponson damaged on bow and stern****Igniter conduit on flare stack****Insulation on generator exhaust and scaffolding****Insulation on compressor exhaust and scaffolding****Rig floor camera****Galley oven****Foxboro field bus modules - 6 damaged****Stand-by generator****gas detector heads****Misc. crane equipment - wind sock and mirrors - etc.****Paint materials - soda blasting material - 1 pallet****crane engine rebuild - water damage (costs assume some parts and labor for a checkup)****Tool boxes in generator building (2)****Helideck skirting****Misc. Gaitronics speakers and electrical**

4.4.4 From the above Table, the following equipment was located in the air gap:

- Number 5, 6 and 7 chain jacks: gratings and aluminium drip pans
- Number 8, and 9 chain jacks: gratings and aluminium drip pans
- Mooring inspection ladder cages
- West boat landing and steps
- ADCP electrical cable severed at waterline
- Deck 10 grating (55 ft off water)
- Boat landing stairs

4.4.5 It can be seen that gratings 55ft above sea level were damaged.

5. ANALYSIS OF MONITORING DATA FOR BRUTUS TLP

5.1 Introduction

5.1.1 Table 7 summarizes the Brutus instrumentation system⁸¹ and its operational condition during Lili. It can be seen that almost all instruments were operational except for the wave probe.

Table 7 - Brutus Instrumentation

| | Method | Sampling Rate (Hz) | Location | Operational |
|----------------|---------------|--------------------|------------------------|-------------|
| Surge | DGPS | 1 | Quarters | Yes |
| Sway | DGPS | 1 | Quarters | Yes |
| Roll | Accelerometer | 2 | Columns | Yes |
| Pitch | Accelerometer | 2 | Columns | Yes |
| Heave | Accelerometer | .3 | Columns | Yes |
| Wind | Anemometer | 2 | 278' / 350' above keel | Yes |
| Wave | Probe | 2 | Drilling Module | No |
| Tendon Tension | Strain Gauge | 2 | Tendon Top | Yes |

5.1.2 Tendon tension data was captured for a tendon in each corner as shown in Figure 34.

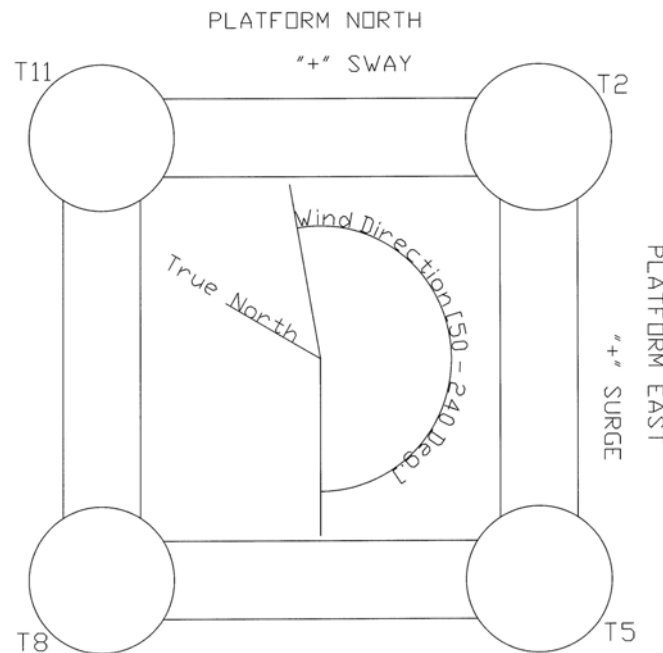


Figure 34 – Location of Instrumented Brutus TLP Tendons

5.1.3 As shown in Section 3, winds changed their mean direction as Lili developed its peak intensity. The change in wind direction observed in the Brutus measurements was from approximately 50 degrees to approximately 240 degrees. These values refer to the direction the wind is blowing from, measured clockwise from True North as shown in Figure 34.

5.1.4 The data was analyzed in both the time and the frequency domain in MATLAB and comparison were made with the unit's design basis. The lessons learned are presented relative to the following main topics:

- Global Performance
- Assessment of Design Recipe
- Vortex Shedding Effects.

5.2 Global Performance

5.2.1 Figure 35 shows the trajectory of Brutus based on the half hour mean offsets. Figure 35 considers 48 hours of monitoring data that included the maximum environmental conditions during Lili.

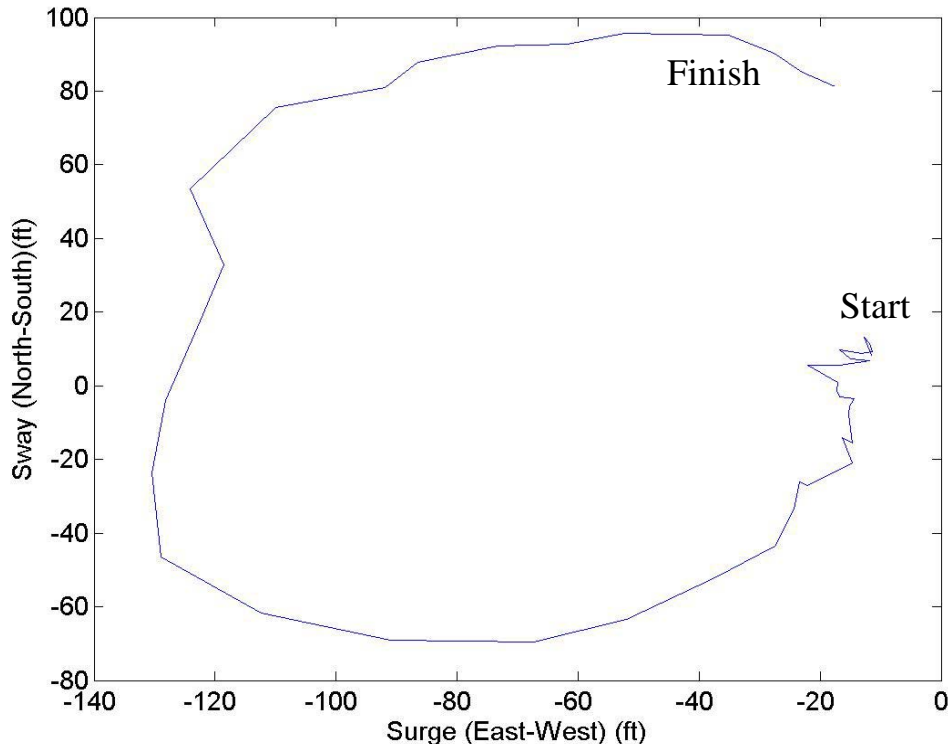


Figure 35 - Brutus' Offset during Hurricane Lili

5.2.2 Brutus followed a path that reflected Lili's directional changes. At the end of the time series, it had not yet returned to its initial position, possibly due to the persistence of currents long after the peak winds and waves had occurred, much as shown in the Genesis ADCP current measurements discussed in Section 3. The residual sway appears to be consistent with a current from 240 degrees clockwise from True North. However it is noted that no current measurements were available at Brutus.

5.2.3 The motion statistics for the entire time series can be seen in Table 8. The maximum offset of 196.7ft was less than 80% of the maximum design offset.

Table 8 - Motion Statistics (Complete Time-Series)

| | Surge | Sway | Offset |
|-------------------------|---------|---------|---------|
| Maximum (ft) | 80.20 | 118.37 | 196.71 |
| Minimum (ft) | -191.69 | -99.70 | 1.58 |
| Mean (ft) | -31.24 | 49.15 | 75.17 |
| Standard Deviation (ft) | 32.25 | 48.62 | 33.83 |
| Variance (ft) | 1039.94 | 2364.29 | 1144.33 |
| Kurtosis | 6.64 | 2.62 | 2.78 |
| Skewness | -2.20 | -1.01 | -0.41 |

5.2.4 The monitoring data was divided into Time Intervals (TI). Three hour long sea states were chosen to match those typically used in physical model tests and computational models. The results are shown in Table 9.

Table 9 - Motions Statistics for 3 Hour TI

| Hours | 3 | 6 | 9 | 12 | 15 | 18 | 21 | 24 | 27 | 30 | 33 | 36 | 39 | 42 | 45 | 48 |
|------------------|-------|-------|-------|---------------|----------------|----------------|--------|-------|-------|-------|-------|-------|-------|-------|-------|-------|
| Surge Mean (ft) | -12.9 | -16.7 | -15.4 | -24.9 | -97.0 | -116.0 | -56.2 | -18.6 | -17.8 | -17.8 | -17.8 | -17.8 | -17.8 | -17.8 | -17.8 | -17.8 |
| Sway Mean (ft) | 10.1 | 4.2 | -8.2 | -33.8 | -55.7 | 42.7 | 92.3 | 82.2 | 81.5 | 81.5 | 81.5 | 81.5 | 81.5 | 81.5 | 81.5 | 81.5 |
| Mean offset (ft) | 16.4 | 17.2 | 17.4 | 42.0 | 111.9 | 123.6 | 108.1 | 84.3 | 83.4 | 83.4 | 83.4 | 83.4 | 83.4 | 83.4 | 83.4 | 83.4 |
| Surge STD (ft) | 6.7 | 5.7 | 4.8 | 10.3 | 33.0 | 16.1 | 21.7 | 3.9 | 2.5 | 2.1 | 1.8 | 1.6 | 1.5 | 1.3 | 1.1 | 0.8 |
| Sway STD (ft) | 5.0 | 6.3 | 7.6 | 13.6 | 19.1 | 32.0 | 6.6 | 2.9 | 1.8 | 1.6 | 1.4 | 1.3 | 1.4 | 1.2 | 1.0 | 0.7 |
| Surge RMS (ft) | 14.6 | 17.6 | 16.1 | 26.9 | 102.5 | 117.1 | 60.3 | 19.0 | 17.9 | 17.9 | 17.9 | 17.9 | 17.8 | 17.8 | 17.8 | 17.8 |
| Sway RMS (ft) | 11.3 | 7.6 | 11.2 | 36.4 | 58.9 | 53.3 | 92.6 | 82.2 | 81.5 | 81.5 | 81.5 | 81.5 | 81.5 | 81.5 | 81.5 | 81.5 |
| Surge VAR (ft) | 45.33 | 32.15 | 23.34 | 105.99 | 1091.94 | 259.25 | 471.57 | 15.58 | 6.35 | 4.52 | 3.37 | 2.51 | 2.17 | 1.66 | 1.21 | 0.65 |
| Sway VAR (ft) | 24.91 | 39.34 | 57.77 | 184.99 | 366.70 | 1022.64 | 43.89 | 8.61 | 3.13 | 2.56 | 1.92 | 1.80 | 1.87 | 1.47 | 1.04 | 0.52 |
| Surge Kurtosis | 36.56 | 3.64 | 3.38 | 3.25 | 2.00 | 3.06 | 1.98 | 7.71 | 2.86 | 3.16 | 3.00 | 3.06 | 2.96 | 3.00 | 3.12 | 3.13 |
| Sway Kurtosis | 18.48 | 14.88 | 3.53 | 2.86 | 3.00 | 1.86 | 3.52 | 6.45 | 2.90 | 3.05 | 3.00 | 3.06 | 3.15 | 3.08 | 2.94 | 3.22 |
| Surge Skewness | 1.51 | -0.66 | -0.16 | -0.56 | 0.11 | 0.00 | -0.09 | -1.59 | 0.05 | 0.01 | 0.01 | -0.06 | -0.02 | -0.01 | 0.01 | 0.00 |
| Sway Skewness | 0.69 | 1.16 | -0.59 | -0.62 | 0.74 | -0.14 | -0.10 | 1.32 | 0.03 | -0.01 | 0.01 | 0.03 | -0.03 | -0.02 | 0.00 | -0.03 |

5.2.5 It can be seen from Table 9 that mean, standard deviation (STD), variance (VAR) and root mean square (RMS) values change significantly for the different TIs due to the non-stationary nature of an event such as Lili.

5.2.6 The peak response to Lili is shown by noticeable differences in all the statistics for TIs 12 – 18 (**bold**). Mean and RMS motion values increase during this time period and correspond to increased TLP offset and environment forces, specifically waves. All motion statistics except for the mean offset in sway return to pre-hurricane values in the final TIs.

5.2.7 The tendon tension statistics for the complete time series can be seen in Table 10.

Table 10 - Tendon Tension Statistics (Complete Time Series)

| | T2 | T5 | T8 | T11 |
|-------------|--------|--------|--------|--------|
| Max (kips) | 3490.0 | 3285.0 | 3754.0 | 3543.0 |
| Min (kips) | 1764.0 | 1672.0 | 1157.0 | 1279.0 |
| Mean (kips) | 2285.0 | 2252.0 | 2218.0 | 2220.0 |
| STD (kips) | 199.4 | 210.3 | 208.3 | 161.7 |
| Kurtosis | 4.08 | 2.66 | 4.97 | 5.53 |
| Skewness | 1.07 | 0.72 | 0.74 | 0.98 |

5.2.8 The maximum measured tendon tension was 80% of the allowable value for the relevant design platform operational condition closest to the conditions during Lili. A minimum bottom tendon tension of 947 kips was calculated from the minimums in Table 10 (which were measured near the top of the tendons). The design analyses⁸⁰ for Brutus predicted minimum tendon tensions that were much closer to a critical condition where tendon tension is lost.

5.2.9 The results for the 3-hour TIs are shown in Table 11. Again the peak response to Lili is indicated by noticeable differences in all the statistics for TIs 12 –18. Mean and RMS tendon tension values for this period increase during this time period and correspond to increased TLP offset and environment forces, specifically waves.

5.2.10 Although the peak environmental conditions during Lili approached 100-year values, the measured responses of Brutus were noticeably lower than the 100-year design responses suggesting a safe side bias in the design models.

Table 11 - Tendon Tension Statistics for 3 Hour TI

| Hours | 3 | 6 | 9 | 12 | 15 | 18 | 21 |
|-----------------|---------|----------|----------|-----------------|-----------------|-----------------|----------|
| T2 mean (kips) | 2159.09 | 2155.25 | 2132.51 | 2235.28 | 2575.80 | 2449.51 | 2294.30 |
| T5 mean (kips) | 2118.98 | 2120.06 | 2065.59 | 2105.90 | 2361.13 | 2525.02 | 2451.42 |
| T8 mean (kips) | 2125.59 | 2120.98 | 2100.50 | 2164.78 | 2326.68 | 2373.86 | 2311.47 |
| T11 mean (kips) | 2143.30 | 2132.35 | 2125.96 | 2206.52 | 2357.66 | 2304.64 | 2269.57 |
| T2 STD (kips) | 56.96 | 84.60 | 92.87 | 131.28 | 191.94 | 162.25 | 114.39 |
| T5 STD (kips) | 38.81 | 59.92 | 70.09 | 102.35 | 204.01 | 144.68 | 111.73 |
| T8 STD (kips) | 59.81 | 118.41 | 133.01 | 201.42 | 295.61 | 222.87 | 127.79 |
| T11 STD (kips) | 40.44 | 76.53 | 90.04 | 144.87 | 225.99 | 179.63 | 121.34 |
| T2 RMS (kips) | 56.95 | 84.60 | 92.87 | 131.28 | 191.94 | 162.24 | 114.39 |
| T5 RMS (kips) | 38.81 | 59.92 | 70.09 | 102.35 | 204.01 | 144.68 | 111.73 |
| T8 RMS (kips) | 59.81 | 118.40 | 133.00 | 201.42 | 295.60 | 222.86 | 127.79 |
| T11 RMS (kips) | 40.44 | 76.53 | 90.04 | 144.86 | 225.98 | 179.62 | 121.34 |
| T2 VAR (kips) | 3243.95 | 7157.61 | 8624.86 | 17234.72 | 36841.41 | 26323.59 | 13086.16 |
| T5 VAR (kips) | 1506.50 | 3590.88 | 4912.15 | 10476.03 | 41621.94 | 20932.06 | 12483.63 |
| T8 VAR (kips) | 3577.38 | 14019.82 | 17690.45 | 40570.39 | 87382.42 | 49670.34 | 16331.43 |
| T11 VAR (kips) | 1635.52 | 5857.25 | 8107.83 | 20986.43 | 51069.71 | 32265.54 | 14724.48 |
| T2 Kurtosis | 3.14 | 3.13 | 3.16 | 3.77 | 3.27 | 3.44 | 3.27 |
| T5 Kurtosis | 3.34 | 3.24 | 3.10 | 3.52 | 2.87 | 3.38 | 3.52 |
| T8 Kurtosis | 3.21 | 3.13 | 3.13 | 3.61 | 3.73 | 3.83 | 3.46 |
| T11 Kurtosis | 3.33 | 3.53 | 3.38 | 3.69 | 4.15 | 3.87 | 3.69 |
| T2 Skewness | 0.01 | 0.18 | 0.18 | 0.49 | 0.29 | 0.29 | 0.18 |
| T5 Skewness | 0.04 | 0.18 | 0.05 | 0.29 | 0.23 | 0.26 | 0.37 |
| T8 Skewness | 0.12 | 0.06 | 0.07 | 0.20 | 0.17 | 0.08 | 0.24 |
| T11 Skewness | -0.04 | -0.04 | 0.04 | 0.07 | 0.08 | 0.08 | 0.24 |

5.2.11 The kurtosis values for all tendons increase during the hurricane, which indicates tendon tensions became more prone to higher extremes, i.e. more variable. In other words, before and after the hurricane, or for normal operating conditions, extreme tendon tensions (maximums and minimums) tend to be closer to the mean tension. The nonlinear environment and/or nonlinear structure response during a hurricane generate maximum and minimum tendon tensions that tend to depart further from the mean. Skewness values also increased with the hurricane.

5.2.12 Figures 36 and 37 illustrate the six minute time series bounding the measured maximum and minimum tension for each tendon. It is interesting to note that maximums do not occur simultaneously, except for tendons T5 and T8. Maximum measured tensions for all tendons occur between 4:30 and 5:30 am GMT on October 3rd, some time after peak measured

winds at 4:00 am GMT. As with the measured maximum tensions, the minimums also occurred at different times, between 11pm GMT on October 2nd and 5am GMT on October 3rd. It should be noted that all minimum tensions occur before their respective maximums.

5.2.13 The responses in Figures 36 and 37 show some ringing and springing characteristics but it is not possible to clearly point to these being responsible for the maximum responses as detailed wave records are not available.

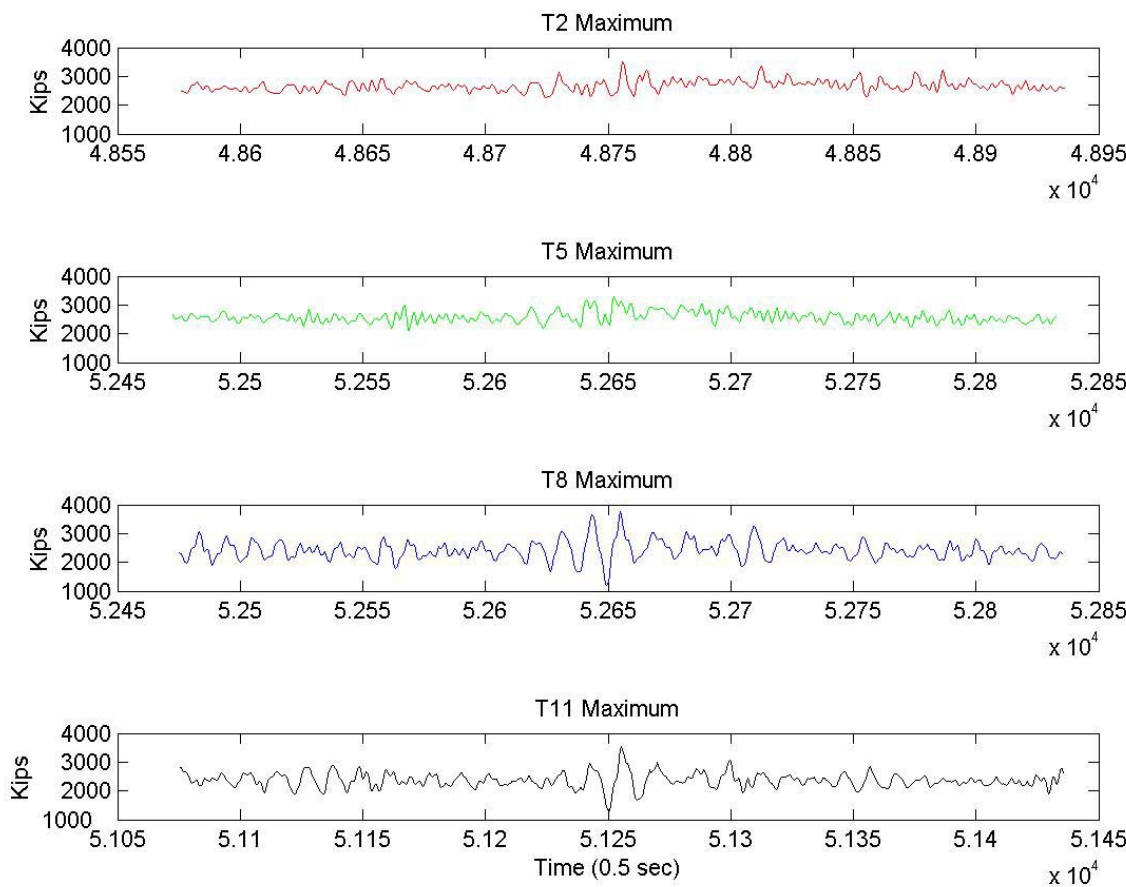


Figure 36 - Maximum Tendon Tensions

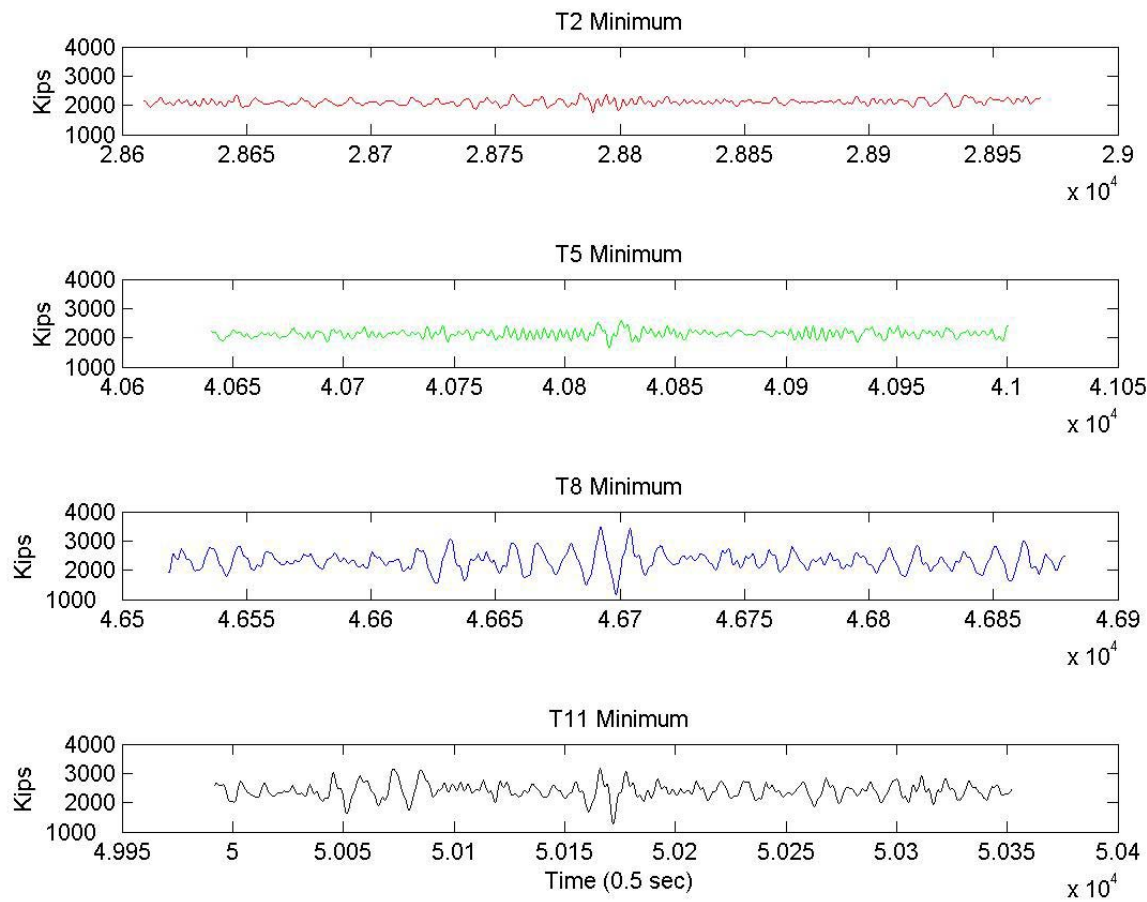


Figure 37 - Minimum Tendon Tensions

5.3 Components of the Design Recipe – Tendon Tension Extremes

5.3.1 The distribution of maximum and minimum tendon extremes was also investigated in the time domain. Standard linear models for a fully developed, wind-generated sea (no swell) assume the water surface elevation is formulated as a stationary, narrow-banded Gaussian (normally distributed) process. The peaks of this process (such as the wave heights or the wave crests), assumed as statistically uncorrelated, are then represented by a Rayleigh distribution:

$$\text{Prob } (X>x) = \exp (-2x^2) \quad (3)$$

Where x is the ratio of an individual wave height H to the significant wave height H_s .

5.3.2 The maximum peaks of the process (that is, the maximum waves in the seastate) can be described by a Gumbel distribution. The probability distribution for the largest individual wave normalized by the significant wave height (X_N) amongst a large number N of waves is:

$$\text{Prob } (X_N < y) = \exp \{ -\exp [-(y - a_N) / b_N] \} \quad (4)$$

$a_N = 0.5 (2\ln N)^{1/2}$ is the modal or most probable maximum value of the wave height normalized by H_s

$$b_N = a_N / (2 \ln N)$$

5.3.3 The same standard models and statistics discussed above for wave heights can be applied to the responses of a linear system to linear Gaussian input. However, non-linear effects are known to cause TLPs to have a non-Gaussian quality to their response.

5.3.4 As a consequence, the maximum and minimum extreme tendon tensions may deviate from a Rayleigh distribution due to non-linearities in the environment or in the structural response, leading to maximum tendon extremes that are greater than those predicted by a Rayleigh distribution or minimum tendon extremes that are lower than those predicted by a Rayleigh distribution. In other words, the probability of exceeding a given level of response may exceed the values predicted by Equations (3) and (4). The non-Gaussian quality of the TLP response can also be verified by kurtosis values exceeding 3.0 such as in Table 11.

5.3.5 In order to cover these non-linear and non-Gaussian deviations, a ‘design recipe’ approach is often used in design. According to API RP 2T⁴⁶ the following needs to be considered:

- Pretension at mean sea level
- Tide / surge variation
- Overturning due to wind and current
- Set-down due to static and slowly varying offset
- Wave forces / wave induced motions about the mean offset
- Foundation mispositioning
- Ringing and springing
- Tendon load sharing
- Vortex shedding
- Other design margins

5.3.6 These can be summarized in the equations⁸⁰ below:

$$T_{\max} = T_{\text{mean}} + [T_{\text{unc}} + T_{\text{mis}} + \Gamma \sqrt{(\gamma^2 T_{\text{rms}}^2 + T_{\text{rra}}^2)}] \quad (5)$$

$$T_{\min} = T_{\text{mean}} - [T_{\text{unc}} + T_{\text{mis}} + \Gamma \sqrt{(\gamma^2 T_{\text{rms}}^2 + T_{\text{rra}}^2)}] \quad (6)$$

5.3.7 In the above equations, T_{\max} and T_{\min} are the maximum and minimum tendon tensions. T_{mean} is the mean tension due to static effects such as pretension, tide / surge variation, overturning due to static wind and current. T_{unc} covers modeling uncertainties and general design margins while T_{mis} covers foundation mispositioning. T_{rms} is the root mean square (RMS) dynamic tendon tension due to low- and wave-frequency components, calculated from a numerical model. A correction factor γ is introduced to account for deviations between numerical predictions of T_{rms} and model test results. T_{rra} accounts for resonant-frequency tension variations due to nonlinear ringing and springing excitation of the TLP in its vertical modes as well as any contribution from VIV and is estimated directly from model tests. The Γ parameter accounts for the non-Gaussian quality of the response based on tendon tension statistics derived from model test data.

5.3.8 The non-Gaussian quality of the response is usually not a concern as it is incorporated in TLP design by means of model tests, but it is important to verify if the current design recipes capture the degree of non-Gaussian quality in an event such as Lili.

5.3.9 A comparison between measured maximum peak tendon tensions and the values implied by a Rayleigh distribution (straight line in the plots) was performed for all instrumented tendons and TIs. A summary of results may be viewed in Figures 38 to 41. Each tendon has at least one maximum peak that deviates from the Rayleigh distribution but the deviations are consistent with those usually observed from model tests and included in design.

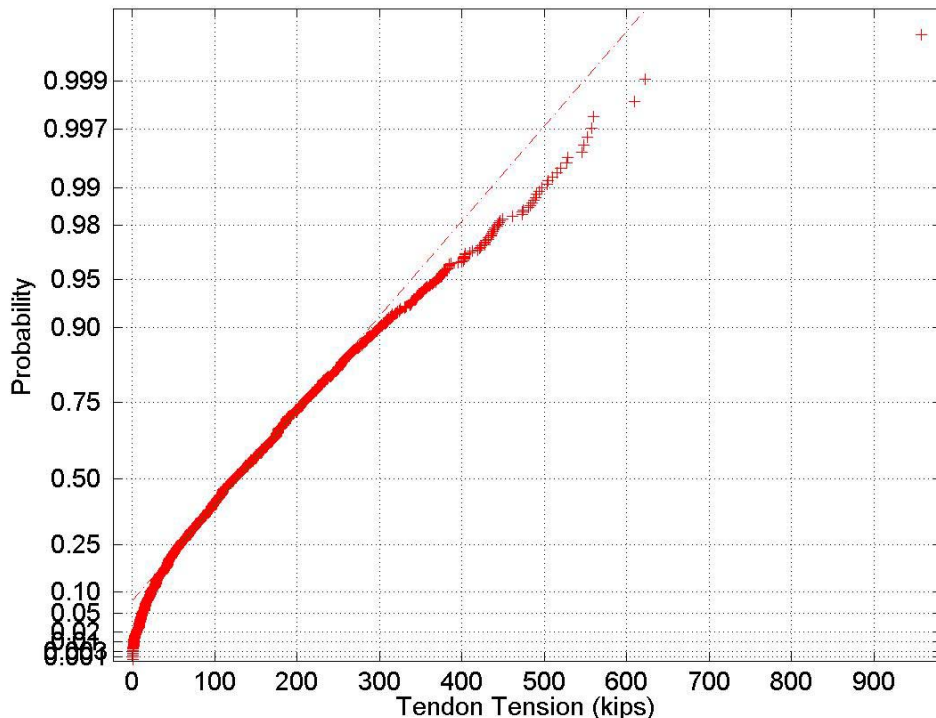


Figure 38 - Probability of T2 Peak Tension for TI 12

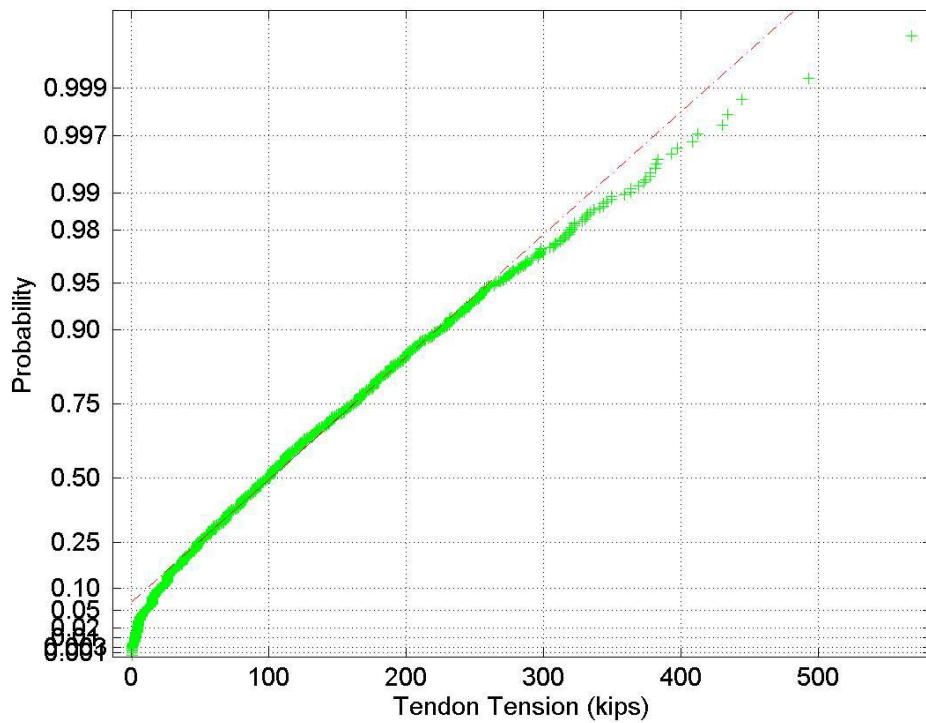


Figure 39 - Probability of T5 Peak Tension for TI 12

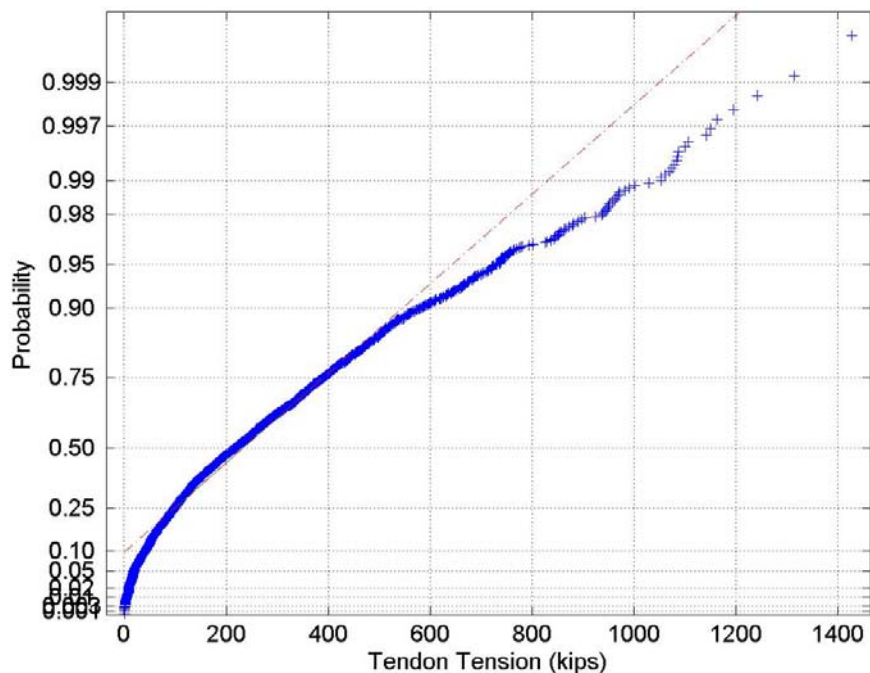


Figure 40 - Probability of T8 Peak Tension for TI 15

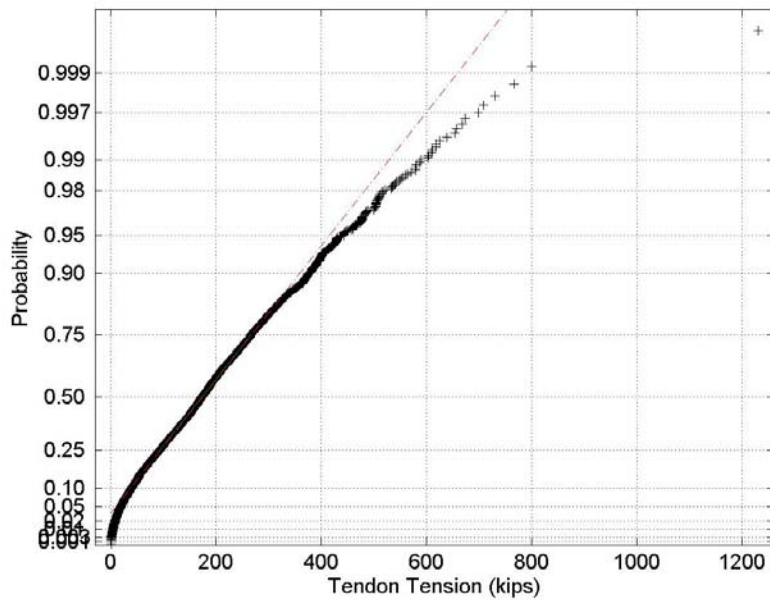


Figure 41 - Probability of T11 Peak Tension for TI 18

5.3.10 Likewise, comparisons between measured minimum peak tendon tensions and a Rayleigh distribution (straight line in the plots) may be viewed in Figures 42 - 45. Minimum tendon peaks exhibit trends similar to maximum tendon peak distributions with extreme values deviating from the Rayleigh distribution but within expectations.

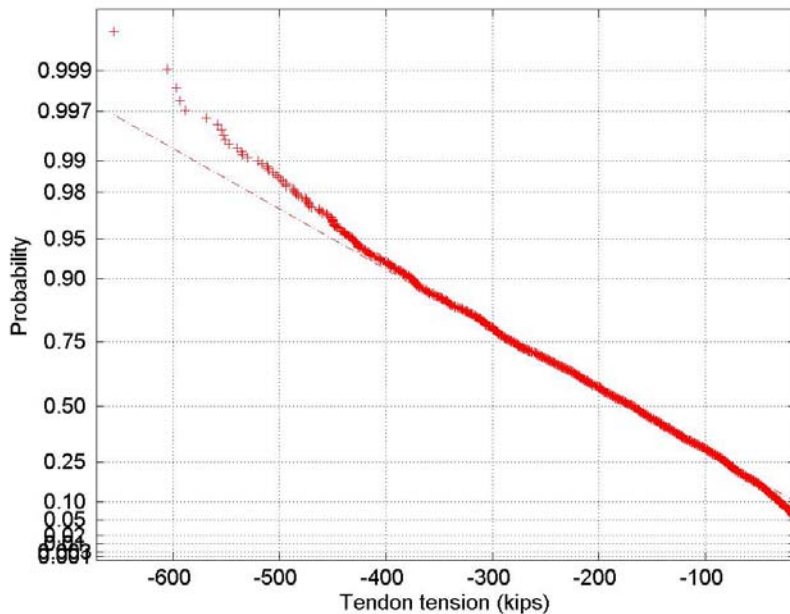


Figure 42 - Probability of T2 Minimum Peak Tendon Tension for TI 15

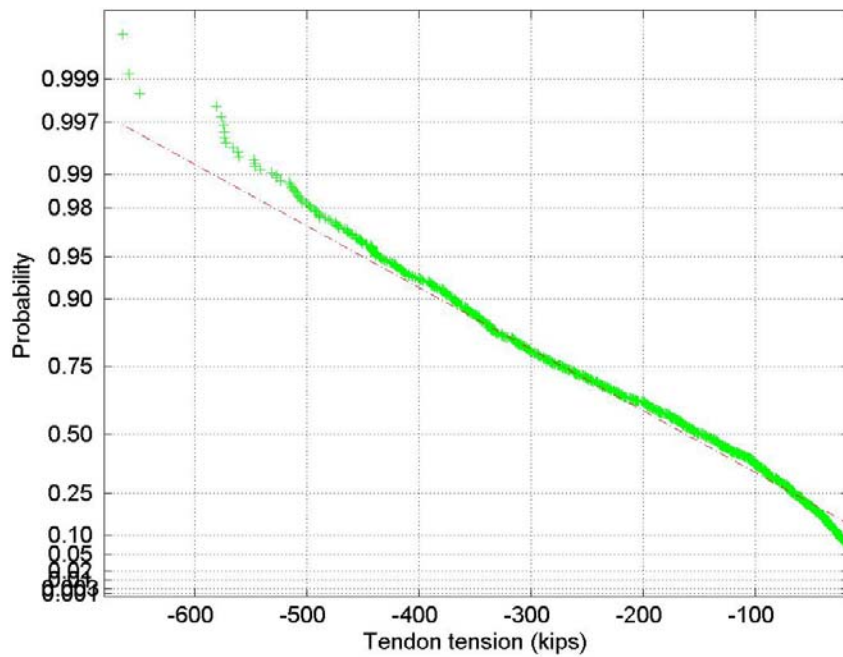


Figure 43 - Probability of T5Minimum Peak Tendon Tension for TI 15

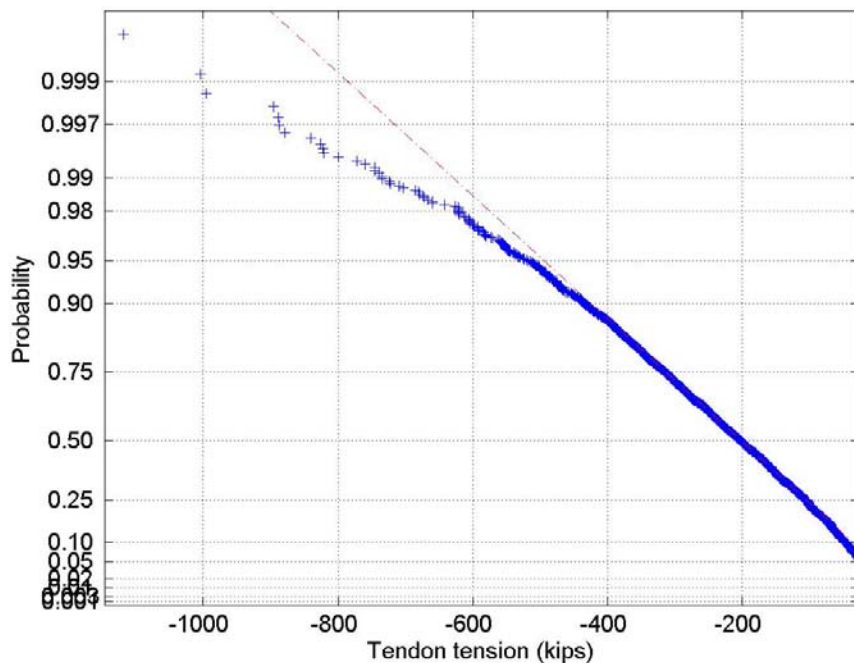


Figure 44 - Probability of T8 Minimum Peak Tendon Tension for TI 18

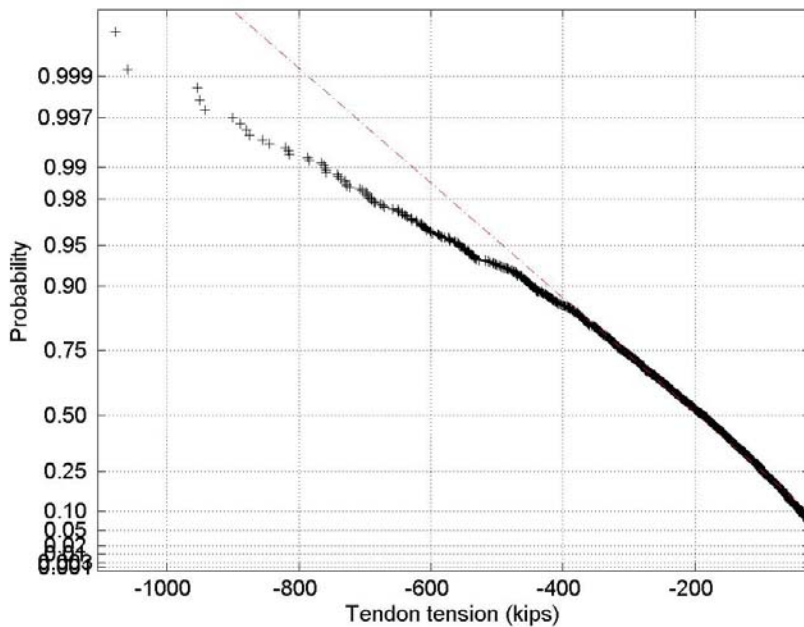


Figure 45 - Probability of T11 Minimum Peak Tendon Tension for TI 15

5.3.11 The calculated Γ values (Equations 5 and 6) for maximum and minimum tensions may be seen in Table 12. The measured Γ values for maximum and minimum tendon tensions exhibit great variability, which is consistent with the results of model tests⁸⁰.

5.3.12 Γ values vary for each tendon and sea state. Minimum tension Γ values are much larger than maximum tension Γ values suggesting that minimum tendon tensions were more non-linear than maximum tendon tensions.

Table 12 - Measured Γ Values

| Hours | Max Tension | | | | Min Tension | | | |
|-------|-------------|-----|-----|-----|-------------|-----|-----|-----|
| | 3 | 6 | 9 | Ave | 3 | 6 | 9 | Ave |
| T2 | 5.0 | 3.2 | 4.3 | 4.2 | 5.6 | 5.0 | 5.9 | 5.5 |
| T5 | 2.6 | 3.1 | 2.9 | 2.9 | 7.2 | 4.7 | 5.8 | 5.9 |
| T8 | 3.3 | 3.8 | 4.7 | 3.9 | 5.9 | 5.0 | 6.4 | 5.7 |
| T11 | 2.4 | 3.9 | 5.2 | 3.8 | 7.0 | 6.1 | 6.5 | 6.5 |

5.4 Design Recipe – Natural Frequencies and Energy Content

5.4.1 Frequency domain analyses were carried out to verify the design estimates for natural frequency and energy content. As previously discussed, considering its entire duration, Hurricane Lili was clearly not a stationary process. For the frequency domain analyses it was assumed stationary for periods of one hour, which were broken down into ten-minute time series to create six independent zero-mean realizations per hour.

5.4.2 Power Spectral Densities (PSD) of the motion and tendon tension data were then computed for these ten-minute realizations. The PSDs of these ten minutes blocks were then averaged to give a single PSD for each hour. This procedure was carried out for all tendon data to reduce the jaggedness and error of the equivalent hourly PSD computed alone. For consistency the same nine hours containing the peak hurricane data in Tables 9 and 11 were analyzed using this averaging method.

5.4.3 Table 13 contains the natural frequencies for Brutus. The response at the wave peak energy (approximately 12 seconds which in good correlation with the hindcast study²) as well as the resonance behavior may be viewed in Figures 46 and 47 which show a typical PSD for surge. Figures 46 and 47 also show wave loading at a frequency corresponding to waves with a length similar to the column spacing. Figure 46 is the result of the PSD averaging method and the resulting PSD estimate is quite smooth, while the PSD in Figure 47 has not been averaged. Figure 47 is a “raw” PSD and clearly illustrates the jaggedness associated with a PSD resulting from a single response realization.

5.4.4 PSD plots were also created for sway, heave, pitch and roll but were not included here to avoid repetition since they do not provide any additional information.

Table 13 - Natural Periods at Relevant Load Condition

| | Period (s) | Frequency (rad/sec) |
|-------|------------|---------------------|
| Surge | 118 | 0.05 |
| Sway | 132 | 0.05 |
| Heave | 3.55 | 1.77 |
| Roll | 3.34 | 1.88 |
| Pitch | 3.2 | 1.96 |

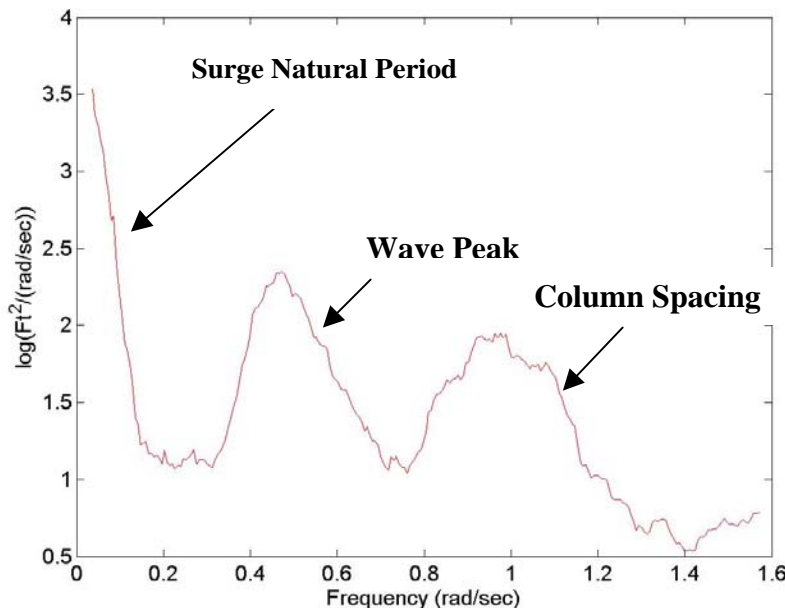


Figure 46 – Example Surge PSD

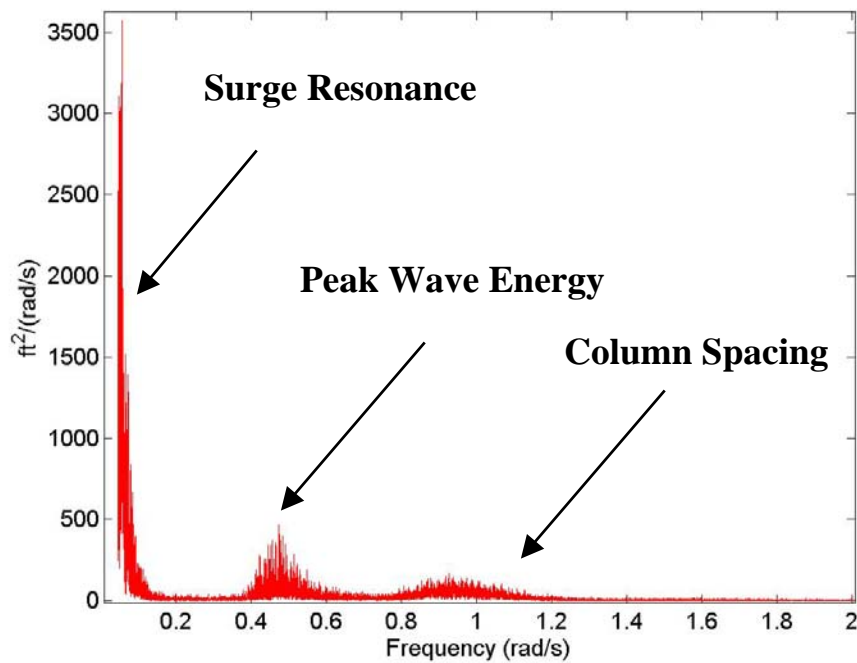


Figure 47 – Example Surge PSD

5.4.5 Figure 48 shows a typical tendon PSD (for T2). The energy at the surge / sway resonance frequencies (around 0.06 - 0.13 rad/sec or 50 – 100 sec) is dominant and was excluded from Figure 48 to permit a better visualization of the other components. Figure 48 also excludes the high frequency vortex shedding components which are discussed later in the report. As with the motion PSDs, resonant behavior may be identified with tendon PSDs.

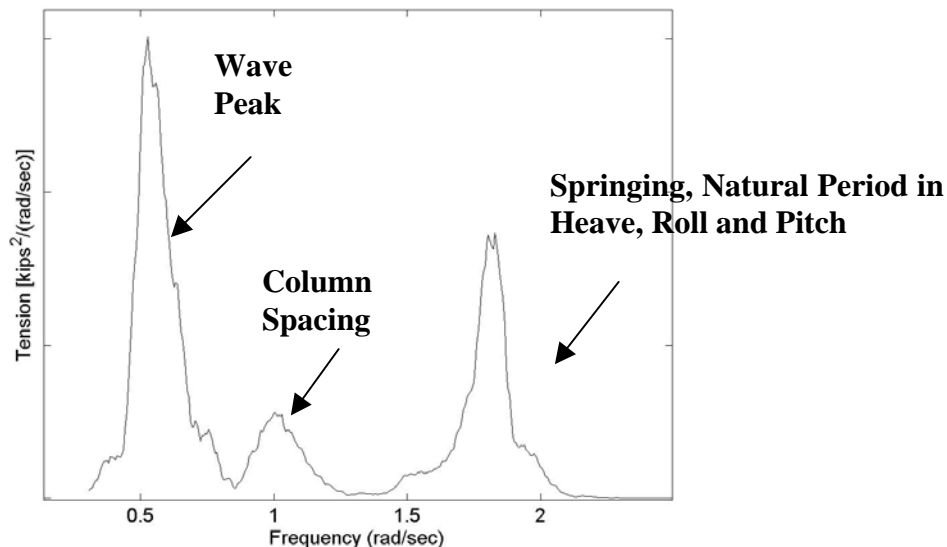


Figure 48 – PSD for Tendon Tension (T2)

5.4.6 PSD plots for each motion (sway & surge) and tendon (4) and for each hour (9) were also generated. The majority of the PSD plots exhibit the same model responses of the platform with only slight differences in energy content attributable either to differences in environment or the random nature of the process. The remaining PSD plots were therefore not included here to avoid repetition.

5.4.7 Coherence plots were created for all the possible tendon-tendon combinations and for each TI. For example, Figure 49 contains coherence plots between the diagonally opposite tendons T5 and T11 during the peak of the hurricane. The coherence plots show that the tendon tensions contain relatively similar energy levels at the same frequencies (peak energy due to motion resonance, wave loading and springing).

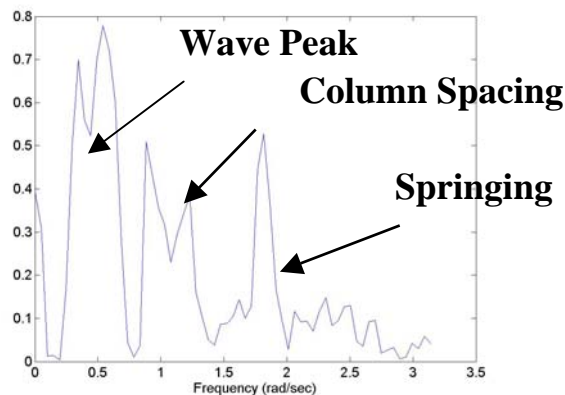


Figure 49 - Coherence between Tendons T5 & T11

5.4.8 Coherence plots were also created between all combinations of motions and tendon tensions. Figure 50 contains the coherence plots between surge motion and the average tension for two tendons, T2 and T5. Adjacent tendon tensions were time averaged to reduce independent tendon response. No unusual behavior is identified and the average tension for T2 and T5 is more highly correlated in the surge resonance frequency.

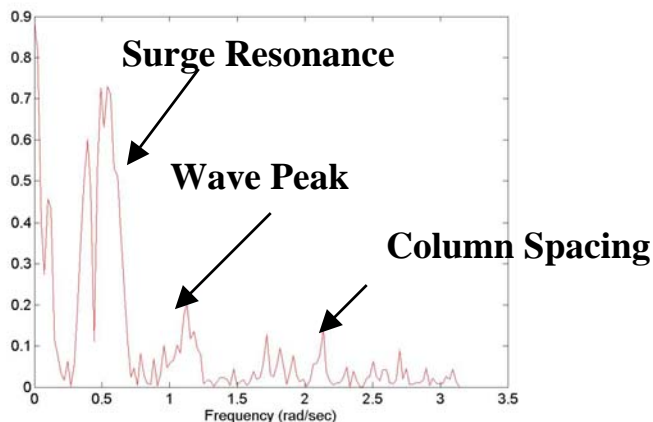


Figure 50 - Coherence between Surge and T2 & T5 Average

5.5 Design Recipe – Damping

5.5.1 Damping may significantly affect design predictions but it is not easy to quantify for a complex dynamic system such as a TLP. Damping estimates were obtained here from spectral analyses of the full-scale measured data using the half bandwidth method.

5.5.2 Investigations^{82,83} of the half bandwidth method as applied to offshore platform response to wave and wind loading suggest that damping estimates using the half-bandwidth method are a function of frequency resolution and typically have errors of the order of ten to twenty percent. The required frequency resolution for half bandwidth estimates for a TLP has been estimated⁸³ to be a minimum of four half bandwidth points around the spectral peak.

5.5.3 Tendon tensions were recorded at 2 Hz and for the ten-minute realizations considered here there are in excess of 100 points around the peaks which should provide sufficient resolution for damping estimates. However, it should be recognized that the underlying process was seen to be inherently non-stationary and the measured data represents purely a set of realizations of a random process. The available information concerning the environmental conditions was less than complete and therefore did not permit an independent verification of the estimated damping values.

5.5.4 Table 14 contains the wave frequency surge and sway damping estimates using the half-bandwidth method for each of the hurricane 9-hour segments taken from the measurements. Likewise, Table 15 contains the results for pitch and roll damping. The damping ratio (coefficient of damping / coefficient of critical damping) estimated for surge and sway from the measurements was in good agreement with the values used in design, which were 11.5-11.8%. The damping estimated for pitch and roll from the measurements exceeded the value used in design, which was of 0.4%.

5.5.5 It is noted that the roll and pitch resonance in the measurements may contain heave resonance as well, since their respective natural frequencies are nearly identical and difficult to filter out. This feature could have an influence in the larger damping values shown in the measurements.

Table 14 - Wave Frequency Surge and Sway % Damping

| | 1 | 2 | 3 | 4 | 5 | 6 | 7 | 8 | 9 | Average |
|-------|------|------|------|------|------|------|------|------|-----|---------|
| Surge | 12.3 | 13.2 | 11.5 | 11.6 | 11.3 | 9.9 | 10.7 | 13.3 | 9.4 | 11.5 |
| Sway | 11.4 | 11.4 | 12.7 | 11.3 | 11.9 | 10.7 | 13.5 | 15.1 | 9.0 | 11.9 |

Table 15 - Resonance Roll and Pitch % Damping

| | 1 | 2 | 3 | 4 | 5 | 6 | 7 | 8 | 9 | Average |
|-------|------|------|------|------|------|------|------|------|------|---------|
| Roll | 2.68 | 2.68 | 2.52 | 2.85 | 2.85 | 3.33 | 2.85 | 3.17 | 2.19 | 2.79 |
| Pitch | 2.85 | 2.35 | 2.52 | 2.52 | 3.01 | 2.52 | 2.19 | 2.52 | 2.52 | 2.56 |

5.6 Design Recipe – Overall Bias

5.6.1 The results previously discussed indicated that the Brutus response during Lili did not approach allowable design values indicating a potential safe side bias in the design recipe. The design transfer functions for Brutus' motions and tendons were available and used in conjunction with the hindcast environmental data, permitting further comparisons between design models and full-scale responses. The transfer functions were for head, beam, and quartering sea conditions, without current and wind effects.

5.6.2 The peak hurricane sea state assumed had significant wave height $H_s = 36.85$ ft and spectral peak period $T_p = 13.0$ sec for use in a JONSWAP spectrum with a peak shape factor equal to 3.3. A theoretical response spectrum was then obtained using the transfer functions derived from numerical models of Brutus. The theoretical power spectrum of response was then compared with the results from a spectral analysis of the measured data. The measured spectrums for the three critical TIs in Tables 9 and 11 were considered.

5.6.3 Comparisons for surge and sway are shown in Figures 51 and 52 which show fairly reasonable correlation between the calculated and measured response power spectrums. Due to geometrical symmetry of Brutus, surge and sway exhibit similar responses. The only notable difference between the measured and model spectrums occurs at a frequency of 1 rad/sec which is believed to be wave energy associated with the column spacing of Brutus.

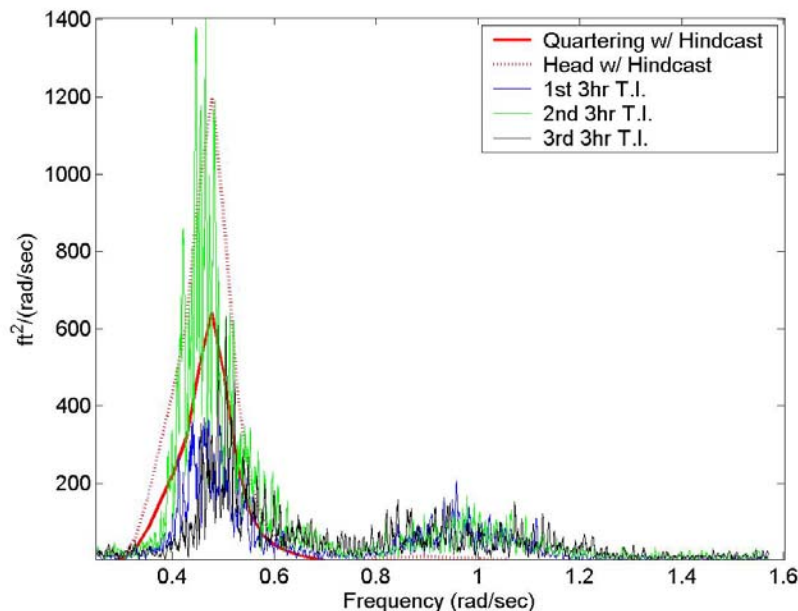


Figure 51 - Surge Response Comparison

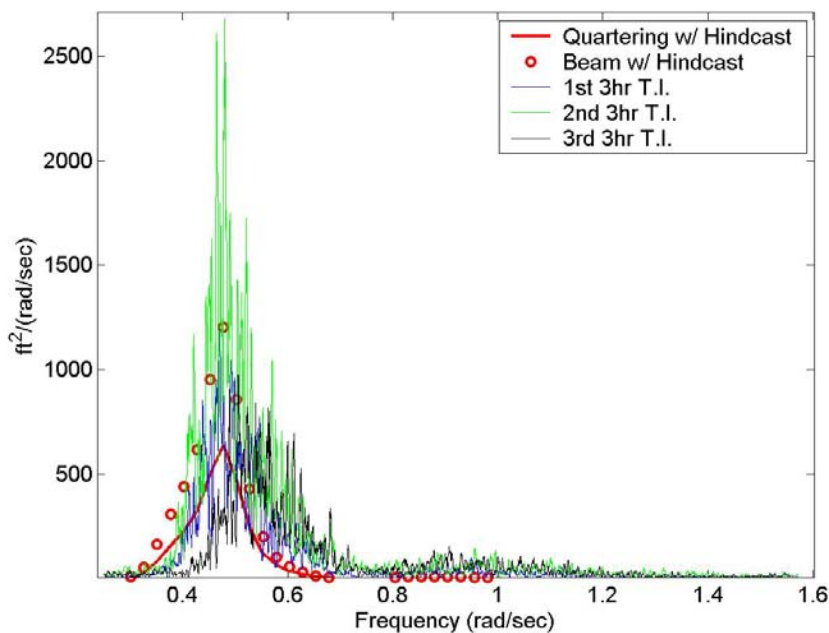


Figure 52 - Sway Response Comparison

5.6.4 Comparisons between measured and calculated tendon tension response spectrums may be viewed in Figures 53-56. The comparison between tendon response spectrums shows the tendons behaving in pairs. The magnitude and shape of the wave energy response for the tendon pairs, T2 & T5, and T8 & T11, differ substantially. The measured responses for tendon pair T2 & T5, shown in Figures 53 and 54, exhibit much lower magnitudes than the theoretical responses for all directions.

5.6.5 However, the theoretical responses for tendon pair T8 & T11, shown in Figures 55 and 56 exhibit magnitudes on par with those obtained from the measurements. It is also important to notice that the measured spectrums for tendons T2 & T5 do not exhibit the same energy peak, at 0.5 rad/sec as tendons T8 & T11. Tendons T8 and T11 had larger maximums and greater variability than the other two tendons, which is consistent with increased energy content.

5.6.6 Directionality of the environment is the most likely explanation for the difference in energy content between tendon pairs but this could not be independently verified.

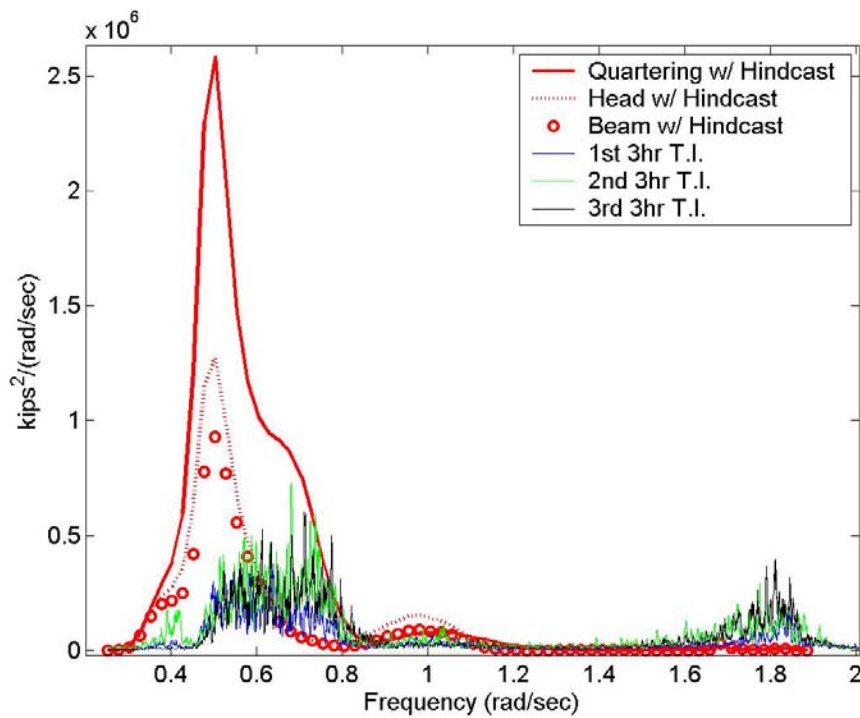


Figure 53 - T2 Response Comparison

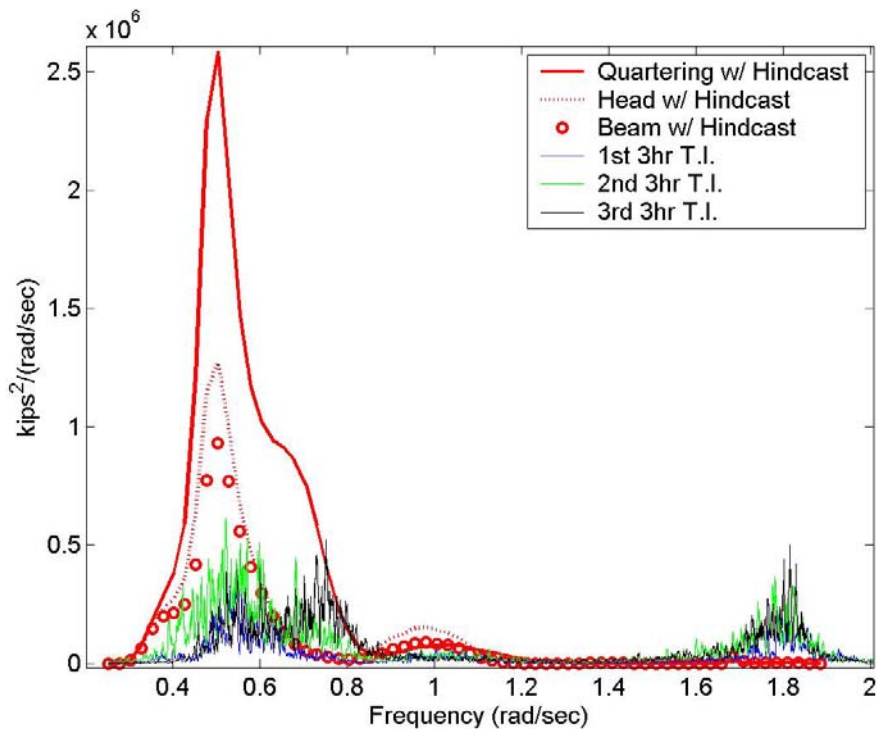
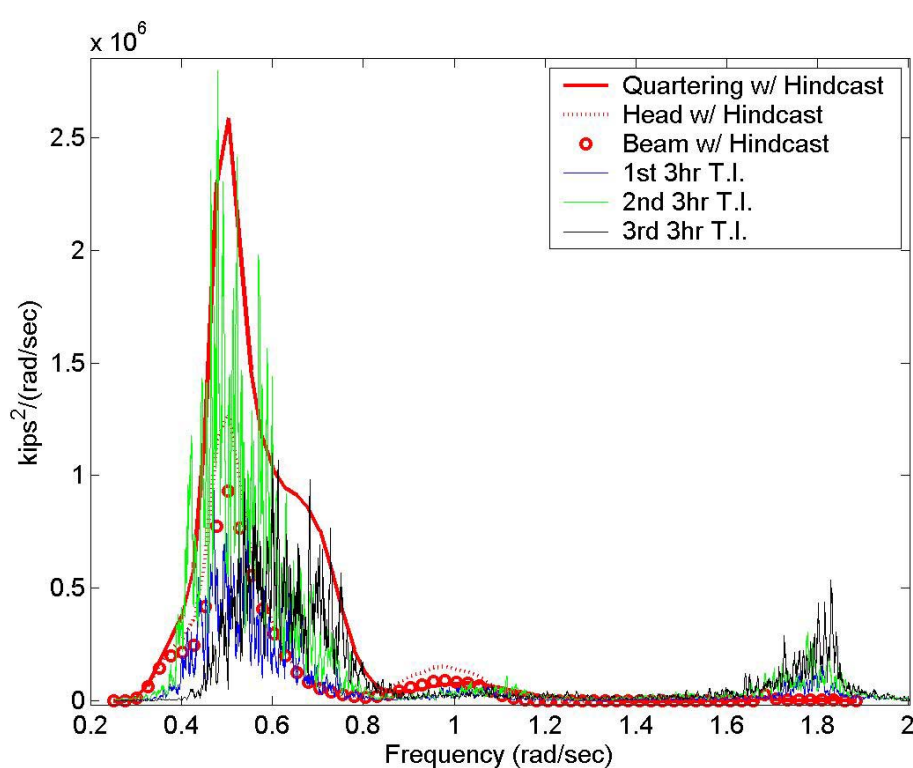
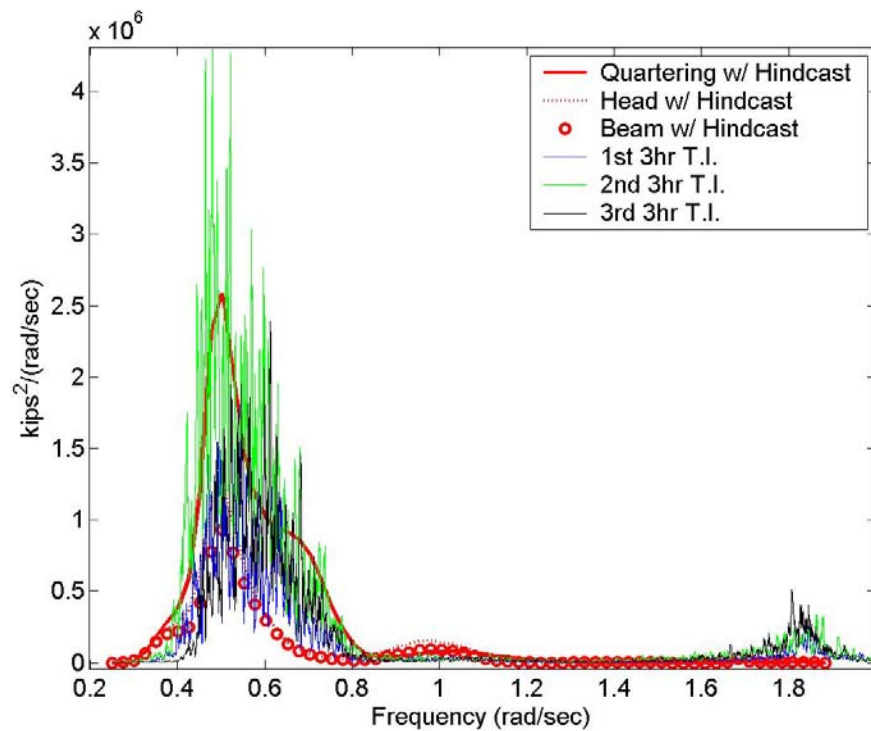


Figure 54 - T5 Response Comparison



5.6.7 Overall the comparisons suggest that although the tendon transfer functions do not accurately represent the individual tendon energy for a particular direction, there is an overall safe side bias in the design models. This is further reinforced by the fact that the design transfer functions do not contain current and wind effects while the measured response spectrums will contain some periodic components of the fluctuating wind and current energy from a continually transient sea state.

5.6.8 The spectral limitations of the model and full-scale measurements must also be recognized. The numerical model transfer functions only yield response results between .04 and .3 Hz, with a frequency step of .004 Hz, which is coarse in comparison to the measured tendon responses, with a range of 0 to 1 Hz and frequency steps of 6.0×10^{-4} Hz. The model response spectrums are from idealized conditions and therefore their response is smooth and stationary. The measured response spectrums have their typical spectral limitations as well, mainly non-stationarity and “jaggedness”.

5.7 Vortex Shedding Effects

5.7.1 Although traditional spectral techniques are informative they give little indication of the energy evolution with respect to time, which is important for a non-stationary process like a hurricane. The spectrogram provides spectral energy with respect to time and as time and frequency resolutions are inversely related, an informative balance is conveyed to the reader. Spectrograms are explained in more detail in the open literature⁸⁵. Frequency and time are plotted along the axes, while energy intensity is represented by color, with red and blue being the maximum and minimum energy, respectively.

5.7.2 Figure 57 gives the spectrogram for T2 tendon tensions for the entire twenty-one hour time series. The intensity of response at the various frequency ranges is given in a log scale (kips^2/Hz) by the colors, with red indicating more intense response. Not only can the natural frequencies and wave energy be identified in the spectrogram as with a PSD, but the evolution of the energy may be seen. The wave energy, approximately .1 Hz, is a prime example of time dependency. At the beginning of the time series, the wave energy is predominately yellow. As the hurricane impacts Brutus, at approximately 4×10^4 seconds, the wave energy increases and becomes predominately red.

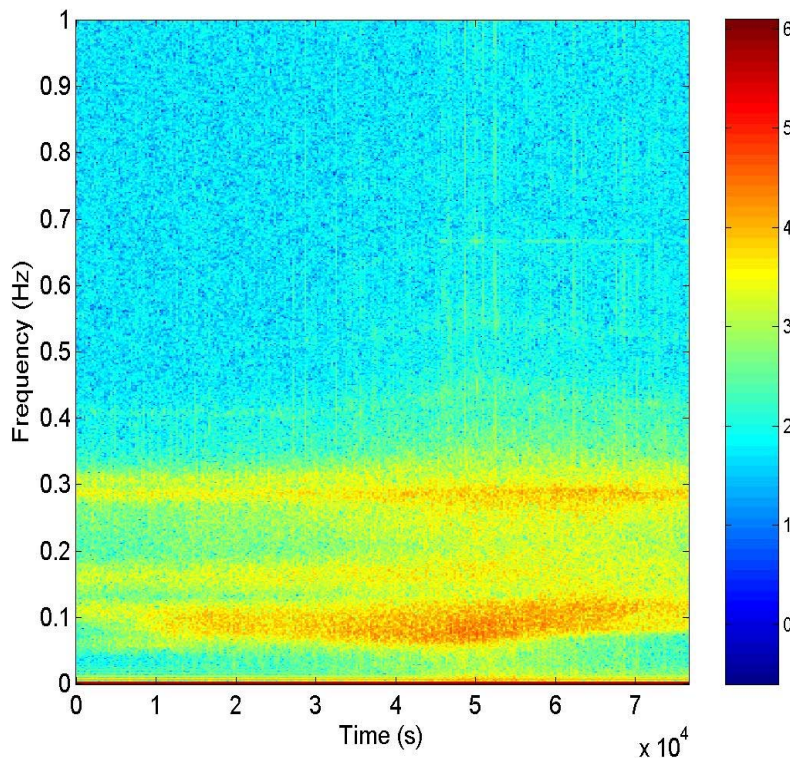


Figure 57 - Spectrogram for T2 Tendon Tension

5.7.3 The spectrogram permits vortex-shedding modes to be easily identified. The spectrogram for T2, Figure 57, shows a faint yellow band of energy at around 0.45 Hz representing the first vortex shedding mode. T2 experienced the most VIV energy of all the tendons and is limited to occurring for only two consecutive hours.

5.7.4 As time progresses and the hurricane intensity increases, the VIV modal frequency also increases. The change in modal frequency is analogous to tightening a guitar string. Increasing or decreasing tension produces parallel changes in modal frequencies. For Brutus, the mean tendon tension is increasing because of the increased platform offset during the peak of the hurricane. Higher vortex shedding modes exhibit the same characteristic and may be viewed (albeit faint) as well. The information from the spectrogram is limited by the frequency of sampling which in this case is of 2 Hz.

5.7.5 VIV of tendons has been seen to excite hull structural modes under intense currents⁵⁵. However, no hull structural modal response was apparent on Brutus during Lili. However, it is noted that the sampling rate of the tendon tensions was too low to capture structural resonance above 1 Hz.

5.7.6 The magnitude of the vortex shedding effects can be roughly estimated from the tendon tension PSD in Figure 58. The vortex shedding excitation spikes are clear for the frequency range exceeding 0.45 Hz. By integrating the energy in this frequency bands a significant

tendon tension amplitude value of around 25 kips was estimated. Such additional tension was not of concern as shown by the maximum and minimum tendon tensions discussed in the time-domain results.

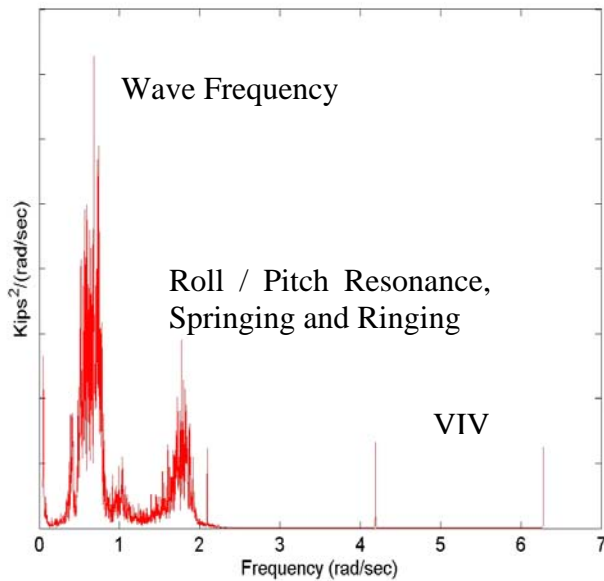


Figure 58 - T2 PSD including High Frequency Response

5.7.7 The possibility of VIM was also considered. For the hindcast peak current velocity of 1.8 knots (Table 2) a vortex shedding frequency of 0.009 Hz (period of 108 sec) was estimated from Equation 1. This coincides with the surge and sway resonant periods given in Table 13 thus making it difficult to clearly separate hull VIM from surge / sway resonance in the tendon tension PSDs for Hurricane Lili. VIM could also be identified by significant yaw of the TLP but this degree of freedom was not monitored. Finally VIM could be verified by significant motions in a direction orthogonal to the direction of the flow but this cannot be clearly defined as Lili changed direction as it developed its peak intensity.

5.7.8 VIM would best be identified during high current and minimal wave conditions such as at the current peak about 24 hours following the hurricane peak winds because hurricane winds and waves would have significantly subsided by then. However, tendon tension data was not available for this period of time.

5.7.9 The overall magnitude of the tendon tensions as well as the comparisons of specific components of the design recipe previously discussed in this report did not suggest any unforeseen tendon tension components. It appears from these observations that VIM was either not present or if present was not of concern vis-à-vis the unit's design recipe. On a side note, the down current columns in a 4-column TLP could affect the vortices shedding from the up current columns. In addition, the flow around the down current columns would no longer be uniform and unidirectional. This would reduce the likelihood of the down current columns inducing vortex shedding.

6. RESULTS FROM MONITORING DATA FOR TYPHOON AND ALLEGHENY

6.1 Introduction

- 6.1.1 The discussion in this section is based on results provided⁶⁴ by Atlantia Offshore concerning a comparison between measurements and predictions for the Typhoon mono-column TLP and contains less detail than the Brutus analysis.
- 6.1.2 Atlantia has also provided⁸⁹ predictions indicating that the tendon tensions at the Allegheny mono-column TLP were well within their design limits but these are not discussed any further as there were no measurements available to compare with such predicted results.

6.2 Typhoon - Global Performance

- 6.2.1 Thirty-six hours (Complete Time Series for Typhoon, CTS) of tendon tension monitoring data, sampled at 4 Hz were available. The maximum measured tendon tension was of 2867 kips which represented 94% of the 100-year maximum tendon tension calculated in design⁶⁴.
- 6.2.2 The minimum measured tendon tension was 788 kips while the 100-year minimum tendon tension calculated in design⁶⁴ was of 253 kips. It follows that, compared to the measured response during Lili, the design cases for Typhoon predicted minimum tendon tensions that were much closer to a critical condition where tendon tension is lost.
- 6.2.3 As discussed in Section 2, Typhoon was close to Lili's track and was subjected to waves, winds and currents that approached 100-year values and the above results indicate a favorable behavior of the unit.
- 6.2.4 Figure 59 contains the statistics for twenty minute time periods for a consecutive thirty-six hours. The peaks or valleys in Figure 59 show the impact of hurricane Lili on Typhoon's tendon tensions. As with Brutus TLP, Typhoon's mean tension and STD values increased as the hurricane impacted the platforms. It is interesting to note that the mean tensions for tendons T1, T5, and T6 remain elevated after the passing of Lili. The mean tension for the other tendons returned to pre-hurricane levels.

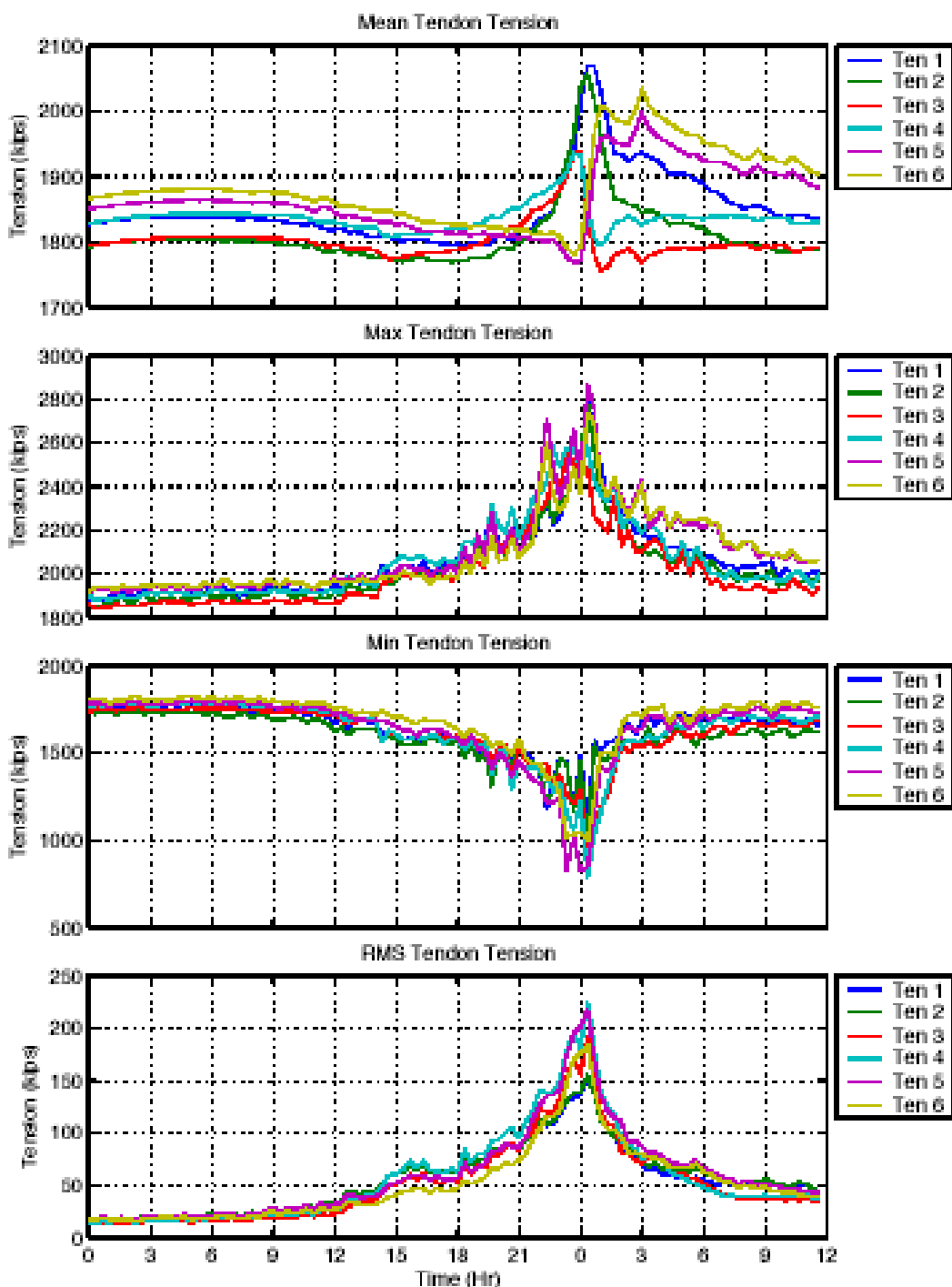


Figure 59 - Time Series of Tension Statistics⁶⁴

6.2.5 It is noted that four of the six tendons experienced both their maximum and minimum tensions during the same twenty-minute time period, between 12:20 and 12:40 am CDT on October 3rd. This could be due to a single environmental event caused the extreme tensions to occur. However, without detailed wave records it is not possible to independently verify this possibility.

6.3 Typhoon Design Recipe – Overall Bias

6.3.1 The design allowables considered in the previous Section include factors, margins and allowances aimed to provide the operator with flexibility in operating the platform.

6.3.2 Additional comparisons were therefore made⁶⁴ between the measurements and design predictions excluding such extra margins. Best estimates of the TLP configuration (weight, draft, etc.) and of the environmental conditions during Lili (from the hindcast study²) were used as an input to the design models. Results are summarized in Table 16.

6.3.3 The maximum measured tendon tension exceeded the predictions by 168 kips while the minimum measured tension was 296 kips less than the minimum predicted tension for Hurricane Lili. Given the environmental conditions at Typhoon and the uncertainties involved, the fact that predictions were so close to the measurements is a positive result. The results however suggest that there is limited margin for reducing conservatism in the design models for some critical headings.

Table 16 - Tendon Tension Statistics for CTS

| | Measured | | | | | | Predicted |
|-------------|----------|--------|--------|--------|--------|--------|-----------|
| | T1 | T2 | T3 | T4 | T5 | T6 | |
| Max (kips) | 2796.4 | 2779.9 | 2553.6 | 2587.0 | 2866.8 | 2737.1 | 2698 |
| Min (kips) | 1106.7 | 981.2 | 849.4 | 787.6 | 827.7 | 994.3 | 1084 |
| Mean (kips) | 1850.7 | 1812.5 | 1801.9 | 1837.3 | 1865.3 | 1884.9 | 1920 |
| STD (kips) | 54.6 | 56.2 | 51.3 | 57.7 | 59.5 | 51.7 | N.A. |

6.4 Typhoon Design Recipe – Tendon Tension Extremes

6.4.1 It is noted that the statistics obtained from the measurements for some tendons are in reasonable agreement with the standard linearized models (Rayleigh distribution) while other tendons show a significant deviation from such models. This is illustrated by the curvature in the maximum tendon tension probability distribution for one of the Typhoon tendons in Figures 60 and 61. A similar non-linearity was observed for the minimum tensions.

6.4.2 Figures 60 and 61 contain example peak tendon tension distributions for T1 and T5. As previous model and measurement comparisons in this report have suggested, each tendon exhibits a different maximum or minimum peak distribution. Tendons T3 and T4 were more Rayleigh distributed than the other tendons.

6.4.3 It is noted that TLP designers account for the effect of such non-linearities on the probability distribution of TLP response by empirical factors derived from model test data or numerical models. The deviations to the Rayleigh distribution observed for some tendons during Lili highlight that TLP designers should maintain care and diligence in performing and interpreting model tests and validating their numerical models.

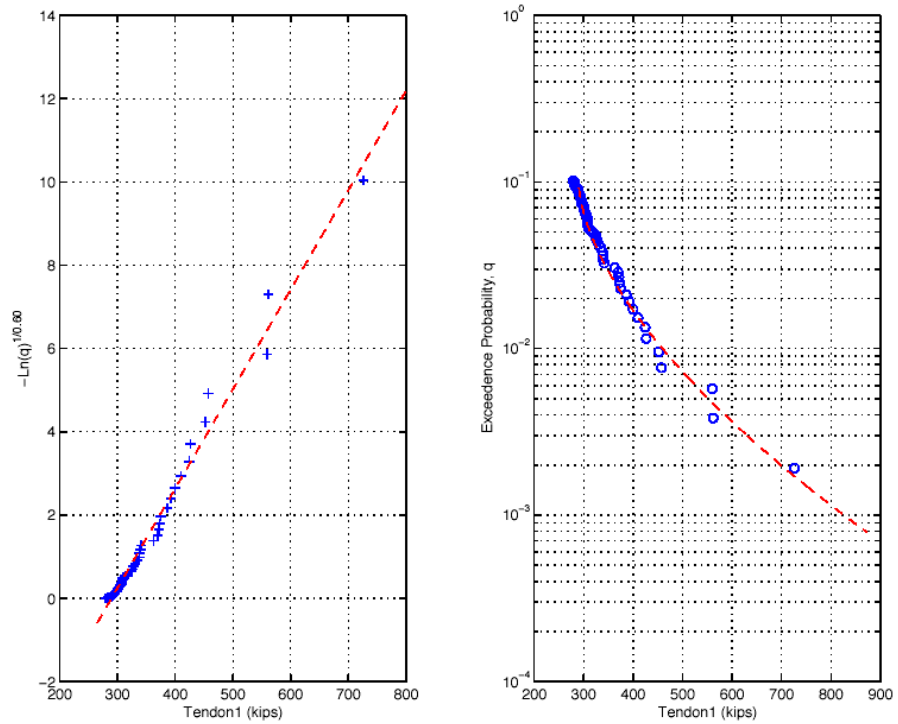


Figure 60: T1 Peak Tension Distribution⁶⁴

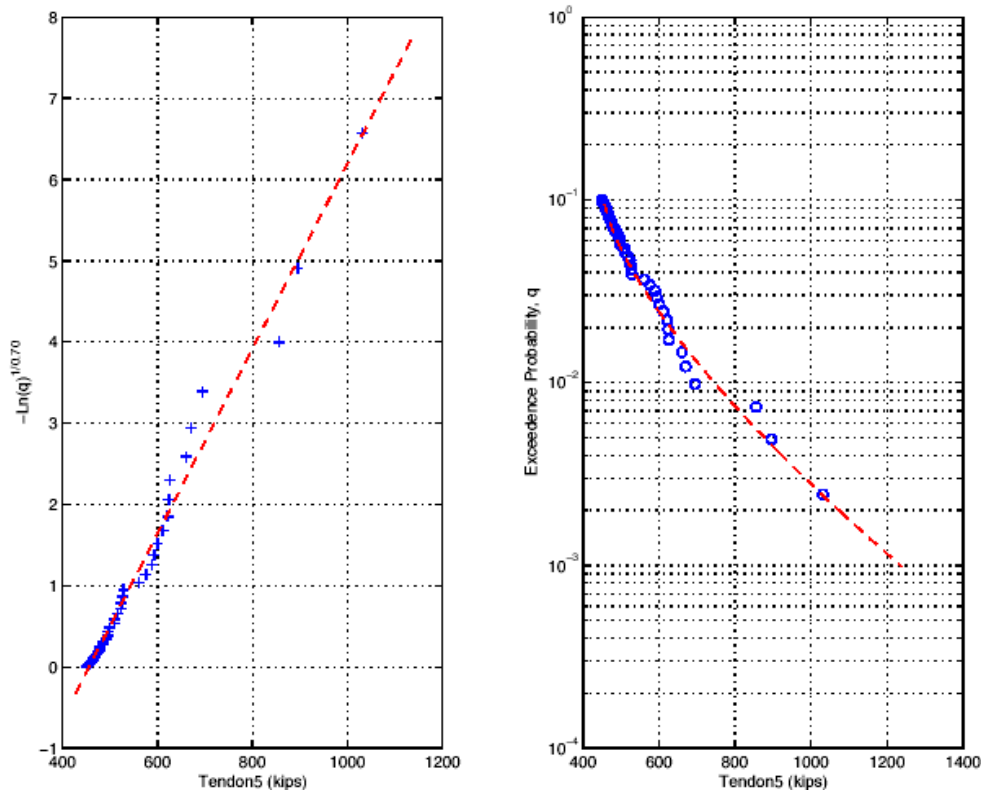


Figure 61 - T5 Peak Tension Distribution⁶⁴

6.5 Typhoon - Vortex Shedding Effects

6.5.1 Figure 62 contain the spectrograms for all six Typhoon instrumented tendons during Hurricane Lili. The vertical axis gives the frequency of response while the horizontal axis gives the time in hours as the storm developed. The intensity of response at the various frequency ranges is given in a log scale (kips^2/Hz) by the colors, with red indicating more intense response. High intensity response is usually expected at around 0.08 Hz (0.5 rad/sec) for the wave peak energy and around 0.28 Hz (1.8 rad/sec) for the TLP resonant vertical modes.

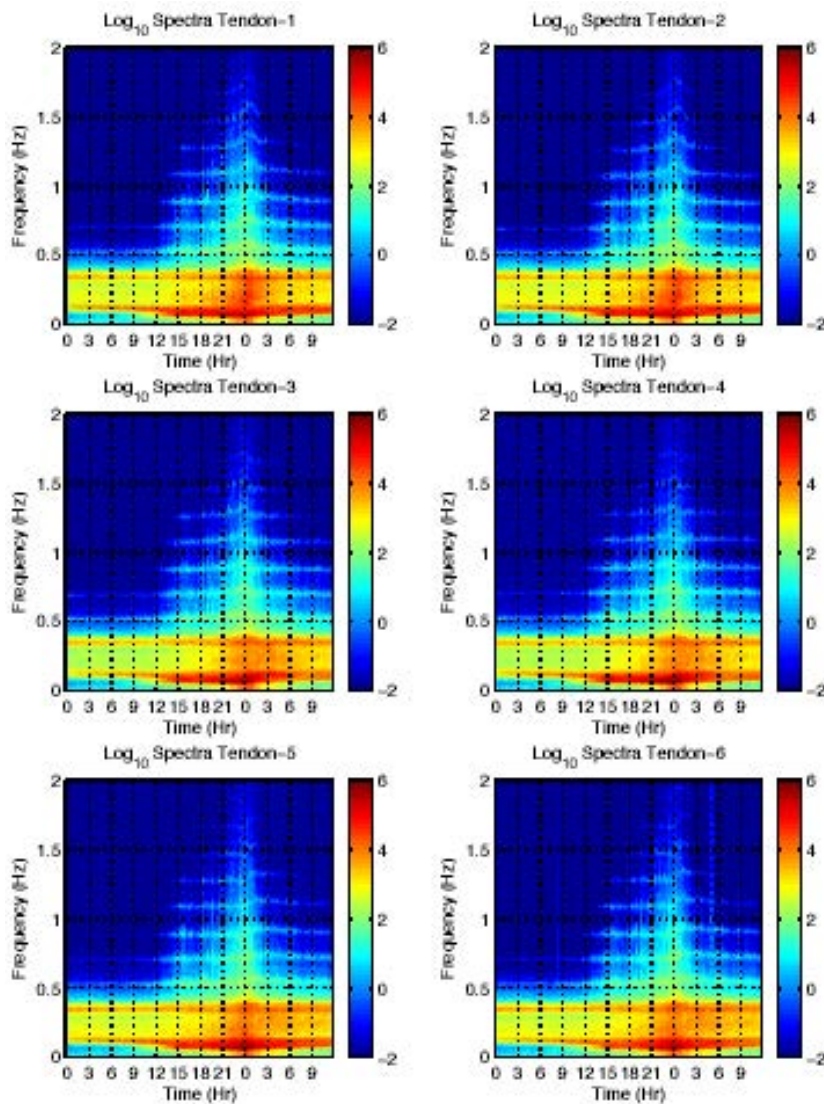


Figure 62 - Spectrograms for Typhoon's Tendons during Lili⁶⁴

6.5.2 Typhoon's tendon modal response during Lili is similar to that of Brutus. The main difference between the two, besides principal tendon dimensions, is sampling resolution. Typhoon's tension was sampled at 4 Hz in comparison to 2 Hz at Brutus and as a result

Typhoon's spectrograms have better resolution. Typhoon's spectrograms are able to more clearly show higher frequency content. Tendon spectrograms for both platforms exhibit resonant bands that increase and decrease as Lili arrives and leaves the platforms.

6.5.3 High frequency components are apparent at 0.5 Hz or higher indicating potential vortex shedding effects on the tendons but their magnitude was small and not a concern. It is noted⁸⁶ that during model tests in extreme wave conditions (with no current), this same vortex shedding excitation of tendons has been observed from an underwater camera. In a sense it is VIV, but does not reach full resonance because it is transient in nature.

6.5.4 Figure 63 shows a similar plot for Allegheny during the Millenium Eddy and relatively high energy levels can be seen for frequencies close to 2 Hz indicating excitation of structural modes. Such excitation was not present during Lili as shown in Figure 62.

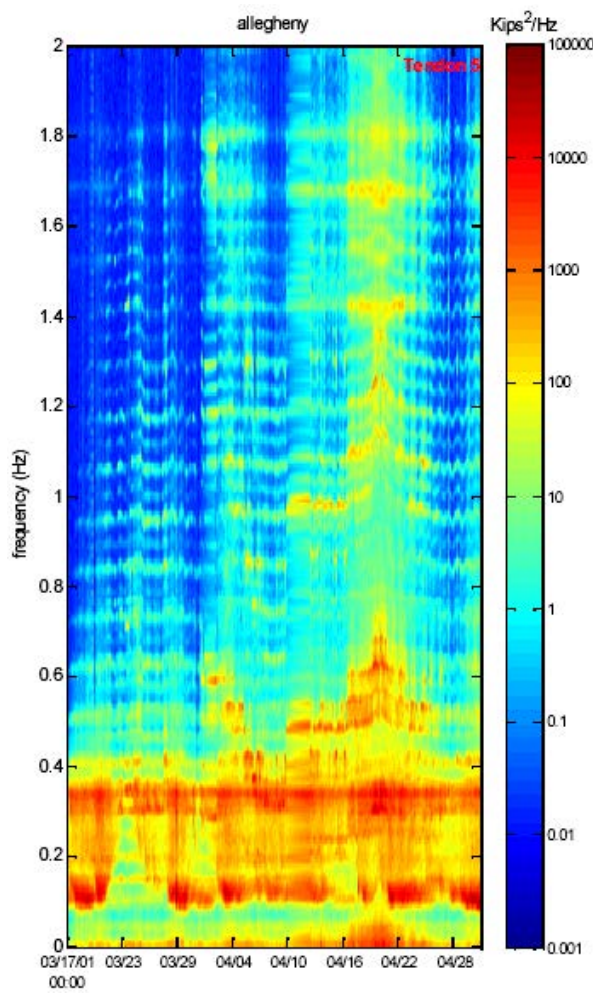


Figure 63 - Spectrograms for Allegheny's Tendon Tensions during the Millennium Eddy⁵⁵

6.5.5 Similarly to Brutus, it would be difficult to detect VIM of the hull for Typhoon but the overall magnitude of the tendon tensions suggested this was not an issue during Lili.

7. CONCLUSIONS AND RECOMMENDATIONS

7.1 Principal Conclusions

7.1.1 *1st Objective: Identify the units that were closest to Lili's track and most likely to be impacted by it.*

7.1.2 The units that were closest to Lili are shown in Figure 7: ChevronTexaco's Genesis Spar and Typhoon Mono-Column TLP, ENI's Morpeth and Allegheny Mono-Column TLPs, Conoco's Jolliet TLP, Shell's Brutus TLP and El Paso's Prince TLP. Typhoon was the unit located closest to Lili's track and subjected to the most severe environmental conditions, Table 2.

7.1.3 *2nd Objective: Collect information on any observed damage to such units and assess its significance. If significant structural damage was observed, identify potential abnormal loading (such as loss of air gap or collision) and failure mechanisms.*

7.1.4 In general, no damage to structural members was observed. Inspection data indicated damage to secondary structures located in the air gap such as ladders and boat landings (up to 55ft above sea level) but no evidence of air gap loss was found. In general, the units were subject to motions that led to damage of some topsides equipment.

7.1.5 *3rd Objective: Assess the environmental conditions during Lili and if these were of a sufficiently large magnitude to test the design of the units affected. Identify and collect any measured data that would assist in assessing the performance of the units. Verify if the performance of the units during Lili stayed within their design limits.*

7.1.6 The hindcast study and the measurements obtained of wind (for Brutus) and of current (for Genesis) suggest that the environmental conditions during Hurricane Lili were sufficient to test the response of Typhoon, Brutus and Genesis relative to their relevant design events.

7.1.7 Motion and tendon tension measurements were obtained for Brutus and verified to be within design limits. Tendon tension measurements were obtained for Typhoon and were also within design limits. Tendon tensions were calculated for Allegheny and found to be within the design limits.

7.1.8 It is noted that no monitoring data was available for Allegheny, Jolliet, Prince and Genesis as their monitoring systems were not operational during Lili. Unfortunately, valuable monitoring data was not recorded precisely when such platforms were subject to a significant environmental event. A contributing factor for this occurrence was that the units were evacuated during Hurricane Isidore and powering of the monitoring system had not been restored (or failed) during Lili. It is understood that some units are currently upgrading the batteries that power their monitoring systems.

7.1.9 *4th Objective: Verify the data collected against current knowledge from the point of view of design environmental conditions and assess any safe / unsafe bias.*

7.1.10 High quality buoy data provided the best indication of winds and waves during Lili and Oceanweather's hindcast model provided an accurate representation of the data measured at the buoys. The measurements obtained from these production units concerning environmental conditions were disappointing and no wave measurements at all were available from any of the units considered here.

7.1.11 Wind measurements were obtained for Brutus but the buoy data was considered more applicable as it was measured nearer to the standard 10m height above sea level and without potential interference from nearby structures.

7.1.12 Some relevant current data was measured for Genesis but the data for the 29m column of water near the surface was discarded due to interference of the side lobes of the Acoustic Doppler Current Profiler (ADCP) unit. Given the complexity of modeling hurricane currents, the design current profiles examined achieved a reasonable level of competence in terms of capturing the global current loading. Relative to the measurements, the hindcast model under-predicted the surface currents and over-predicted deep currents.

7.1.13 Overall the analysis of Hurricane Lili data suggested that the design and hindcast models were reasonably competent in predicting key hurricane environmental data.

7.1.14 *5th Objective: Verify the data collected against current knowledge from the point of view of design response / performance models and assess any safe / unsafe bias.*

7.1.15 Detailed analyses of the monitoring data suggested an overall safe side bias in the design models for Brutus with room for future investigation. Minimum tendon tension was an important criterion for the design of Brutus in its intact condition and it was noted that the minimum tendon tensions during Lili did not approach a critical condition of zero tension at all.

7.1.16 Detailed analysis of the monitoring data indicated that, given the uncertainties involved on the environmental conditions, the design models for Typhoon predicted tendon tensions that were reasonably close to the measurements. The results however suggest that there is no room for reducing conservatism in such design models for some critical headings.

7.1.17 *6th Objective: Review past operational experience and briefly document key issues of concern to the industry. These are understood to be prediction of meteorological data, its translation into design bases, and the impact of vortex shedding effects on the behavior of risers and TLP tendons as well as on the motions and therefore global performance of deepwater floating production installations. Assess if the data collected during Lili sheds new light into these issues.*

7.1.18 High frequency tendon tension response components during Lili were apparent at 0.5 Hz or higher for both Brutus and Typhoon indicating potential vortex shedding effects on the tendons. However, the magnitude of such effects was small and did not significantly contribute to the total tendon tension. No significant riser VIV was reported. Such behavior was in contrast to that observed, for example, for Allegheny during the Millennium Eddy where VIV on the tendons and risers was enough to excite modes of vibration on the TLP

structure.

7.1.19 It is difficult to clearly identify VIM for TLPs as the vortex shedding frequency may be close to the surge and sway resonant periods. The overall magnitude of the tendon tensions as well as the comparisons of specific components of the design recipe carried out in this report did not suggest any unforeseen tendon tension components. It appears from these observations that, for Brutus and Typhoon, VIM was either not present or if present was not of concern vis-à-vis the unit's design recipe.

7.1.20 More technically detailed comments and conclusions are given in 7.2 and 7.3. Recommendations are given in 7.4.

7.2 Design Environmental Conditions

7.2.1 The hindcast wind velocities appear to be lower than those calculated from the Brutus measurements based on the API RP 2A¹⁰ wind profile. The following should be noted concerning such discrepancy:

- Winds measured from large offshore platforms may be biased due to topsides induced flow distortion effects and this could have affected the measurements for Anemometer 21. Anemometer 31 was mounted at the crown of the derrick and less likely to be affected by flow around the topsides. Anemometer 31 was mounted at a height significantly greater than the standard reference 10m level and simple wind profiles factors may not apply very well in this case.
- According to Oceanweather⁶⁵ if the Brutus measured wind data were to be incorporated into the hindcast wind field, the resulting hindcast wave heights would have become seriously biased high in relation to the measurements taken at the buoys. The wind measurements taken at the buoy were at 5m and 10m above sea level and thus much closer to the standard reference 10m level.

7.2.2 It was observed that hurricane surface current values and current profiles used by designers differ between themselves far more than the values used for winds and waves. There are at least two models that have been used extensively to predict currents during hurricanes: a mixed-layer model⁶⁶ and a Turbulence Closure model⁶⁷. Both models have given similar mixed-layer averages for some platform designs⁶⁸ but the Turbulence Closure model tends to give higher surface current velocity values.

7.2.3 A validated Turbulence Closure model⁶⁷ applied to the Genesis location in conjunction with the ADCP current measurements considered to be reliable predicted maximum surface current velocity values that were not a matter of concern for the unit's continuing operations.

7.3 TLP Global Performance and Design Recipe

7.3.1 Although the peak environmental conditions during Lili approached 100-year values, the measured responses for Brutus and Typhoon were within the design limits.

7.3.2 In the case of Brutus, the comparisons suggest that although the tendon transfer functions did not accurately represent the individual tendon energy for a particular direction, there is an overall safe side bias in the design models. This is further reinforced by the fact that the design transfer functions do not contain current and wind effects while the measured response spectrums will contain some periodic components of the fluctuating wind and current energy from the continually transient sea state during Lili.

7.3.3 The limitations of the spectral analysis of full-scale measurements must be kept in mind, particularly the impact of directionality and of the non-stationary nature of the underlying process. In addition it must be recognized that Lili was essentially one realization of an inherently random process. The input model response spectrums are from idealized conditions and therefore their response is smooth and stationary.

7.3.4 The most likely explanation for the favorable outcome is that Lili's behavior was fundamentally different from the following standard design assumptions: peak environmental conditions lasting for 3-hours, constant direction of environmental loading, stationary narrow-banded process, collinear wave, wind and current. Comparisons between measured and predicted tendon response spectrums emphasized the importance of environment directionality on response.

7.3.5 The damping estimated from the Brutus measurements was reasonably consistent with the values used in design considering the limitations of the spectral analysis of full-scale measurements as previously discussed and also potential limitations of the single-degree-of-freedom, half-bandwidth method used here. It is noted that the roll and pitch resonance in the measurements may contain heave resonance as well, since their respective natural frequencies are nearly identical and difficult to filter out. This feature could have an influence on the larger damping estimates given by the measurements.

7.3.6 Design practices for TLPs usually predict maximum tendon tension by combining components due to pretension at mean sea level, tide / surge variation, overturning due to wind and current, setdown due to static and slowly varying offset, wave forces and wave induced motion about the mean offset, foundation mispositioning, ringing / springing, tendon load sharing, VIV. General design margins are usually incorporated to provide the operator with a degree of flexibility in the unit's operation. A conservative design combination of parameters is usually developed relative to a real environmental event such as Lili.

7.3.7 Minimum tendon tension is an important criterion for TLPs and it was noted that the minimum tendon tensions during Lili did not approach zero for both Typhoon and Brutus. This is also a positive indication of the performance of TLPs under a major event such as Hurricane Lili.

7.3.8 Some tendon tensions indicated a clearly non-Gaussian quality to their response due to non-linearity in either the environmental conditions or the TLP response itself (or both). The non-Gaussian nature of tendon tension response is usually captured in design by empirical factors based on model testing and numerical models. TLP designers should maintain care and diligence in performing and interpreting model tests and validating their numerical

models. Feasible theoretical improvements to capture such non-Gaussian response include the use of Generalized Extreme Value distributions as well as application of a Hermite Polynomial model. Another potentially helpful advance is the application of a multivariate statistical description to the sea climate, in order to estimate extreme response.

- 7.3.9 The apparent lack of response of some of the tendons in Brutus at the wave frequency range was intriguing and a departure from numerical models.
- 7.3.10 The monitoring data for the TLPs indicated the robustness of current global performance analysis methods but further investigation is necessary to indicate how such design methods could be improved. As noted, loss of tendon tension is an important criterion in TLP design but tendon tensions during Lili remained relatively high – this is an area where further investigation may lead to more economical designs.

7.4 Recommendations

- 7.4.1 Damage was observed to deck equipment in some units due to the motions during Lili. A review of the procedures for securing critical equipment during major environmental events is recommended. API RP 2A¹⁰, for example, has useful equipment tie-down procedures for hurricanes that can be used as a starting point.
- 7.4.2 Damage was observed to equipment located in the air gap of some of the units. Such damage appears to be consistent with design predictions for wave crest, wave run-up and green water loading but a more detailed assessment should be carried out in the future.
- 7.4.3 Several units were subject to severe environmental loading not only during Lili, but also during previous major environmental events. The impact of all such events on the integrity of structural components, tendons, moorings, anchors and risers should be carefully investigated.
- 7.4.4 The data measured during Lili provided evidence of vortex shedding effects on TLP tendons but the magnitude of such effects did not increase the overall tension values beyond design predictions. On a more general note, vortex shedding may affect risers and tendons but also the global motions of spars. Such motions may have a knock-on effect on other areas such as the integrity of structural components, moorings and risers. This study provided evidence of the competence of the powerful tools available to the industry (both in terms of analysis and measurement) when modeling an event such as Lili. The industry should work diligently in applying such tools and expertise to achieve similar competence in modeling VIV and VIM to reduce undue operational costs.
- 7.4.5 This study has also provided evidence that some operators and designers are indeed working diligently to address the complex issues related to metocean data and its translation into design bases as well as those issues related to VIV and VIM in deepwater structures. It is believed that an industry wide effort into reviewing and documenting existing prediction methods and best design practices on such issues would be beneficial for the future operation of deep water production units in the Gulf of Mexico.

- 7.4.6 The offshore industry has previously conducted useful studies where computer programs for advanced analysis (such as pushover analysis of platforms) were benchmarked against each other and against model tests or monitoring data. Computer programs presently used for the prediction of motions, tendon / mooring loads and riser response should be subject to similar benchmarking. The outcome of such study would provide an insight into specific areas where future research would be most beneficial.
- 7.4.7 There is a clear economical benefit in designing operations that can be maintained during high currents.
- 7.4.8 Extensive literature is available related to reliability-based methods for TLP design. A co-coordinated effort to collate such information and develop a risk-based approach to the design and integrity management of TLPs worldwide could be beneficial to the industry. A similar approach to the design of risers could be also beneficial.

8. REFERENCES

1. American Global Maritime Inc.: 'Assessment of Performance of Deepwater Floating Production Facilities', Proposal GMH-188, February 2003.
2. Cardone, V.J., Cox, A.T., Lisaeter, K.A., Szabo, D.: 'Hindcast of winds, waves and currents in Northern Gulf of Mexico in Hurricane Lili (2002)'. Paper OTC 16821, Offshore Technology Conference, Houston 2004.
3. Ward, E.G.: 'Ocean data gathering program – An overview'. Paper OTC 2332, Offshore Technology Conference, Houston 1974.
4. Cardone, V.J., Cox, A.T., Greenwood, J.A., Evans, D.J., Feldman, H., Glenn, S.M., Keen, T.R.: 'Hindcast study of winds, waves and currents in Hurricane Andrew, Gulf of Mexico, 1994'. Final Report to the Minerals Management Service, Herdon, Va., 1994.
5. Petruskas, C., Finnegan, T.D., Heideman, J.C., Vogel, M., Santala, M., Berek, G.P.: 'Metocean criteria/loads for use in assessment of existing offshore platforms'. Paper OTC 7484, Offshore Technology Conference, Houston 1994.
6. Puskar, F.J., Aggarwal, R.K., Cornell, C.A., Moses, F., Petruskas, C.: 'A comparison of analytically predicted platform damage to actual platform damage during Hurricane Andrew'. Paper OTC 7473, Offshore Technology Conference, Houston 1994.
7. Krieger, W.F., Banon, H., Lloyd, J.R., De, R.S., Digre, K.A., Nair, D., Irick, J.T., Guynes, S.J.: 'Process of assessment of existing platforms to determine their fitness for purpose'. Paper OTC 7482, Offshore Technology Conference, Houston 1994.
8. Marshall, P.W., Bea, R.G.: 'Failure modes of offshore platforms'. Proc. Intl. Conf. Behavior of Offshore Structures, 2, 1976, pp. 579-635.
9. Bea, R.G., Mortazavi, M., Stear, J., Jin, Z.: 'Development and verification of template offshore capacity analysis tools (TOPCAT)'. Paper OTC 11935, Offshore Technology Conference, Houston 2000.
10. American Petroleum Institute: 'Recommended practice for planning, designing and constructing fixed offshore platforms'. API RP 2A, 21st Ed., 2000.
11. Efthymiou, M., van de Graaf, J.W., Tromans, P.S., Hines, I.: 'Reliability based criteria for fixed steel offshore platforms'. Journal of Offshore Mechanics and Arctic Engineering, 119, 1997, pp. 120-124.
12. Minerals Management Service: 'Workshop: Assessment of existing OCS platforms'. September 23-24, 2003, New Orleans, USA.
13. Bea, R.G., Ramos, R., Valle, O., Valdes, V., Maya, R.: 'Risk assessment and management based hurricane wave criteria for design and requalification of platforms in the Bay of Campeche'. Paper OTC 8692, Offshore Technology Conference, Houston 1998.
14. Tromans, P.S., van de Graaf, J.W.: 'Statistical verification of predicted loading and ultimate strength against observed storm damage for an offshore structure'. Paper OTC 6573, Offshore Technology Conference, Houston 1991.
15. Harland, L.A., Taylor, P.H., Vugts, J.H.: 'The extreme force on an offshore structure and its variability'. Applied Ocean Research, 20, 1998, pp. 3-14.
16. Hellan, Ø.: 'Nonlinear pushover and cyclic analyses in ultimate limit state design and reassessment of tubular steel offshore structures'. PhD Thesis, The Norwegian Institute of Technology, 1995.

17. Erb P.R., Finch C.L., Manley G.R. 'The Hutton TLP Performance Monitoring and Verification Program', Paper OTC 4951, Offshore Technology Conference, Houston, 1985.
18. Mercier, J.A., Leverette, S.J., Bilault, A.L.: 'Evaluation of Hutton TLP response to environmental loads', Proc. Offshore Technology Conference, Houston, Texas, 1982.
19. Hauch S. and Haver S. "Measured Motion Characteristics of the Heidrun TLP" Proceedings of the 17th International Conference on Offshore Mechanics and Arctic Engineering, OMAE98-1391, 1998.
20. Marthinsen, T., Muren, J.: 'Snorre TLP – comparison of predicted and measured response', Proc. Seminar on Tensioned Buoyant Platforms, University College London, Bentham Press, London, 1993.
21. Leverette, S.J., Rashedi, R.: 'Reliability-based design methodology for TLP design'. Proc. 4th SNAME Offshore Symposium, Houston, Texas, 1995.
22. Mercier, J.A.: 'Reliability-based design code for floating systems', Proc. 2nd SNAME Offshore Symposium, Houston, Texas, 1991.
23. Banon, H., Toro, G., Jeffreys, R.: 'Development of reliability-based global design equations for TLPs', Proc. of the 13th International Conference on Offshore Mechanics and Arctic Engineering, OMAE'94, Houston, Texas, 1994.
24. Mathisen, J., Rashedi, R., Moerk, K., Zimmer, R., Skjøng, R.: 'Reliability-based load and resistance factor design code for TLP hull structure', Proc. of the 13th International Conference on Offshore Mechanics and Arctic Engineering, OMAE'94, Houston, Texas, 1994.
25. Leverette, Bradley and Bliault: 'An integrated approach to setting environmental design criteria for floating production facilities', Proc. BOSS'82, 1982.
26. Bea, R.G, Allin Cornell, C., Vinnem, J.E., Geyer, J.F., Shoup, G.J., Stahl, B.: 'Comparative risk assessment of alternative TLP systems: Structure and foundation aspects', Proc. of the 11th International Conference on Offshore Mechanics and Arctic Engineering, OMAE'92, Calgary, Canada, 1992.
27. Kung, C.J., Wirsching, P.H.: 'Fatigue and fracture reliability and maintainability of TLP tendons', Proc. of the 11th International Conference on Offshore Mechanics and Arctic Engineering, OMAE'92, Calgary, Canada, 1992.
28. Hovde, G., Moan, T.: 'Fatigue reliability of TLP tether systems', Proc. of the 13th International Conference on Offshore Mechanics and Arctic Engineering, OMAE'94, Houston, Texas, 1994.
29. Ang, A. H.-S.: 'A study of the reliability of a Tension Leg Platform', Report No. CG-M-1-86, Vol. 2, US Coast Guard Office of Marine Safety, Security and Environmental Protection, Washington, D.C, 1986.
30. Naess, A., Ness, G.M.: 'Second-order, sum-frequency response statistics of tethered platforms in random waves'. Applied Ocean Research, Vol. 14, No.1, pp. 23-32, 1992.
31. Winterstein, S., Marthinsen, T.: 'Nonlinear effects on TLP springing response and reliability'. Proc. 1st Intl. Conf. Computational Stochastic Mechanics. Ed. P.D. Spanos and C.A. Brebbia, Computational Mechanics Publications, Southampton, 1991.
32. Naess, A., Moe, G.: 'The statistics of springing response of a TLP', Proc. of the 11th International Conference on Offshore Mechanics and Arctic Engineering, OMAE'92, Calgary, Canada, 1992.
33. Banon, H., Harding, S.J.: 'Methodology for assessing reliability of Tension Leg Platform tethers', Journal of Structural Engineering, Vol. 115, No. 9, pp. 335-344, Houston, 1989.

34. Das, P.K., Faulkner, D., Guedes da Silva, A.: 'Limit state formulations and modeling for reliability-based analyses of orthogonally stiffened cylindrical shell structural components', Rep. NAOE-91-26, Dept. Naval Architecture and Ocean Engineering, Glasgow University, 1991.
35. Faulkner, D., Birrel, N.D., Stiansen, S.G.: 'Development of a reliability-based code for the structure of tension leg platforms', Proceedings Offshore Technology Conference, Houston, 1983.
36. Lotsberg, I.: 'Probabilistic design of the tethers of a Tension Leg Platform', J. Offshore Mechanics and Arctic Engineering, Vol. 113, pp. 162-170, 1991.
37. Rooney, P., Lereim, J., Madsen, H.O.: 'Application of probabilistic methods for verification and calibration of a TLP tether system design based on partial coefficients', Proc. of the 8th International Conference on Offshore Mechanics and Arctic Engineering, The Hague, Netherlands, 1989.
38. Stahl, B., Geyer, J.F.: 'Ultimate strength reliability of Tension Leg Platform systems', Proceedings Offshore Technology Conference, Houston, Texas, 1985.
39. Ximenes, M.C.C., Mansour, A.E.: 'Fatigue system reliability of TLP tendons including inspection updating', Proc. of the 10th International Conference on Offshore Mechanics and Arctic Engineering, 1991.
40. Stansberg, C.T.: 'Statistical properties of nonlinear wave-induced high frequency responses in random waves', Proc. Seminar on Tensioned Buoyant Platforms, University College London, Bentham Press, London.
41. American Petroleum Institute: 'TLP Model Code JIP – Summary Document for API'. API Project 93-20. Report prepared by Offshore Systems and Analysis Corporation, Houston, October 1994.
42. American Petroleum Institute: 'Bulletin on Stability Design for Cylindrical Shells', Bulletin 2U, 1st Edition 1987, 2nd Edition, Washington, DC, 2000.
43. American Petroleum Institute: 'Bulletin on Design of Flat Plate Structures', Bulletin 2V, 1st Edition 1987, Washington, DC, 2nd Edition 2000.
44. Balint S., Capanoglu, C., Kamal, R.: 'Background to new edition of API Bulletin 2U: Stability design of cylindrical shells'. Paper OTC 14188, Offshore Technology Conference, Houston, 2002.
45. Balint S., Serrahn, C.S., Chang, B.C.: 'Background to new edition of API Bulletin 2V: Design of flat-plate structures'. Paper OTC 14187, Offshore Technology Conference, Houston, 2002.
46. American Petroleum Institute: 'Recommended practice for planning, designing and constructing tension leg platforms'. API RP 2T. 2nd Edition, Washington, DC, 1997.
47. American Petroleum Institute: 'Recommended practice for planning, designing and constructing floating production systems'. API RP 2FPS. 1st Edition, Washington, DC 2001.
48. American Petroleum Institute: 'Design and analysis of stationkeeping systems for floating structures'. API RP 2SK. 2nd Edition, Washington, DC, 1996.
49. American Petroleum Institute: 'Design of risers for floating production systems (FPSs) and tension leg platforms (TLPs)'. API RP 2RD. 1st Edition, Washington, DC, 1998.
50. Huang, K., Chen, X., Kwan, C.T.: 'The impact of vortex-induced motions on mooring system design for spar-based installations'. Paper OTC 15245, Offshore Technology Conference, Houston 2003.
51. Mairs, H.L., Koch, S.P., Gordon, R.B., Cuellar, R.: 'The storm current response of Gulf of Mexico hurricanes'. Paper OTC 6833, Offshore Technology Conference, Houston 1992.
52. van Dijk, R.R.T., Voogt, A., Fourchy, P., Mirza, S.: 'The effect of mooring system and sheared currents on vortex induced motion of truss spars'. Proc. of the 22nd International Conference on Offshore Mechanics and Arctic Engineering, OMAE'03, Cancun, Mexico, 2003.

53. Texas A&M, University Department of Oceanography. 'Quarterdeck On-Line'. Volume 6, Number 1, May 1998. Internet link: <http://www-ocean.tamu.edu/Quarterdeck/QD6.1>
54. Schaudt, K.J.: 'Operations and deepwater currents in the Gulf of Mexico'. Deepwater Infrastructure Forum, Coasts, Oceans, Ports and rivers Institute of the American Society of Civil Engineers, Houston, 2004.
55. Leverette, S., Rijken, O., Dooley, W., Thompson, H.: 'Analysis of TLP VIV responses to Eddy currents'. Paper OTC 15289, Offshore Technology Conference, Houston, 2003.
56. Goni, G., Trinanes, J.: 'Near-real time estimates of upper ocean heat content (UOHC) and tropical cyclone heat potential (TCHP) from altimetry'. Website of the National Oceanic Atmospheric Administration (NOAA). Internet Link: <http://www.aoml.noaa.gov/phod/cyclone/data>
57. Allen, D.W.: 'Various design impacts of loop currents on offshore structures'. Deepwater Infrastructure Forum, Coasts, Oceans, Ports and rivers Institute of the American Society of Civil Engineers, Houston, 2004..
58. De Luca, M.: 'Current affairs'. Offshore Engineer, Sunday, February 01, 2004
59. Email communications with El Paso, dated July 2003.
60. Atlantia Offshore Limited: 'Allegheny Seastar® TLP: Annual structural inspection report for year 3'. Doc. No. 22111-TR-0005, 25 Feb. 2003.
61. Rigzone: 'Shell Global Solutions Retrofits VIV Strakes on Medusa Spar'. Rigzone.com, Tuesday, March 30, 2004. Internet link to http://www.rigzone.com/news/article.asp?a_id=11952
62. Roshko, A.: 'Experiments on the flow past a circular cylinder at very high Reynolds number'. Journal of Fluid Mechanics, 1961, 10:345-356.
63. Minerals Management Service. Technology Assessment and Research. 'VIM/SPAR Industry Forum', Project Number 482, February 2004.
64. Atlantia Offshore Limited: 'Typhoon Seastar® TLP: Hurricane Lili response'. Doc. No. 22116-TR-0001, 4th Feb 2004.
65. Email Communications with Oceanweather Inc., March 2004.
66. Mellor, G., and Yamada, T., 1982, 'Development of a Turbulence Closure Model for Geophysical Fluid Problems'. Reviews of Geophysics and Space Physics, Vol. 20, p. 851-875.
67. Cooper, C. and Thompson, H., 1989, 'Hurricane-driven currents on the outer continental shelf - I. model formulation and verification', J. Geophys. Res. (Oceans).
68. Email Communications with ChevronTexaco, Feb 2004.
69. Bleck, R., G. R. Halliwell, Jr., A. J. Wallcraft, S. Carroll, K. Kelly, and K. Rushing, 2002. Hybrid coordinate ocean model (HYCOM) user's manual: Details of the numerical code. Available on the internet at hycom.rsmas.miami.edu.
70. Email Communications with ChevronTexaco, Dec 2003.
71. Doppler Principles of Operation, Internet link to <http://www.current-meter.com/prin-dop.html>
72. Email communications with RD Instruments, March 2004.
73. Allegheny Seastar® TLP - Atlantia Offshore Limited Website, Internet link to <http://www.atlantia.com/projects/allegheny>
74. Typhoon Seastar® TLP - Atlantia Offshore Limited Website, Internet link to <http://www.atlantia.com/projects/typhoon>
75. Kibbee, S.E., Chianis, J.W., Davies, K.B., Sarwono, B.A.: 'A mini-platform for deepwater: the Seastar TLP. Proc. SNAME 4th Offshore Symposium, Tension Leg Platform Technology, Houston, 23/24 February 1995.
76. Atlantia Offshore Limited: 'Typhoon Seastar® TLP: Special underwater inspection report'. Doc. No. 22113-TR-0004, 19 Dec. 2002.

77. Communications with ChevronTexaco, October 2003
78. MODEC's MOSES TLP – MODEC International Website. Internet link to <http://www.modec.com/en/project/tlp/prince.html>
79. Wybro, P.G.: 'Development of deepwater fields using MOSES small TLP'. Proc. SNAME 4th Offshore Symposium, Tension Leg Platform Technology, Houston, 23/24 February 1995.
80. Young, P.: 'Brutus TLP global performance evaluation'. Shell Report CE-224, October 1998.
81. MMS study 'assessment of performance of deepwater floating production facilities during hurricane Lili', Private Communication by Shell dated September 2003.
82. Campbell, R.B. and Vandiver, J.K., 1980, "The Estimation of Natural Frequencies and Damping Ratios of Offshore Structures," Proc. of Offshore Technology Conference, OTC 3861, Houston, Texas.
83. Garrett, D.L., Gu, G.Z., Watters, A.J., 1995, "Frequency Content Selection for Dynamic Analysis of Marine Systems," Proc. of the 14th International Conference on Offshore Mechanics and Arctic Engineering, OMAE'95, 1, pp 393-399.
84. Kijewski, T. and Kareem, A., 1999, "Analysis of Full-Scale Data from a tall building in Boston: Damping Estimates," Proc. of the 10th International Conference on Wind Engineering.
85. Oppenheim, A.V. and R.W., Schafer, 1989, "Discrete-Time Signal Processing," Prentice-Hall, pp. 713-718.
86. Email communications with Atlantia Offshore, March 2004.
87. Forristall, G.Z., Larrabee, R.D., Mercier, R, 1991, 'Combined oceanographic criteria for deepwater structures in the Gulf of Mexico'. Proc. of Offshore Technology Conference, OTC 6541, Houston, Texas.
88. Cooper, C.K., 1992, 'A preliminary case for the existence of hurricane alleys in the Gulf of Mexico'. Proc. of Offshore Technology Conference, OTC 6831, Houston, Texas.
89. Atlantia Offshore Limited: 'Allegheny Seastar® TLP: Hurricane Lili Reponse'. Doc. No. 23125-TR-1001, 8 June 2004.
90. NORSOOK, 1999, Actions and Action Effects, N-003, Rev. 1
<http://www.standard.no/standard/index.db2>
91. Kokkinis, T., Sandstrom, R.E., Jones, H.T., Thompson, H., Greiner, W.L., 2004, 'Development of a stepped line tensioning solution for mitigating VIM effects in loop eddy currents for the genesis spar', Proc. of the 23th International Conference on Offshore Mechanics and Arctic Engineering, OMAE'04.

ACKNOWLEDGEMENTS

The Minerals Management Service funded the present work. The contribution to this work of Charles Smith, MMS Contracting Officer's Technical Representative (COTR) is gratefully acknowledged.

Diego Martinez of Global Maritime processed the Brutus monitoring data in MATLAB and assisted in its interpretation and in other useful technical input during the course of the project. Jack Mercier of Global Maritime provided input concerning TLP technology.

Prof. Robert G. Bea of the University of California at Berkeley provided useful discussions and technical input during the course of the project.

Shell International Exploration and Production Inc. provided the monitoring data for Brutus. Peter Young and George Rodenbusch provided the monitoring data as well as comments during the course of the work.

Atlantia Offshore Inc. provided inspection reports as well as monitoring data, data analysis and comments relevant to Typhoon and Allegheny. The contribution of Steve Leverette, Mike W. Spillane, Oriol Rijken and Guy Mansour is acknowledged.

Richard G. Adams, Cortis K. Cooper, James Stear, Hugh M. Thompson and Jeffrey K. Schmoll of ChevronTexaco provided assistance with the data for Genesis and Typhoon as well as comments to the work.

William Dooley of ENI Petroleum assisted with releasing the data for Allegheny.

Arnold Crochet of El Paso Corporation provided information on the Prince TLP. Bart Heijermans and James Brokmeyer of El Paso Corporation provided support to this initiative.

Vince Cardone of Oceanweather Inc. made the hindcast data available to this project and provided useful discussions and feedback.

The support of the above companies and individuals is gratefully acknowledged. Every effort was made to reflect the comments from the operators and designers who provided input to this work. The report, however, solely reflects the opinions, conclusions and recommendations of the author.